University of Cincinnati

Date: 3/8/2016

I, Amrita Mandal, hereby submit this original work as part of the requirements for the degree of Doctor of Philosophy in Molecular & Developmental Biology.

It is entitled:

Roles of Retinoic Acid and Wnt signaling during Zebrafish Development

Student's name: **Amrita Mandal**

This work and its defense approved by:

Committee chair: Joshua Waxman, Ph.D.

Committee member: Louis Muglia, M.D., Ph.D.
M

Committee member: Brian Gebelein, Ph.D.

Committee member: Jerry Lingrel, Ph.D.

Committee member: Katherine Yutzey, Ph.D.

19727

Roles of retinoic acid and Wnt signaling during zebrafish development

A dissertation submitted to the

Division of Graduate Studies and Research

of the University of Cincinnati

In partial fulfillment of the requirements for the degree of

Doctor of Philosophy

In the graduate program of Molecular and Developmental Biology in the college of Medicine

2016

by

Amrita Mandal

M.Sc, University of Calcutta, Kolkata, India, 2010

B.Sc, Presidency College, Kolkata, India, 2008

Committee Chair: Joshua Waxman, PhD

Katherine Yutzey, PhD

Brian Gebelein, PhD

Louis Muglia, MD, PhD

Jerry Lingrel, PhD

Abstract

Retinoic acid (RA) and canonical Wnt/β-catenin (Wnt) signaling are two major pathways that direct early embryonic development. Abnormalities in either pathway lead to congenital birth defects of the limb, heart and central nervous systems. This thesis is comprised of three studies that provide novel insights into the roles of RA and Wnt signaling during zebrafish development. Utilizing a ligand trap method, we created new zebrafish transgenic RA reporters, which act as a direct sensor for RA. We have shown these novel transgenic lines are responsive to RA and report previously unknown areas of activity. These reporters will be valuable tools to aid in studying early embryonic RA signaling and responses.

Crossregulation of RA and Wnt signaling has been reported in different cell types and physiological conditions with clinical and physiological relevance. Both RA and Wnt regulate Dact (Dapper antagonist of catenin) proteins, thus this family of proteins might act as a linker between these two pathways in various developmental processes. With that aim we have examined the dynamic expression pattern and regulation of *dact3* genes in zebrafish. Our analysis has shown *dact3b* but not *dact3a* is negatively regulated by RA in the hindbrain.

Multiple congenital defects include both cardiac and craniofacial abnormalities, which suggest there is close relationship between adjacent cardiac and pharyngeal field. Signaling pathways that regulate progenitor specification in the cardiopharyngeal field (CPF) are not yet well understood. Previous studies have shown that Wnt promotes cardiac specification and inhibits pharyngeal muscle (PM) development during somitogenesis. Our work demonstrates that contrary to previous studies, Wnt signaling promotes PM loss only prior to gastrulation, and interestingly this timing correlates with increases in cardiac specification. We also find that

excess Wnt leads to an increase of differentiated first heart field (FHF) and a decrease in second heart field (SHF) and PM markers.

Altogether, these results provide a novel tool to study RA signaling as well as opens up new areas to study RA and Wnt cross regulation in the context of *dact3b.* Additionally we have provided new insights on the role of Wnt during fate specification in the CPF.

Acknowledgments

I would like to thank my family and friends for their support and encouragement throughout my graduate studies. This thesis is dedicated to my mother who has instilled in me the value of education and living a compassionate life.

I thank my advisor, Joshua Waxman and the dissertation committee for their support and mentorship.

Table of Contents

List of Figures

Chapter 1

Chapter 2

Chapter 3:

Chapter 4

Chapter 5

Chapter 1:

Introduction

Overview

Two important pathways that regulate early embryonic development are RA and Wnt signaling. Zebrafish being optically transparent with high fecundity and short developmental time is an ideal organism to study the *in vivo* dynamics of signaling pathways. In order to study RA signaling *in vivo*, there is a need to create efficient and reliable tools to visual RA signaling. With that aim, we have created and characterized a novel stable transgenic RA reporter. Both RA and Wnt signaling regulate Dact proteins. Investigating Dact expression and regulation provides an excellent context to gain insight into the possible cross talk between these two signaling pathways. Wnt signaling plays multiple roles during organ progenitor specification. It is not yet known if Wnt signaling plays any role during cardio-pharyngeal field development. Therefore, three distinct goals of my thesis were to: 1) Characterize a novel RA sensor line; 2) Analyze expression and regulation of *dact3* genes in zebrafish; 3) Decipher the role of Wnt in balancing cardiac and pharyngeal muscle fate in zebrafish.

Retinoic acid signaling during development

RA is an active metabolic derivative of Vitamin A (Vit-A) and implicated in various biological and pathological conditions with significant clinical relevance. Animals depend on nutrition for the source of Vit-A, since it cannot be synthesized de novo in the body. Retinol homeostasis begins with its dietary uptake in the intestine, storage in liver, and adipose tissues and then transportation in the blood to the target cells via binding with the carrier protein retinol binding protein 4 (RBP4) [1]. Some cells also have a transmembrane protein named Stra-6, which acts as a receptor for RBP4 for efficient retinol uptake [2]. In target tissues, retinol is

reversibly oxidized to retinaldehyde via two classes of enzymes: alcohol dehydrogenases (ADH) or retinol dehydrogenase (RDH) [3, 4]. Next, retinaldehyde is irreversibly oxidized to retinoic acid by retinaldehyde dehydrogenases (RALDH). RA then enters the nucleus of target tissues and binds with the RAR/RXR heterodimer leading to target gene transcription (Figure 1). Humans have three types of aldehyde dehydrogenases: Aldh1a1, Aldh1a2 and Aldh1a3 (also called Raldh) [5]. Zebrafish, however, only have Raldh2 and Raldh3 in their genomes [6]. Retinol can also be converted to retinyl ester for future storage via cellular retinol binding proteins (CRBP) [7]. RA levels are precisely controlled in the embryo via complimentary expression of RA synthesizing and degrading enzymes. In RA non-target tissues, it is metabolized to an inactive derivative via P450 family of cytochromes cyp26 enzymes [8].

RA acts as a ligand for nuclear hormone receptors RAR/RXR heterodimer, which are ligand activated transcription factors [8-10]. Binding with RA leads to conformational changes in the receptors converting them from transcriptional repressors to activators, which eventually lead to permissive changes in chromatin conformation of the target genes and recruitment of transcription initiation machinery to begin target gene transcription [11]. RARs bind the most commonly available forms of RA: all trans RA as well as 9-cis RA. RXRs can only bind to 9-cis RA [12]. There are three highly conserved RARs in human, mice, xenopus and chicken: RARα, RARβ and RARγ. Due to whole genome duplication and subsequent gene loss, zebrafish lack the *RARβ* receptor and have two paralogs for each of the other two receptors [13]. Genetic knockdown studies in mice have described considerable redundancy of these receptors. Only the double knockout *RAR/RAR* or *RAR/RXR* mice are embryonically lethal. Previous studies have shown that ligand binding to only the RAR portion can rescue RA synthesis abnormalities [14]. The primary role of RXR is to act as a scaffold for RAR in order to promote proper DNA

binding to the highly conserved RA response elements (RAREs) located in the promoters of RA target genes [15]. Classic RARE sequence is a 5-bp-spaced direct repeat of a hexameric consensus motif popularly known as DR5 site [9]. There are reports of other DR sites such as DR1, DR2 and DR4 which also serves as RAR/RXR binding sites on the promotes of RA target genes [16].

RA is important for growth, patterning and homeostasis of most of the vital organs in the body, such as heart, liver, kidney, pancreas, limb and central nervous system (CNS). Requirements of RA have been discovered using Vit-A deficient (VAD) animal models [8] . VAD quail dies 4 days after hatching due to malformations in the CNS, cardiovascular system and hindbrain [17]. *Raldh2-/-* mice also have greatly reduced posterior hindbrain, cardiac abnormalities and die at midgestation [18-20]. These abnormalities arise due to the requirement of RA early in development to set up the anterior-posterior axis patterning of neural plate and proper hindbrain segmentation. Zebrafish *raldh2* mutants (*neckless* fish) also have malformed hindbrains, increase in cardiac specification and lack pectoral fins (equivalent to limb in mammals) [21]. Within the cardiac field, RA is important for heart tube patterning, looping, and outflow tract septation. RA is known to restrict cardiac progenitor pools in zebrafish. Loss of RA in zebrafish causes excess cardiac specification via fate transformation of the adjacent organ progenitors in the ALPM [22].

Transcription based reporters of RA signaling

To understand the role of RA in normal development, it has been fundamental to gain knowledge about its spatial and temporal regulation in vivo. With that aim, transgenic mice were

created using three copies of a DR5 RARE from the *RARβ2* isoform placed upstream of *lacz* under a mouse minimal heat shock inducible *hsp68* gene promoter (Figure 2A). This *RARE-hsp68-lacZ* construct had expression in a specific A-P domain with a sharp anterior boundary where the primitive streak ends [23]. This type of regionalized expression supports the role of RA in A-P patterning and the absence of expression in the anterior forebrain was due to presence of RA degrading enzymes. Similarly, a second mouse transgenic reporter line was created using three copies of a DR5 RARE sequence upstream of a minimal thymidine kinase promoter [24]. While useful tools, a few caveats of these transgenic reporters were: 1) they had later onset of reporter expression (E7.5) than anticipated and they could not explain the early role of RA in mesoderm migration or neural plate formation; 2) these reporters need fixation, which hinders the ability to look at live embryos and tissues.

Since zebrafish embryos develop *ex utero*, direct visualization and optical clarity make them an excellent tool to study signaling pathways in live animals. The first zebrafish RA reporter was created using three copies of RARE from the mouse *RARβ* gene upstream of the mammalian minimal thymidine kinase promote. The same study also used a zebrafish specific *GATA2* promoter to make additional transgenic embryos [25]. Transgene expression in these embryos was localized in the neural tube, spinal cord, retina, somites, heart, pronephric ducts, facial muscle, and branchial arches. These are known regions of RA receptor and RA target gene expression [11, 13, 26]. Treatment with a *Raldh2* inhibitor DEAB at gastrulation was able to eliminate or reduce reporter expression, suggesting this transgenic is RA responsive. Compared to the zebrafish reporter, expression was broader and more complex in the mouse reporter lines, although none of these reporters were able to reflect all endogenous RA availability. In order to create a more sensitive zebrafish RA reporter, 12 concatenated DR5 RARE sequences adapted

from *Hox* gene promoters were used to create the *Tg(12XRARE-ef1a:gfp)* line (Figure 2C) [11]. Although increasing the number of DR5 RARE copies resulted in higher sensitivity to RA and earlier initiation of reporter expression, this transgenic reporter expression was restricted to the anterior spinal cord, ventral eye and pronephros. Recently, another RA reporter line has been reported using genetically encoded probes for RA (GEPRA), which exploits fluorescence resonance energy transfer to report ambient intracellular [27]. In these reporters, the ligand-binding domain of RARβ is fused to cyan (CFP) and yellow fluorescent (YFP) proteins (Figure 3). Binding of RA causes changes in the ligand binding domain conformation, which results in conversion of cyan to yellow. Using GEPRA it was possible to report RA as early as 75% epiboly [27]. By comparison and validation of multiple reporters for a signaling pathway, we can establish optimal strategies to study physiological RA signaling.

Dact proteins: at the crossroad of Wnt and RA signaling

Dact proteins (also known as Dapper/Frodo) were initially discovered as binding partners for the Wnt signaling master regulator disheveled (Dvl) in a yeast two-hybrid screen [28]. As an interacting partner for Wnt master regulator Dvl, Dact proteins play roles in many Wnt signaling-mediated cellular responses. Three family members, Dact1, Dact2 and Dact3 have been described in humans and mice. Dact1 is the best-studied member of the family, which can negatively regulate both canonical and non-canonical branches of Wnt signaling. Dact1 can directly interact with TCF3 and inhibits β-catenin/LEF interaction [29]. Additionally, Dact1 associates with HDAC1 and promotes LEF/HDAC1 interaction leading to repression of downstream Wnt target gene transcription. In zebrafish, Dact1 acts as a positive regulator of Wnt

in a *wnt8* hypomorphic background. Dact2 is required for proper convergent extension movements via its role in Wnt/Ca^{+2}-PCP signaling during zebrafish development [29]. Expression and regulation of zebrafish *dact3* is yet unknown. Mice Dact3 shares 27% and 24% similarity to Dact1 and Dact2 respectively. Human Dact3 shares high similarity (85%) with mice Dact3 [30]. Dact3 is most abundantly found in the adult brain cortex of mice. Other areas of expression include branchial mesenchyme, pharyngeal arches, and craniofacial mesenchyme [30]. Unlike *Dact1* null mice, which die prenatally due to severe urogenital defects [31, 32], *Dact3* knock-out mice are viable but have reduced body weight, suggesting a possible role in postnatal growth. Employing the unilateral ureteral obstruction model in the *Dact3* null background results in enhanced kidney fibrosis along with up regulation of *β-catenin*, *dvl2* and Wnt target fibrotic gene expression. Dact3 also prevents Wnt signaling mediated EMT and myofibroblast activation, thus attenuating Wnt induced kidney fibrosis [33]. Negative regulation of Wnt by *Dact3* has also been established in the context of colon cancer. *Dact3* is epigenetically repressed through bivalent histone modifications in colon cancer cells, as well as patient-derived tumor cells. Pharmacological intervention of the chromatin status to increase *dact3* expression results in reduction of Wnt/βcatenin signal and enhanced apoptosis of colon cancer cells [34]. Thus, *dact3* can be used as a potential therapeutic agent in controlling aberrant Wnt signaling during colon cancer. Although all three Dact proteins have distinct expression patterns and developmental roles, one common theme is they all have a role in Wnt signaling mediated cellular responses. Through microarray analysis and drug treatment performed in our lab, RA signaling was found to positively regulate *dact1* and *dact2* expression in zebrafish embryos (Figure 4). Interestingly, Wnt and RA signaling cross talk in various cell types and physiological conditions [35-37]. For example, RARγ can directly interact with and repress *βcatenin* activity in

chondrocyte function [38]. However, it is not known what regulates *dact3* expression and if it is also regulated by RA similar to the other *dact* genes. Our study in chapter 3 is the first to describe *dact3a* and *dact3b* expression and regulation in zebrafish.

Wnt signaling in cardiac development

The Wnt families of proteins are cysteine rich secreted glycoproteins, which mediate a plethora of cellular functions during embryonic development and adult homeostasis. Wnt signaling is branched into canonical and non-canonical pathways depending on the type of Wnt ligands and downstream factors used [39]. β-catenin is the major downstream transcriptional co-activator of canonical Wnt signaling. In the absence of Wnt ligand, β-catenin is phosphorylated by the members of the degradation complex, which include axin, APC, GSK3β and CK-1. This phosphorylation event is followed by eventual proteasomal degradation of β-catenin. When a Wnt ligan is available, it binds with the trans-membrane frizzled (Frz) receptor and LRP5/6 co-receptor complex leading to plasma membrane recruitment of the degradation complex and release of β-catenin. Next, β-catenin travels to the nucleus and binds with TCF/LEF transcription factor leading to Wnt target gene transcription. Another important player of Wnt signaling is Dvl, which binds with the cytosolic β-catenin and prevents its destruction by the degradation complex [40, 41] (Figure 5).

Vertebrate cardiac development occurs in two waves of specification. First heart field (FHF) progenitors arise from lateral splanchnic mesoderm and subsequently migrate to the cardiac crescent. Later the cardiac crescent fuses to form the linear heart tube. Next, chamber specific gene expression, looping and constriction of atrioventricular canal eventually forms the multi

chambered beating heart. FHF derived structures include the left ventricle and parts of atria. Late differentiating second heart field (SHF) progenitors are derived from the cranial paraxial mesoderm and SHF cells are progressively added to both the poles of the heart and contribute to the right ventricle, outflow tract and parts of the atria [42-46]. Canonical Wnt signaling has multiple developmental stage specific roles during cardiogenesis [47-49], Using zebrafish and mouse ES cells, it has been shown that Wnt regulation of cardiac development requires precise temporal control [50, 51]. Wnt signaling promotes initial cardiac specification via its role in inducing mesoderm formation. This initial increase of cardiogenesis has been shown to happen at the expense of adjacent hematopoietic and endothelial fate in the mesoderm [52]. Later Wnt inhibition is required for proper cardiac differentiation. These data suggest that Wnt signaling has diverse functions during cardiac development depending on the developmental stage (Figure 6).

Wnt signaling in pharyngeal muscle development

Pharyngeal muscles are a subset of head muscles, which include three main subgroups: 1. Pharyngeal mesoderm derived PM (or branchiomeric muscle) that is involved in feeding, breathing, jaw movement, facial expression and pharyngeal laryngeal function; 2. Prechordal mesoderm derived extra ocular muscles (EOM) that help in eye movement and rotation; 3. Somite derived neck and tongue muscles. Genes that regulate initial head muscle specification upstream of the general skeletal muscle differentiation marker MyoD are distinct for head and trunk muscle [53]. For example *pax3*, which is essential for skeletal muscle specification in the trunk, is not expressed in the head muscle [54]. In accordance with this differential regulation, a

study in chicken has shown Wnt signaling from the dorsal neural tube inhibits skeletal myogenesis in the head, while the same signal promotes trunk myogenesis [55]. However, it is not known if Wnt inhibition of PM is conserved across other vertebrates. There has been no study to investigate if there is any developmental stage specific requirement of Wnt signaling during PM formation. Our work in Chapter 4 explored these questions.

Cardio-pharyngeal field development

The recent identification of a cardiopharyngeal field (CPF) refers to the developmental domain encompassing multipotent progenitors, which are specified into FHF, SHF and PM [56]. During early embryonic development, multipotential progenitors are specified and fate is restricted to certain organ types [57]. A balance of different signaling cues within the cell or surrounding environment determines specific lineages and organ field boundaries. Various congenital abnormalities include cardiac and craniofacial abnormalities, suggesting misregulation of signaling pathways regulating individual or common progenitor specification underlie the molecular etiology of these diseases. DiGeorge syndrome in which hemizygous deletion of chromosome 22q11.2 deletion includes the gene *TBX1* results in malformed pharyngeal apparatus and hypoplastic outflow tract [58]. Prevalence of cardio-craniofacial abnormalities calls for better understanding of the regulation of these progenitor specifications.

Extensive research in the ascidian *Ciona* in the past few years established the presence of a multi-lineage primed cardio-pharyngeal progenitor, which undergoes a few asymmetric divisions and eventually specifies into the cardiac and pharyngeal lineage via regulatory antagonism between transcription factors *NK4* (cardiac) and *Tbx1/10* (pharyngeal) [59] (Figure 7). During

lineage specification, two B7.5 blastomeres are divided into atrial tail muscle (ATM) and tail ventricular cells (TVC). Using targeted gene disruption and transcriptional profiling, TVCs were shown to be primed for both cardiac and pharyngeal fate. Subsequently, TVC is divided into a small first heart field precursor (FHP) and a large secondary TVC, which is further asymmetrically divided in to atrial siphon muscles (ASM) and second heart field precursors (SHP). *NK4* (*Nkx2.5* homolog in *Ciona*) is necessary to repress *TBX1/10* expression and inhibit ectopic induction of muscle determinant *Ebf/COE* in the SHP. *TBX1/10* inhibits cardiac marker *GATAa* expression and subsequent cardiac specification. Thus, the antagonism between transcription factors specifies CPF in *Ciona*. Owing to the complexity of vertebrate embryos, we do not yet know if there is similar cross antagonism present to specify fate in the cardio-pharyngeal field.

Contrary to the previous notion of a common origin for FHF and SHF, single cell clonal analysis of *mesp1,* the earliest cardiac marker has shown FHF and SHF arise from temporally distinct progenitor populations during gastrulation with discrete molecular signatures [60]. Genetic marker expression and ontogeny of SHF and PM are more closely related to each other than to FHF [61]. Recent retrospective clonal analysis suggested specific regions of SHF share common origins with subsets of PM. Muscles derived from the 1st pharyngeal arch, as well as EOM, share clonal relationships with the right ventricle. Whereas the 2nd BA derived muscle shares progenitors with outflow tract, pulmonary trunk and aorta. Further analysis suggested the presence of a 3rd subgroup, which includes non-somite derived neck muscles, venous pole and pulmonary trunk of the heart [62] (Figure 8). There is significant overlap among the cardiac (*nkx2.5, isl1*) and pharyngeal marker (*tcf21, tbx1*) expression in the pharyngeal mesoderm. Work from Harel et al has argued cardiogenesis and myogenesis in the CPF is network properties of a

set of transcription factors rather than specific properties of a single gene [63]. Using single and double mutant mice for some of these markers, they have discovered a regulatory network of *tbx1, tcf21, lhx2* and *pitx2* acting upstream of cardiogenesis and myogenesis in the pharyngeal mesoderm [63].

Experimental rationale

Generation and characterization of a novel RA reporter

Abnormalities in RA signaling can lead to congenital birth defects. In order to treat RA related abnormalities, it is important to study its temporal and spatial activity in an *in vivo* model. Previous RA reporters in mice and zebrafish did not recapitulate broader availability of endogenous RA and the initiation of expression was also delayed [11, 23-25]. These reporters were created using the RAR/RXR binding DR5 RARE sequences. Thus, reporter activity is dependent on successful RAR/RXR heterodimer formation and binding to RARE. Additional factors such as other co-activators, repressors and transcription factors known to bind with either of the receptor can also affect the sensitivity of the reporter. We hypothesized creating a reporter by fusing only the RAR ligand binding domain (RLBD) with the Gal4 DNA binding domain (GDBD) will act as a direct sensor for RA since reporter activity would depend only on the availability and subsequent binding of RA to RLBD [64]. A previous study has shown fusion of N or C terminal domain of RAR with the VP16 domain creates hyperactive but not constitutively active RAR [11]. We hypothesized fusion of VP16 with the RLBD-GDBD construct will also create a hyperactive RA reporter. Thus, we also created a putative hypersensitive RA reporter.

We have analyzed the expression pattern and sensitivity to RA for these novel reporters using both standard fluorescence and confocal microscopy. Characterization of these novel sensors will add value to study RA biology in vivo and new insights into endogenous RA activity.

Dact3 **expression and regulation**

Dact proteins are modulators of both canonical and noncanonical Wnt signaling [28, 29, 65]. Microarray and drug treatment data from our lab has found *dact1* and *dact2* are positively regulated by RA. Thus, there is the potential that Dact proteins can act as an important linker for cross-regulation between Wnt and RA signaling. There is no report of a zebrafish *Dact3* orthologs until now. We performed phylogenetic analysis and found two paralogs of *dact3a* and *dact3b* in zebrafish with 100% conservation of the PDZ binding domain, which is important for binding with the Wnt master regulator Dvl. We have also performed *in situ* hybridization to analyze the dynamic expression pattern for *dact3a* and *dact3b* in zebrafish. Further we have analyzed the regulation of *dact3* by key signaling pathways (Wnt, RA, BMP and FGF) using appropriate transgenic reporter lines in zebrafish. Experimental approaches such as these will help us understand the role of *dact3* during zebrafish development as well as provide new insights into the cross-regulation between Wnt and RA signaling.

Wnt signaling in cardiac & PM specification

Wnt signaling plays important roles in mesoderm patterning and mesoderm derived organ development [66]. Previous studies have shown Wnt promotes cardiac specification before

gastrulation, while in chicken Wnt plays an antagonistic role during PM formation [50, 51, 55]. Since cardiac and pharyngeal fields lie in close proximity in the lateral marginal zone before gastrulation, we hypothesized that the source of excess cardiomyocytes comes at the expense of PM fate. Recent clonal analyses in *Ciona* and mice have established a common origin for SHF and PM, which is distinct from FHF [60, 67, 68]. Based on this information, we further wanted to explore if Wnt signaling specifically promotes FHF derived structure at the expense of SHF and PM. First, we have used heat shock inducible zebrafish reporters to explore the stage specific requirement of Wnt during PM development. Next, we analyzed the expression of cardiac and pharyngeal markers upon Wnt manipulation. These analyses will give novel insights into the role of Wnt signaling in establishing CPF.

Significance of studies

Improper balance of RA signaling can be teratogenic and cause perinatal mortality [8, 69]. For that reason, the levels of RA are strictly regulated in common medicines for acne given to pregnant women and women of child bearing age [12]. While RA is essential for proper development, excess RA can be teratogenic with lethal consequences, which are collectively known as RA embryopathies. Due to the ability of RA to promote differentiation and apoptosis in tumor cells, all-trans RA is commonly used as a therapeutic agent in cancer. Various synthetic retinoids are currently in clinical trials for thyroid cancer, lung cancer, head-neck cancer, etc [69]. Recently retinoids are also being used as a drug for neurodegenerative diseases such as Alzheimer's and Parkinson's disease for its role in inhibiting the formation of amyloid-beta fibrils, the main etiology of such diseases [70, 71]. Vit-A deficiency syndromes, which result in

abnormally low RA levels, can lead to complete blindness. Thus, it is important to understand the role of RA during normal development in order to better understand ways for treatment for these pathological conditions. Zebrafish is a powerful in vivo tool to study signaling pathways [72]. Due to its optical transparency and *ex-utero* development there is no need for invasive procedures or fixation. This allows imaging of RA signaling in a live organism efficient and reliable. Our novel RA sensor described in Chapter 2 will not only help to study RA signaling at intercellular, tissue specific and whole organism levels but also to study anatomical structures where reporter signaling is present independent of RA.

Expression of the Dact3 protein is epigenetically repressed in colorectal cancer and pharmacological perturbation can lead to apoptosis of cancer cells [34]. Thuss studying the expression and regulation of *dact3* is important and can shed light on possible therapeutics for colon cancer. The availability and function of *dact3* during zebrafish development has not been studied yet. Our study described in Chapter 3 is the first to analyze developmental stage specific expression of *dact3a* and *dact3b* in zebrafish. We have also found a previously unexplored role of RA in negatively regulating *dact3b* expression in the zebrafish hindbrain. Since Dact proteins are well known regulators of Wnt signaling, our work provides a novel platform to study possible cross regulation of RA and Wnt signaling during hindbrain development mediated by *dact3b*.

The heart is the first organ to form and function in all vertebrates. Proper function of the heart is essential for efficient oxygen transport and blood circulation. Heart disease accounts for the highest number of congenital deaths in the United States. Using stem cell based approaches to generate cardiomyocytes and heal injured hearts is a promising therapeutic strategy. Therefore, it is important to study the signaling pathways responsible for regulating cardiac

specification and differentiation *in vivo*. Prevention and treatment of human diseases in which both the heart and head muscles are affected needs an understating of the development of the respective organ field. Both cardiac and head muscles arise from common mesodermal progenitor population. Using heat-shock inducible zebrafish transgenic embryos and marker analysis, our study has unveiled a novel role of Wnt signaling in balancing cardiac and pharyngeal muscle fate specification in the CPF. More precisely, our data suggests Wnt signaling promotes FHF derived structures, while it inhibits PM and SHF development. Collectively these data adds to our current understating of CPF fate allocation in vertebrates. Understanding aspects of CPF development will help advance therapies for patients with cardio-craniofacial defects.

Figures:

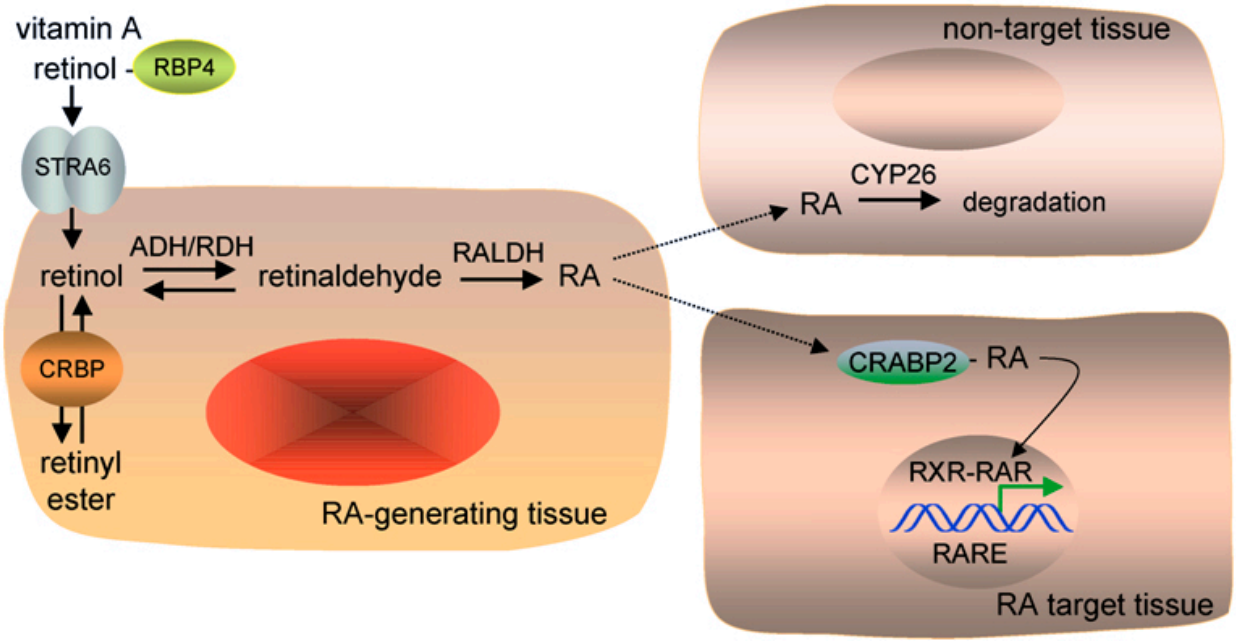

Figure 1: RA signaling pathway

RA is metabolized from the alcoholic form of Vit-A via multiple pxidayives steps. Adapted from Duster et al.,

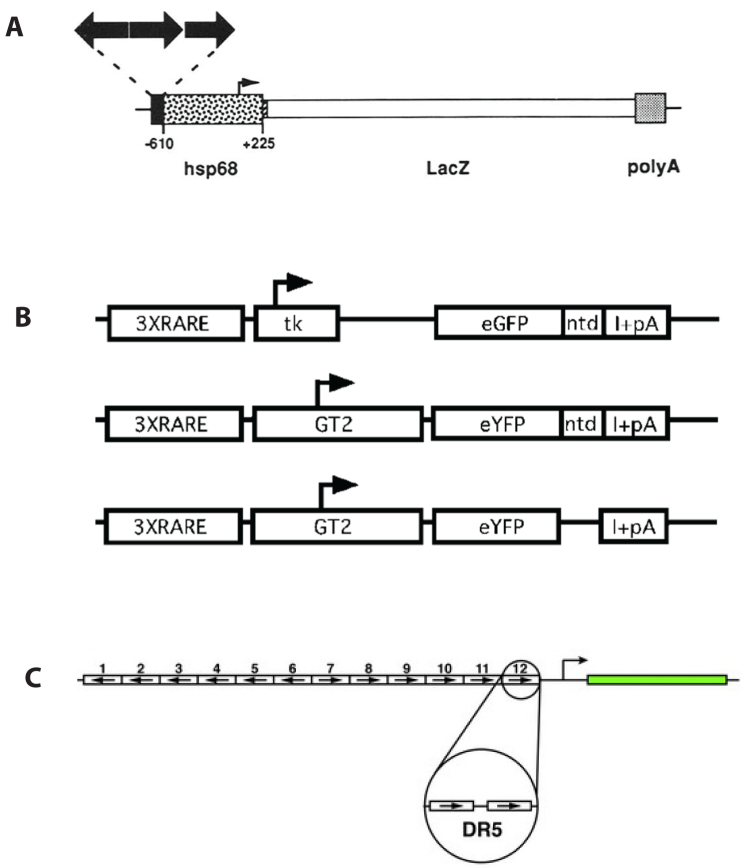

Figure 2: RA signaling reporters in mice and zebrafish

A) Recombinant construct used to make a transcriptional reporter *RAREhsplacz* to test RA signaling activity. It has three copies of RARE from RARβ promoter upstream of *hsp68lacZ.* B) RARE driven zebrafish construct: 1. Three copies of RARE is fused upstream of viral basal promoter thymidine kinase (tk). 2. Three copies of RARE from *RARβ* promoter is fused to zebrafish *GATA-2* basal promoter along with a nuclear localization signal (*ntd*) 3. Similar construct as 2, only difference it lacks the *ntd* domain. C) Schematic of 12XRARE reporter. Direct repeat 5 (DR5) RARE sequence from *Hox* gene promoters is placed upstream of EGFP. Adapted from Rossant et al., [23], Perz-Edwards et al.,[25], Waxman et al., [11].

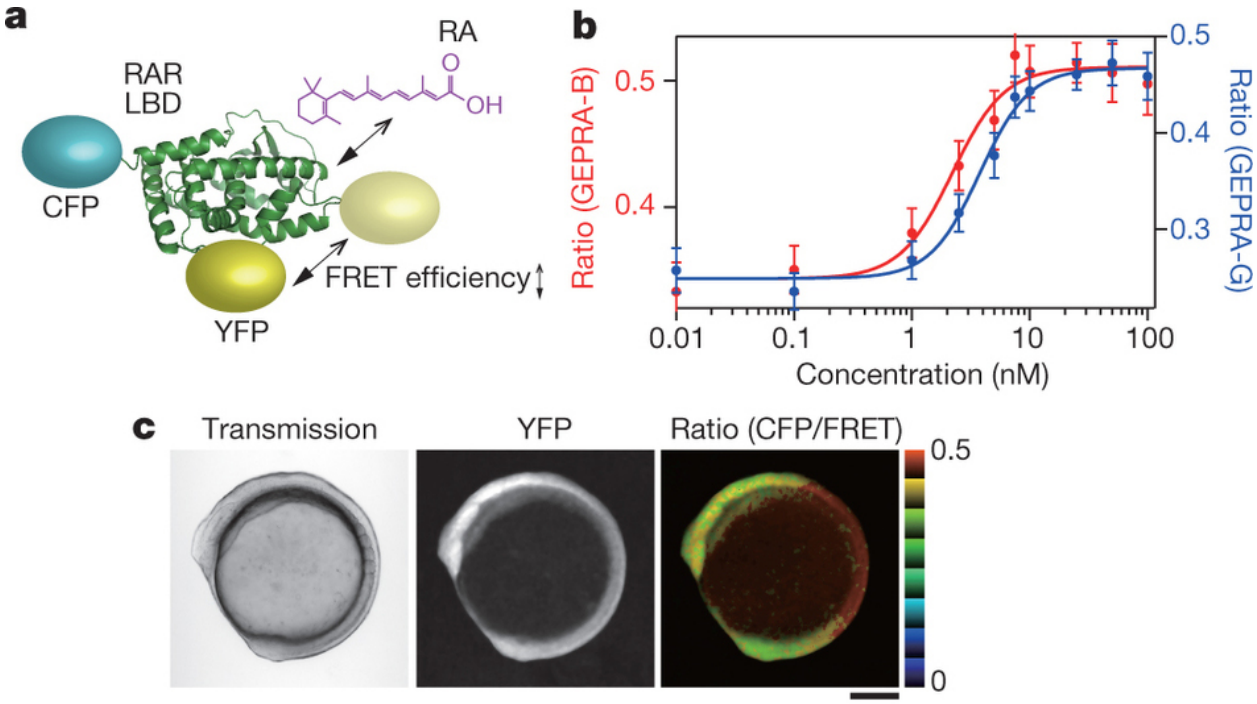

Figure 3: Genetically encoded probes for RA (GEPRA)

a) Schematics for GEPRA construct. Ligand binding domain of RARβ is fused to CFP and YFP. Light yellow color denotes RA unbound state. Upon RA binding fluorescence energy transfer leads to conversion from CFP to YFP. b) Titration curve for different GEPRA constructs. c) Transmission ratio. Blue suggests no RA and red suggest highest RA concentration. Adapted from Schimozono et al., [27].

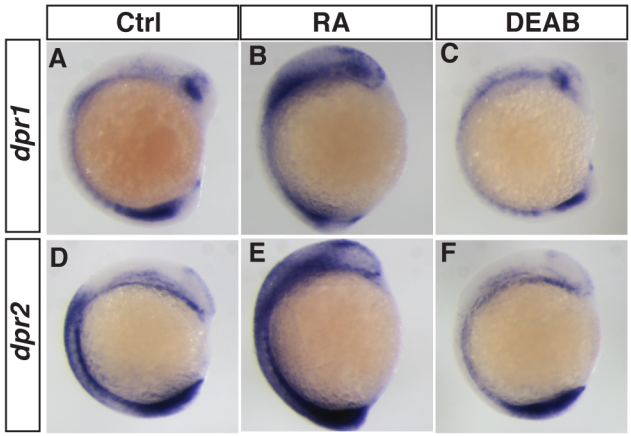

Figure 3: RA signaling positively regulates *dpr1* and *dpr2* expression

Embryos were treated at 50% epiboly and fixed for in situ at 8somites. RA treatment increases *dpr1* and *dpr2* expression significantly (B, E). Treatment with RA antagonist DEAB leads to reduced expression (C, F)

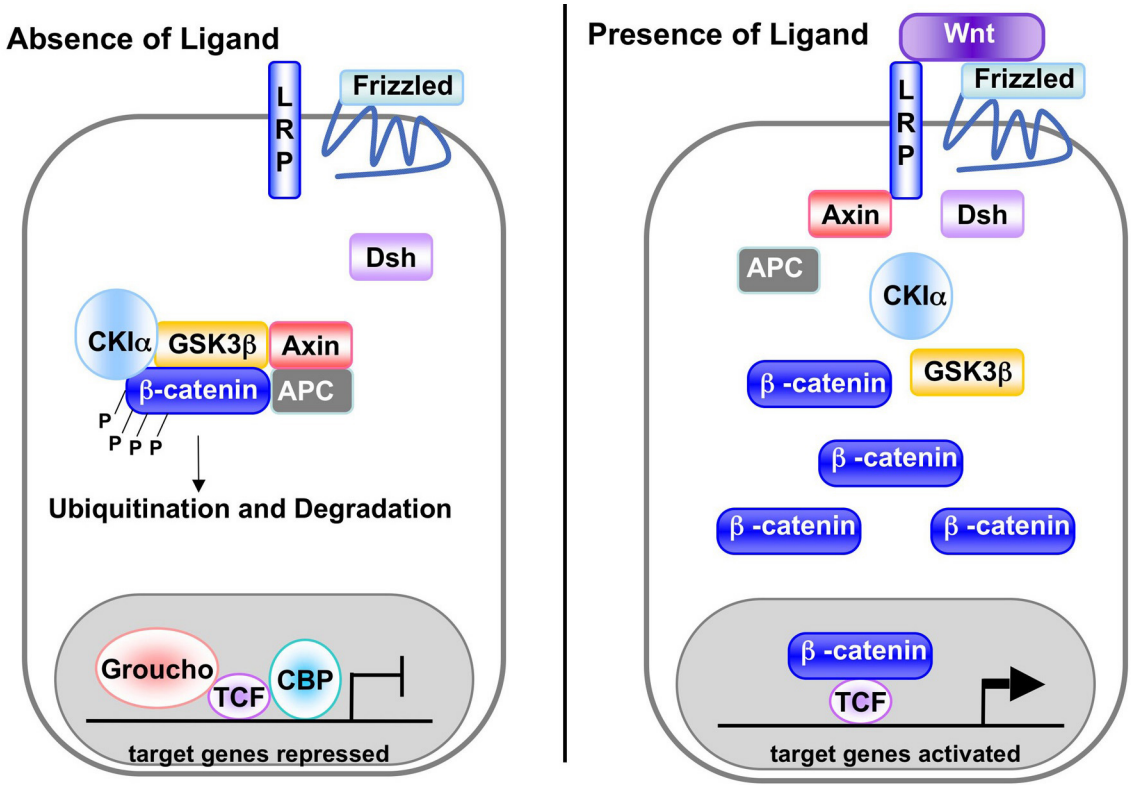

Figure 5: Canonical Wnt signaling pathway

A) In the absence of Wnt, ß-catenin is phosphorylated and degraded by APC/GSK-3 death complex B) In the presence of Wnt ligands, it binds to Frizzled and LRP receptor complex which lead to ß-catenin release and ß-catenin then enters the nucleus where it interacts with TCF proteins to regulate Wnt target gene expression.

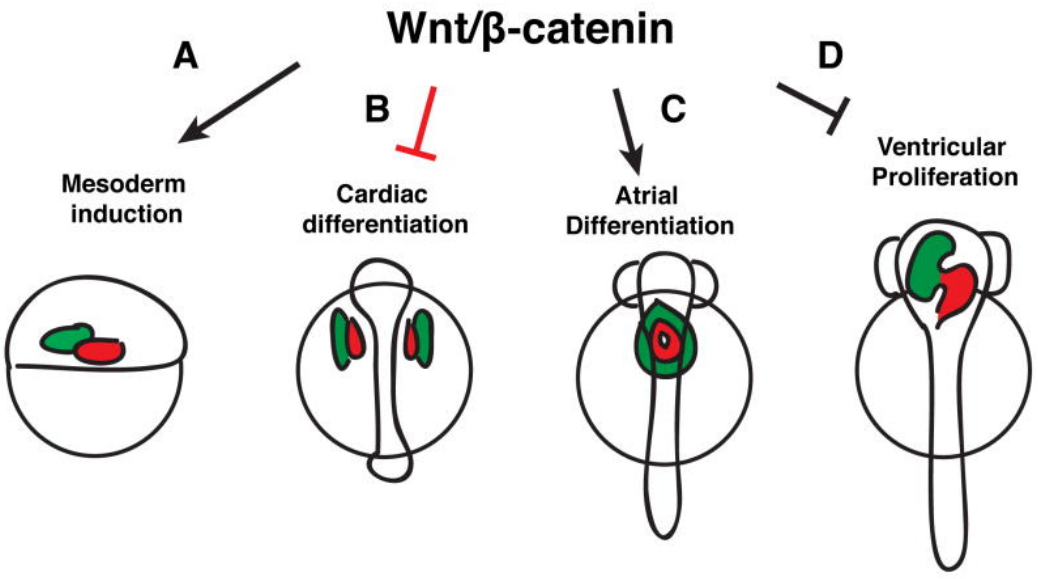

Figure 6: Multiple developmental stage dependent role of Wnt in zebrafish cardiogenesis

A) Before gastrulation Wnt promotes cardiac specification via its role in mesoderm induction B) Wnt inhibits cardiac differentiation after gastrulation C) Wnt preferentially promotes atrial differentiation D) Wnt inhibits ventricular differentiation. Red: Atrium, Green: Ventricle. Adapted from Dohn et al., [51]

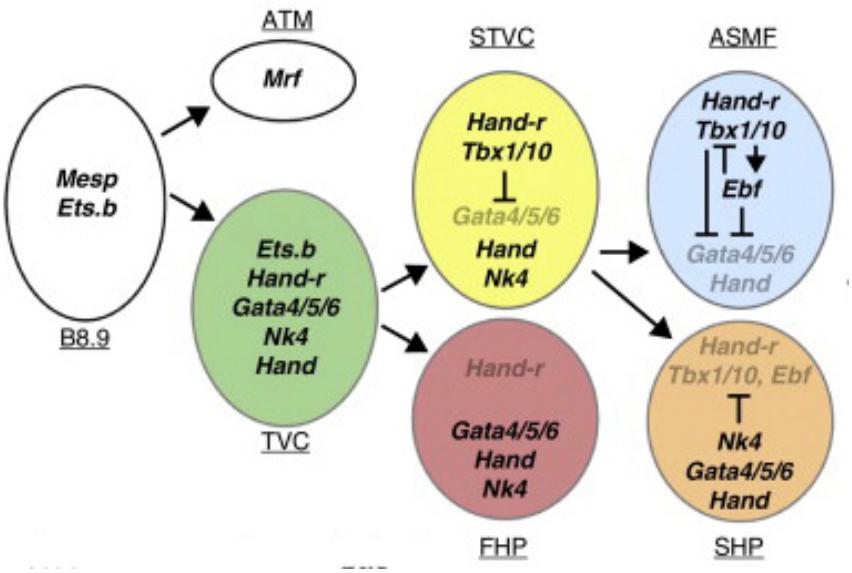

Figure 7: Regulatory cross-antagonism during cardio-pharyngeal progenitor fate specification in *Ciona*

B8.9 blastomere founder cell expresses earliest mesoderm marker *mesp*. Then it is divided in to TVC and ATM. TVC is a multilineage primed progenitor for heart and PM. TVC is then asymmetrically divided in to *NK4* and *Gata4/5/6* expressing FHP. STVC is the common progenitor for SHF and PM. Cross antagonism between transcription factors such as *NK4* and *Tbx1/10* then specifies SHP and ASMF respectively. ATM-anterior tail muscle cell, TVC- trunk ventral cell, FHP-first field precursor, STVC-secondary TVC. ASMF-atrial siphon muscle founder cell, SHP-secondary heart precursor. Adapted from Kaplan et al., [68].

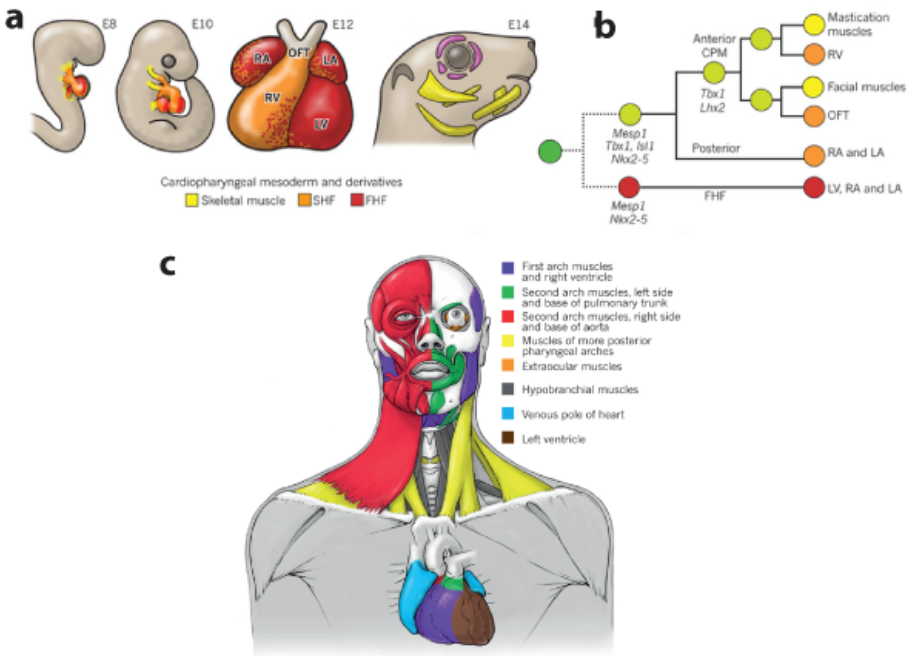

Figure 8: Cardio-pharyngeal derivatives in mammals

a) Schematic showing contribution to FHF (red), SHF (orange) and skeletal muscle (yellow) at different embryonic stages in mice. E14: yellow denotes all branchiomeric muscles (derived from pharyngeal mesoderm). Purple indicates extra ocular muscles (derived from prechordal plate mesoderm). b) Lineage tree describing contribution of single progenitor (dark green) to FHF (red), parts of SHF (orange) and specific subsets of pharyngeal muscle (yellow). c) Heterogeneity of human head and heart. Structures with similar origin are color-coded. Adapted from Rui et al., [67].

Chapter 2

Transgenic retinoic acid sensor lines in zebrafish indicate regions of available embryonic retinoic acid

Amrita Mandal[1,2], Ariel Rydeen[1,2], Jane Anderson[1], Mollie R.J. Sorrell[1], Tomas Zygmunt[3], Jesús Torres-Vázquez[3], Joshua S. Waxman[1]*

1-The Heart Institute, Molecular Cardiovascular Biology Division and Development Biology Division, Cincinnati Children's Hospital Medical Center, Cincinnati, OH, 45229, USA

2-Molecular Developmental Biology Graduate Program, University of Cincinnati and Cincinnati Children's Hospital Medical Center, Cincinnati, OH, 45229, USA

3- Department of Cell Biology, Helen L. and Martin S. Kimmel Center for Biology and Medicine at the Skirball Institute, New York University School of Medicine, New York, NY 10016, USA.

***Correspondence:** Email: joshua.waxman@cchmc.org, phone: 513-636-7232, fax: 513-636-5958

Running title: Zebrafish RA sensor lines

Key words: nuclear horomone receptors, retinoic acid signaling, transgenic zebrafish, Gal4 fusion proteins

Bullet points:

- Transgenic zebrafish lines were made incorporating fusion proteins that act as RA sensors.
- The RA sensor lines report available embryonic RA.
- Hyperactive RA sensor lines indicate RA is available throughout the embryo.
- The transgenic RA sensors complement existing tools and will help elucidate the mechanisms of RA signaling in vivo.

Grant Sponsor: NIH

Grant Numbers: R01 HL092263, R01 HL092263-01A1, R00 HL901126, R01 HL112893-A1

Abstract

Background: Retinoic acid (RA) signaling plays a critical role in vertebrate development. Transcriptional reporters of RA signaling in zebrafish, thus far, have not reflected the broader availability of embryonic RA, necessitating additional tools to enhance our understanding of the spatial and temporal activity of RA signaling *in vivo*. **Results:** We have generated novel transgenic RA sensors in which a RA receptor (RAR) ligand-binding domain (RLBD) is fused to the Gal4 DNA binding domain (GDBD) or a VP16-GDBD (VPBD) construct. Stable transgenic lines expressing these proteins when crossed with UAS reporter lines are responsive to RA. Interestingly, the VPBD RA sensor is significantly more sensitive than the GDBD sensor and demonstrates there may be almost ubiquitous availability of RA within the early embryo. Using confocal microscopy to compare the expression of the GDBD RA sensor to our previously established RA signaling transcriptional reporter line, *Tg(12XRARE:EGFP)*, illustrates these reporters have significant overlap, but that expression from the RA sensor is much broader. We also identify previously unreported domains of expression for the *Tg(12XRARE:EGFP)* line. **Conclusions:** Our novel RA sensor lines will be useful and complementary tools for studying RA signaling during development and anatomical structures independent of RA signaling.

Introduction

The requirement of RA signaling was first studied in the 1940's and 50's using Vitamin A deficient rat embryos [73-75]. Since these initial pioneering studies, inappropriate RA signaling has been found to cause a similar spectrum of developmental defects in all vertebrates, with increases and decreases in RA signaling affecting many organs and tissues, including the hindbrain, forelimbs, and heart [4, 12, 20, 76-86]. RA signaling's earliest known function is in posteriorization of the embryonic axis [8, 87, 88], which is an evolutionarily conserved function in chordates [89]. In vertebrates, later developmental roles of RA signaling include promoting differentiation of the epicardium [90], proliferation of the myocardium [91], outgrowth of the forelimbs [92], and patterning of the cardiac outflow tract [93].

RA is the most active metabolic derivative of Vitamin A (retinol) and is produced through a series of oxidative reactions by alcohol and aldehyde dehydrogenases within specific locations of the embryo [8]. During development, RA acts as a morphogen and is a ligand for members of the nuclear hormone family of receptors - the RA receptors (RARs) [8-10, 26]. RARs function at the transcriptional level as heterodimers with the retinoid X receptors (RXRs), which together bind RA response elements (RAREs). Most often, RAR/RXRs heterodimers bind what are referred to as direct repeat 5 (DR5) sites, defined by a 5 nucleotide spacer between the RAR and RXR binding elements. However, they do have some flexibility and can also bind DR1 and DR2 sites [9].

The knowledge of general RAR binding rules has led to the generation of a number of synthetic reporters that contain concatenated DR5 RARE sites, which have been used both *in vitro* and *in vivo* in transgenic mice as transcriptional reporters of RA signaling [23, 24, 94].

More recently, similar strategies were used to create zebrafish with transgenic RA signaling reporter lines [25]. However, a number of the earlier zebrafish lines, which used the same synthetic promoters as utilized in mice, exhibited significant positional effects due to their insertions, even though they were still responsive to RA. Moreover, these RA signaling reporter lines were not expressed in some of the tissues known to require RA signaling [25]. Despite the transgenic RARE reporter mice having broader expression compared to the transgenic zebrafish [23, 24], it is still not clear as to whether or not they too reflect all RA signaling.

In an attempt to make a more sensitive RA signaling reporter, we recently constructed a new synthetic RA signaling reporter composed of 12 concatenated DR5 RARE elements [Fig. 1C; 11], instead of the 3 used previously in mice and zebrafish [23-25]. Like its predecessors, we also used this construct *in vitro* in cell culture and *in vivo* to make stable transgenic lines in zebrafish. While the *12XRARE* transgenic reporter lines in zebrafish were less sensitive to positional effects and were highly responsive to RA signaling, it is clear that these reporters still do not reflect expression in all tissues with RA signaling [11]. Therefore, we have sought to generate additional *in vivo* tools that will complement our current RA signaling reporter transgenic lines and aid in our understanding of the locations and mechanisms of RA signaling within the embryo.

Previous *in vitro* studies have used Gal4 DNA binding domain (GDBD)/RAR domain fusion proteins to elucidate the functional domains of RARs [94, 95]. More recently, groups have adapted this method, in what is referred to as a ligand trap strategy, for use with many other nuclear hormone receptors in stable transgenic zebrafish to identify the ligands for orphan nuclear hormone receptors [64]. An advantage of the GDBD-RAR fusion is that it should function primarily as a ligand sensor, rather than as a ligand dependent transcriptional reporter of

RXR/RAR interactions. We have used this strategy to make GDBD and VP16-GDBD (VPBD) fusion proteins with the ligand binding domain of the zebrafish RARab (RLBD) [Fig. 1A, B; 96, 97]. We have characterized these transgenic lines and find that both fusion proteins are responsive to RA, although the VPBD-RLBD fusion is significantly more sensitive and more accurately reflects the locale of RA based on the expression domains of the RA producing and degrading enzymes. We also compare the expression of a *GDBD-RLBD;UAS:mCherry* transgenic reporter line to one of our previously reported *Tg(12XRARE-ef1a:EGFP)* lines using confocal microscopy. We conclude that these novel RA sensor lines will complement existing tools and aid in the *in vivo* analysis of RA and RA signaling during development and other contexts.

Results

GDBD-RLBD;UAS transgenes produce a RA sensor

In order for the GDBD-RLBD fusion protein lines to report RA, they need to be crossed with UAS reporter lines (Fig. 1B). To examine the efficacy of the *Tg(β-actin:GDBD-RLBD)* trangene, we crossed stable transgenic carriers to two distinct UAS reporter lines: a *Tg(5XUAS:EGFP)* [98], which we refer to as *UAS:EGFP*, and a *Tg(14XUAS-E1b:NfsB-mCherry)* [99], which we refer to as *UAS:mCherry*. Reporter expression in either the *Tg(β-actin:GDBD-RLBD);(UAS:EGFP)* or *Tg(β-actin:GDBD-RLBD);(UAS:mCherry)* embryos was detectable using *in situ* hybridization (ISH) by the tailbud stage (TB) stage (Fig. 2A, B, K, L). UAS reporter expression initially appeared to be predominantly expressed in the spinal cord (Fig. 2A-D, K-N). However, by the 16s stage, expression was observed in a bit broader domain, discernibly expanding to the somites and notochord, and later to the pronephros (Fig. 2E-J, O-T). The region of expression within the embryos was largely similar between the two lines, except that in the *Tg(β-actin:GDBD-RLBD);(UAS:EGFP)* embryos there was stronger and persistent expression in the anterior somites and expression in the ventral eye (Fig. 2I, J, S, T). Importantly, reporter expression from both lines was restricted to a mid-region of the embryos where we and others have previously established there is high RA signaling during these stages of development [11, 26, 100, 101].

The fluorescent expression from both transgenic lines was delayed relative to the ISH expression. In the *Tg(β-actin:GDBD-RLBD);(UAS:EGFP)* transgenic embryos, expression was visible by the 16s stage (Fig. 3A), while expression from the *Tg(β-actin:GDBD-RLBD);(UAS:mCherry)* transgenic embryos was not typically visible until shortly after the 16s

stage (Fig. 3E). Bright fluorescence was observed in a central portion of the embryo by 24 hours post-fertilization (hpf) with both UAS lines, which was maintained past 48 hpf (Fig. 3B-D, F-H). Although the domains of expression from these reporters was largely similar, the *Tg(β-actin:GDBD-RLBD);(UAS:mCherry)* line was significantly more variegated, which is likely due to silencing caused by the additional repetitive elements used with that UAS construct [99, 102]. The other major difference we observed in fluorescent reporter expression, other than the variegation due to silencing, was that the *Tg(β-actin:GDBD-RLBD);(UAS:EGFP)* line had expression in the eyes and stronger expression in the somites (Fig. 3D), as mentioned with the ISH. We think that the expression in the eye is reflecting availability of RA because our previously created transcriptional RA reporter also has expression in the eye after 24 hpf [11]. We postulate that the difference we observe between the UAS reporters could either be due to positional effects of the transgene or the shorter UAS repeats [102].

The expression of the *β-actin:GDBD-RLBD;UAS* lines in the mid-region of the embryo was strongly suggestive that reporters are RA responsive. To confirm that the reporters are RA responsive, we modulated RA signaling using RAR agonists, RAR antagonists, and an aldehyde dehydrogenase inhibitor. Consistent with the GDBD-RLBD being responsive to RA, treatment with RA or the RARα agonist AM580 both produced essentially ubiquitous expression in the *Tg(β-actin:GDBD-RLBD);(UAS:EGFP)* and *Tg(β-actin:GDBD-RLBD);(UAS:mCherry)* embryos (Fig. 4A-C, A'-C', H-J, H'-J'). Similarly, the pan-Cyp inhibitor Ketoconazole (Keto), which inhibits the function of the RA degrading Cyp26 (P450) enzymes, or the use of morpholinos (MOs) for *cyp26a1* and *cyp26c1* produced an expansion of the domain of reporter expression (Fig. 4D, D', K, K' and Fig. 5A-D). Conversely, the retinaldehyde dehydrogenase inhibitor diethyl-aminobenzoic acid (DEAB), which inhibits RA production [103], and the

competitive RARα antagonist RO41-5253 (referred to as RO41) [104], which should interact with the RLBD, both inhibited expression of the reporter. Altogether, our analysis suggests that our new transgenic lines are functioning as sensors of embryonic RA.

A hypersensitive transgenic RA sensor

Although the *GDBD-RLBD:UAS* reporters are sensitive to RA and expressed in regions of the embryo where there is RA signaling, we found it interesting that the reporter expression did not initiate until the TB, likely after RA signaling initiates based on *aldh1a2* expression [85], and were expressed in a relatively restricted domain within the embryos, similar to RA responsive genes and the *Tg(12XRARE-ef1a:EGFP)* lines, here referred to as *Tg(12XRARE:EGFP)* [11, 100, 105]. Therefore, we wanted to explore ways of increasing the sensitivity of the RA sensor. Our previous study found that fusion of the VP16 transcriptional activation domain to either the N- or C-termini of RARs creates a hyperactive RAR, not a constitutively active RAR [11]. Therefore, we wanted to determine if a similar fusion would make a hypersensitive RA sensor. We fused the VP16 domain to the N-terminus of the GDBD-RLBD protein (VPBD-RLBD), made stable transgenic lines, and crossed them to the UAS reporter lines.

We found that in *Tg(β-actin:VPBD-RLBD);(UAS:EGFP)* embryos expression was pretty broad by the TB stage (Fig. 6A, B) and maintained through the 8s stage when fluorescence was easily oberserved (Fig. 6C-E). In contrast to the more limited expression of the *β-actin:GDBD-RLBD;UAS* transgenic lines, the broad expression of the VP16-RA sensor was reminiscent of the broad, posterior expression of *aldh1a2* at the same stages within the early embryo [85, 106].

Furthermore, given the role of RA signaling in patterning the hindbrain, the sharp anterior border of reporter expression at the TB stage was reminiscent of the expression patterns of RA responsive genes in the hindbrain, including *hoxb1b*, *vhnf1*, and *hoxb1a* [106, 107]. Interestingly, we also found expression in the very anterior of the embryo and the polster (Fig. 6A, C, E), suggesting there may be available RA in the anterior of the embryo in addition to more posteriorly. A candidate source of this expression is Aldh1a3, which is expressed in the anterior of the embryo [108, 109]. However, its stronger anterior expression does not initiate until mid-somitogenesis [108, 109], suggesting that Aldh1a2 cannot also be ruled out as a potential source. Importantly, at these stages, *Tg(β-actin:VPBD-RLBD);(UAS:EGFP)* reporter expression was largely lacking in a large anterior region of the embryo (Fig. 6A-E), which correlates with the early anterior expression domain of *cyp26a1* [26, 83]. By the 16s stage, *Tg(β-actin:VPBD-RLBD);(UAS:EGFP)* expression was still absent in the majority of the anterior brain and anterior hindbrain (Fig. 6F-H). However, expression expanded to the eyes, where *aldh1a3* is expressed [108, 109], and was in the hatching gland, the derivative of the polster. At the 8s and 16s stages, lower levels of expression were found in the posterior hindbrain and extended anteriorly up to the level of the otic vesicle, which forms at rhombomeres 5 and 6 (Figs. 6C, E, F, H). By the 16s stage, strong expression was in the posterior spinal cord and extended to the most posterior somites, but was absent in the tip of the tail (Fig. 6F, I, L). The presence and absence of reporter expression again parallels the opposing domains of *aldh1a2* expression and *cyp26a1* in the trunk and tail [83, 85]. Expression was maintained in the anterior brain and eyes, and the somites and spinal cord of the embryos past 48 hpf (Fig. 6I-N). Similar domains of expression were also observed in the *Tg(β-actin:VPBD-RLBD);(UAS:mCherry)*

embryos. However, expression was significantly variegated in these lines, so it is not presented here.

To determine if the *Tg(β-actin:VPBD-RLBD);(UAS:EGFP)* embryos were sensitive to modulation of RA, we used the same pharmacological agents that were used to analyze the *β-actin:GDBD-RLBD;UAS* transgenic lines. Treatment with RA or AM580 produces relatively ubiquitous expression (Fig. 7A-C, G-I), while Keto expanded and enhanced the domains of expression (Fig. 7D, J). Interestingly, treatment with DEAB or RO41 were both able to reduce expression, but never able to completely eliminate expression (Fig. 7K, L). Of these two inhibitors, it is interesting that RO41, the competitive RARα antagonist, was typically much more effective at reducing expression (Fig. 7F, L). DEAB treatment could reduce expression as indicated by ISH (Fig. 7K). However, we often could not detect significantly lower expression via fluorescence in live embryos (Fig. 7L). Therefore, our characterization of the *Tg(β-actin:VPBD-RLBD);(UAS:EGFP)* transgenic line suggests that the VPBD-RLBD fusion protein creates a more sensitive RA sensor than the GDBD-RLBD and that the reporter's expression and absence of expression correlate better with the expression of RA producing and degrading enzymes, respectively, than the more restricted *β-actin:VPBD-RLBD;UAS* or the *12XRARE* reporters [11].

Comparison of the transgenic GDBD-RLBD RA sensor and RARE reporter lines

The more restricted expression of the *β-actin:GDBD-RLBD;UAS* RA sensor reporters was conspicuously similar to the *12XRARE:EGFP* transgenic reporter lines [11]. Both are expressed predominantly in the mid-region of the embryo where we postulate that there is higher

sustained RA signaling (Figs. 2 and 3) [11, 105]. Therefore, we wanted to directly compare the temporal and spatial expression from the different reporters. Hemizygous *Tg(β-actin:GDBD-RLBD);(UAS:mCherry)* adults were crossed with homozygous *Tg(12XRARE:EGFP)* adults and the triple transgenic embryos were imaged using confocal microscopy at stages from 20s through 78 hpf. As suggested from our ISH and live fluorescent analysis of the current and previously published reporters [11], the fluorescent expression from the *β-actin:GDBD-RLBD;UAS:mCherry* transgenes was initiated earlier than the *12XRARE:EGFP* transgene (Fig. 8A-C). By the 20s stage, *β-actin:GDBD-RLBD;UAS:mCherry* reporter expression was easily visible in skin epithelial cells, the spinal cord, a few pronephros cells and notochord (Fig. 8A, C). By comparison, EGFP was more weakly expressed and just initiating in a couple pronephros cells and the spinal cord of the *Tg(12XRARE:EGFP)* embryos (Fig. 8B). By 24hpf , the *β-actin:GDBD-RLBD;UAS:mCherry* reporter expression had expanded in the skin epithelial cells, the spinal cord, the pronephros and notochord (Fig. 8D, F). By comparison, the *12XRARE:*EGFP reporter was still more weakly expressed, but more visible in the pronephros of embryos (Fig. 8E). By 30 hpf, the expression of both reporters was stronger and significantly expanded (Fig. 8G-I). Expression of the *β-actin:GDBD-RLBD;UAS:mCherry* reporter was still expressed in the skin epithelial cells, the spinal cord, pronephros and notochord (Fig. 8G, I), but now axons projecting anteriorly from the spinal cord were also visible (Fig. 8G, I, insets). At 30 hpf, in the *Tg(12XRARE:EGFP)* embryos the spinal cord expression was significantly stronger and expanded in the A-P axis in the spinal cord and pronephros (Fig. 8G, I). Additionally, there were also extremely low levels of expression in the somites and notochord, which we have not reported previously (Fig. 8H). Despite the overlap in most tissues, we never observed expression in the skin epithelial cells in the *Tg(12XRARE:EGFP)* embryos. By 30 hpf, we also observed

expression in the dorsal eye (Fig. 9A), which we had not reported previously and correlates with the localization *aldh1a2* expression [108-110]. Expression in the ventral domain of the eye was reported previously and correlates with *aldh1a3* expression [Fig. 9A; 108, 109, 110]. As mentioned above, we did not find eye expression using the *UAS:mCherry* line, but did observe it in the *UAS:EGFP* embryos (Figs. 2I and 3D).

Through 72 hpf, the expression of both reporters became sharply defined at the hindbrain-spinal cord boundary (Fig. 8J-O), compared to earlier when the boundary between these neural regions was not quite as distinct (Fig. 8G-I). Expression was maintained at these later stages in all the same tissues as at 30 hpf for both reporters (Fig. 8J-O; Fig. 9B). Interestingly, both these reporters labeled the ventral motor neurons (Fig. 8J-O), which we did not report previously for the *Tg(12XRARE:EGFP)* lines using standard fluorescent microscopy [11]. The extension and expansion of the ventral motor neurons projecting from the spinal cord was easily observable through these stages and individual axons could be followed due to the variegated nature of expression from the *UAS:mCherry* transgene. Furthermore, by 78 hpf, the pectoral fin motor neuron projections could be seen terminating at the base of the fins [Fig. 9A, B; 111], while there was additional expression of individual neurons seen medial to the retina in the brain (Fig. 9D).

Discussion

Our characterization of the *β-actin:GDBD-RLBD;UAS* transgenic reporters suggests that they are responsive to and report the availability of embryonic RA. Interestingly, the regionalized expression from the *GDBD-RLBD;UAS* reporter lines in the mid-region of the embryo posterior to the hindbrain overlaps considerably with our previously reported *12XRARE:EGFP* transgenic line [11]. The expression of the RA sensor reporter initiates earlier and is expressed more broadly than the *12XRARE:EGFP* reporter line, as one might predict because it should report the availability of RA and precede target gene transcription, while the RARE reporter is dependent upon RA plus RAR/RXR interactions. The broader expression of the RA sensor reporter also reinforces the notion that there are tissues that are likely responsive to RA, but are not strongly represented by expression in the *12XRARE:EGFP* transgenic line [11]. Since it is likely that the RLBD interacts with transcriptional activators and repressors [9, 10], even though theoretically it should not be dependent on RXR [64], we cannot rule out that the transcriptional regulatory proteins that interact with the GDBD-RLBD fusion protein through the RLBD influence the temporal and spatial expression of the reporter [9]. Importantly, the regionalized expression of the RA sensor and RARE transgenic lines does correlate with the expression of RA target genes and sensitive tissues during early and mid-somitogenesis stages [85, 100, 105-107, 112]. However, when compared to the *β-actin:VPBD-RLBD;UAS* reporter our characterization also suggests that they both may be reporting higher levels of sustained RA.

When comparing the expression of the *β-actin:GDBD-RLBD;UAS* and *12XRARE:EGFP* reporters to the *β-actin:VPBD-RLBD;UAS* reporter, it is clear that the *β-actin:VPBD-RLBD;UAS* reporter is expressed much more broadly throughout the transgenic embryos and strongly

correlates with *aldh1a2, aldh1a3* and *cyp26a1* expression [83, 85, 106, 108, 110]. Because we cannot eliminate reporter expression in *β-actin:VPBD-RLBD;UAS* transgenic embryos this suggests a couple possibilities, which are not mutually exclusive: there is some transcriptional activation of the UAS reporter from the VPBD domain that is independent of RA or that there are low levels of RA that can still be detected by the VPDB-RLBD fusion protein that we cannot eliminate. Although we have not yet distinguished between these possibilities, an argument in favor of the latter possibility is that if there were RA-independent reporter expression, we would not expect to the have localized reporter expression that strongly correlates with RA producing and degrading enzymes. Moreover, previous studies have also demonstrated that there is still RA responsive gene expression in zebrafish embryos even with high concentrations (5μM) of DEAB treatment [106], which confirms that DEAB treatments likely do not completely eliminate embryonic RA or RA signaling. Therefore, assuming that the *β-actin:VPBD-RLBD;UAS* transgenic reporter is reporting available embryonic RA, our analysis suggests the thought-provoking hypothesis that RA may be available almost entirely throughout the embryo, including the most anterior tissues of the embryos, which has not been previously suggested to receive embryonic RA at earlier stages.

While we propose that VPBD-RLBD; UAS transgenic lines will also be useful, informative and complementary tools, the enhanced sensitivity to RA at this point may actually limit its general utility because we have found that it does not demonstrate significant fluctuations in reporter expression when RA signaling is modulated. Nevertheless, this analysis promotes the idea that in the future similar strategies using alternative transcriptional activation domains combined with the GDBD-RLBD fusion protein may be able to create highly sensitive

reporters that accurately report the availability of low concentrations of RA while eliminating the possibility of ligand-independent transcriptional activation.

In addition to being indicators of RA sensitivity and availability, our confocal analysis of the RA sensor and *12XRARE:EGFP* transgenic lines suggests that these transgenes will likely be useful tools for studying the development of RA independent processes. In particular, we envision that these lines will be useful for studying the development of specific populations of neurons in the brain and spinal cord, due the expression of the fluorescent proteins in the axons, as well as the nephrons, where expression persists as long as we have tracked expression in the embryos. Together, our current and previous studies using transgenic zebrafish with the Gal4 fusion method set the precedence for the creation of similar lines for studying RA signaling and the function of other nuclear hormone receptors in other model organisms. Overall, the novel RA sensors complement the utility of the existing *12XRARE:EGFP* transgenic lines and enhance the available toolset to study the mechanisms of RA signaling dependent developmental processes *in vivo*.

Experimental Procedures

Zebrafish maintenance and lines used

Adult zebrafish were maintained and embryos were raised using standard zebrafish aquaculture conditions. UAS transgenic lines used in crosses were *Tg(5XUAS:EGFP)* [98] and *Tg(14XUAS:NfsB-mCherry)* [99]. For the stable *β-actin:GDBD-RLBD* and *β-actin:VPBD-RLBD* transgenic lines, multiple transgenic lines were recovered from individual founders designated *Tg(β-actin:GDBD-RLBD)*^{cch1}, *Tg(β-actin:GDBD-RLBD)*^{cch4}, *Tg(β-actin:VPBD-RLBD)*^{cch2}, *Tg(β-actin:VPBD-RLBD)*^{cch5}, and *Tg(β-actin:VPBD-RLBD)*^{cch6}. Each transgene in the stable lines segregated according to a standard Mendalian ratio, suggesting the integrations were at single loci. Expression from each of the Tg(*β-actin:GDBD-RLBD)* and Tg(*β-actin:VPBD-RLBD)*, respectively, was overtly found to be indistinguishable. Therefore, the lines *Tg(β-actin:GDBD-RLBD)*^{cch1} and *Tg(β-actin:VPBD-RLBD)*^{cch2} are presented in the current study, but all lines are available. For experiments, hemizygous *Tg(β-actin:GDBD-RLBD)* carriers were crossed with hemizygous *Tg(UAS:EGFP)* carriers and *Tg(β-actin:GDBD-RLBD);(UAS:mCherry)*, which were hemizygous for each transgene, were crossed to hemizygous *Tg(UAS:mCherry)* carriers. The *Tg(12XRARE-ef1a:EGFP)*^{sk72} was reported previously [11].

Construction of the transgenes and fusion proteins

For constructing the Tol2 Gateway destination vector with the *α-crystallin:DsRED* (*α-cry:DsRED),* PCR amplification was used to add ClaI restriction sites to the 5' and 3' ends of the

previously reported *α-cry:DsRED* plasmid [113]. This fragment and the vector pDestTol2p2A were then digested with ClaI and the fragment was ligated into the pDestTol2p2A using standard cloning methods. The *GDBD-RLBD* and *VPBD-RLBD* constructs were then cloned upstream of the *β-actin* promoter using the Tol2/Gateway system [114] and transgenic animals were made using standard Tol2 methods [115].

The GDBD-RLBD was made using PCR to fuse the amino acids 156-457 of zebrafish RARαb, which comprise the D-F domains, to amino acids 1-147 of the Gal4 protein, which contains the DNA binding domain. Amino acids 413-490 of VP16 were fused to the N-terminus of the GDBD-RLBD to make the VPBD-RLBD construct. For this fusion, the start methione was deleted from the GDBD and added to the VP16 domain. Both constructs were initially cloned into pCS2p+ as an intermediate vector prior to cloning into the pDestTol2p2A-αcry:Dsred destination vector along with the *β-actin* promoter for making transgenic animals.

Drug treatments and morpholinos used

Embryos were treated with 1μM RA (Sigma), 0.5μM AM580 (Biomol), 25μM Keto (Sigma), 1μM DEAB (Sigma), and 0.75μM RO41 (Biomol) beginning at the shield stage. 0.003% w/v 1-phenyl 2-thiourea (PTU; Sigma) was used beginning prior to 24 hpf to prevent pigmentation.

Sequences for *cyp26a1* MOs used were:

MO1 5'-TCTTATCATCCTTACCTTTTTCTTG

MO2 5’-TAAAAATAATACACTACCTGCAAAC.

Sequence for the *cyp26c1* MO was reported previously [112]. A mixture of 2 ng *cyp26a1* MO1 and 1 ng *cyp26a1* MO2 and 6 ng *cyp26c1* MO were injected into one cell *Tg(β-actin:GDBD-RLBD);(UAS:EGFP)* embryos. Deficiency of both Cyp26a1 and Cyp26c1 has been shown previously to more effectively cause increases in embryonic RA [112]. 1 ng of p53 MO was used to prevent not-specific p53 mediated cell death [116].

Imaging

Images were taken using a Zeiss M2BIO fluorescent stereomicroscope and Axiocam2 camera. Confocal images were taken using a Nikon_A1 inverted confocal microscope. Images were prepared using Adobe Photoshop.

ISH

ISH was performed essentially as reported previously [117].

Acknowledgements

We thank Steve Farber for informative discussions. TZ and JTZ were supported by NIH grants R01 HL092263 and R01 HL092263-01A1. AM, AR, JA, MRJS, and JSW were supported by NIH grants R00 HL901126 and R01 HL112893-A1 and a CCHMC Trustee Award.

Figure Legends

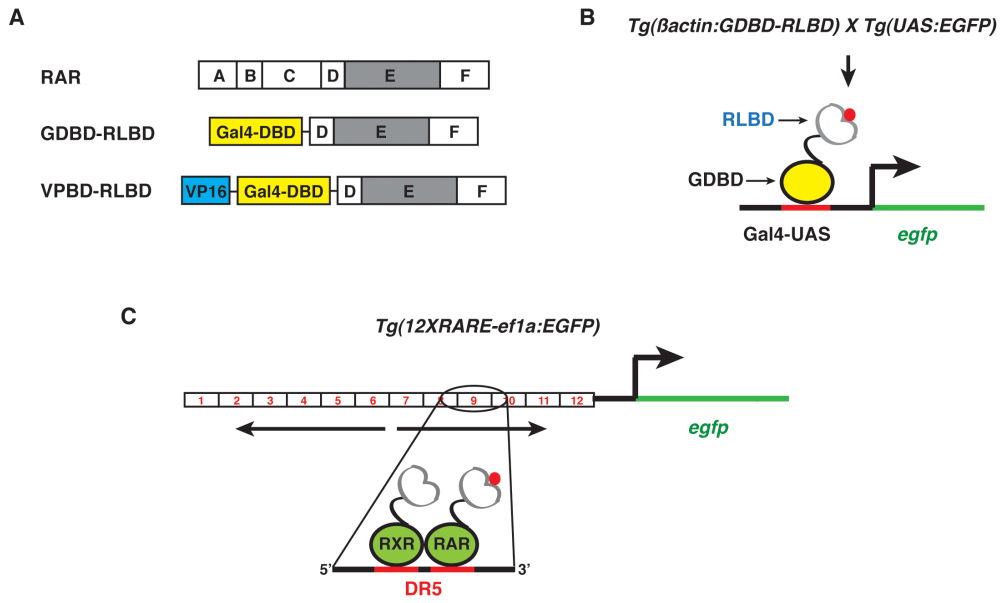

Figure 1. Constructs used and schematics of RA reporters. **(A)** Conserved domains found in RARs [9]. The A domain has some limited transcriptional activation ability. The B domain has an unknown function. The C domain is the DNA binding domain. The D domain is a hinge domain. The E domain is the ligand-binding domain and contains the major transcriptional activation domain. The F domain has an unknown function. The Gal4-DNA binding domain (GDBD; yellow) was fused to the D-F domains, which contain the RAR ligand-binding domain, to make the GDBD-RLBD fusion protein. The VP16 activation domain (blue) was fused to the N-terminus of the GDBD-RLBD to make the VPBD-RLBD fusion protein. **(B)** Schematic of how the RLBD fusion proteins work. The GDBD-RLBD fusion protein should bind the UAS elements and activate transcription in the presence of RA (red dot). **(C)** Schematic of the previously reported 12XRARE transgene for comparison to the ligand trap method. RA (red dot) interacts with RARs, which drive transcriptional activation through RAR/RXR heterodimers acting on DR5 RAREs.

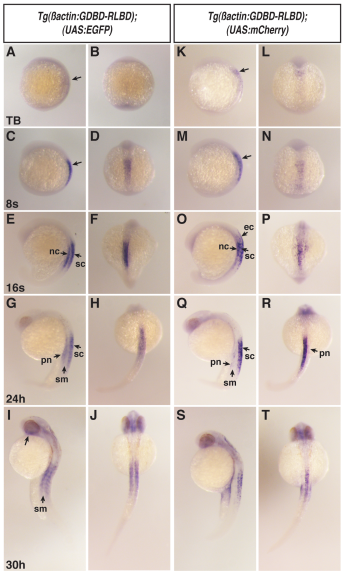

Figure 2. RA sensor reporters are expressed in established domains of RA responsive gene expression. **(A, B, K, L)** Reporter expression in both the *Tg(β-actin:GDBD-RLBD);(UAS:EGFP)* and *Tg(β-actin:GDBD-RLBD);(UAS:mCherry)* lines initiates in the spinal cord (arrows in A and K) by the tailbud (TB) stage. **(C, D, M, N)** RA sensor reporter expression is strengthened in the anterior spinal chord by the 8 somite (s) stage (arrows in C and M). **(E, F, O, P)** RA sensor reporter expression is maintained in the anterior spinal cord (sc) and noticeable expanded to the adjacent tissues, including the notochord (nc) and ectoderm (ec), by the 16s stage. **(G, H, Q, R)** RA sensor reporter expression was maintained in the tissues of the mid-region (anterior trunk and spinal cord), but was now more easily observed in the somites (sm) and pronephros (pn). **(I, J, S, T)** Both the *Tg(β-actin:GDBD-RLBD);(UAS:EGFP)* and *Tg(β-actin:GDBD-RLBD);(UAS:mCherry)* lines initiate some expression in the brain by 36 hpf. However, we only found eye expression (arrow in I) in the *Tg(β-actin:GDBD-RLBD);(UAS:EGFP)* line. Views in A, C, E, G, I, K, M, O, Q, S are lateral. Views in B, D, F, H, J, L, N, P, R, T are dorsal. In all images anterior is up.

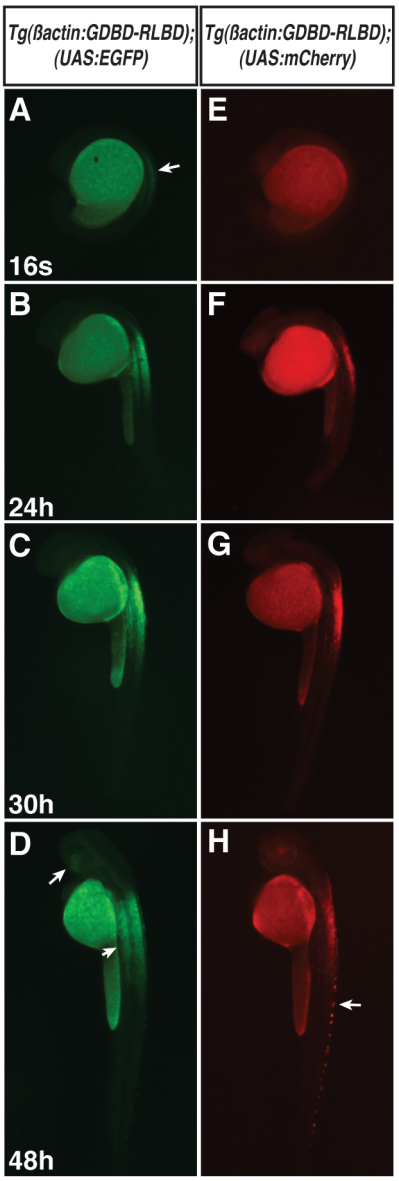

Figure 3. Fluorescence in the *Tg(β-actin:GDBD-RLBD);(UAS:EGFP)* and *Tg(β-actin:GDBD-RLBD);(UAS:mCherry)* lines. **(A, E)** Fluorescence in the *Tg(β-actin:GDBD-RLBD);(UAS:EGFP)* line is found in the spinal cord (arrow) by the 16s stage, although expression in the *Tg(β-actin:GDBD-RLBD);(UAS:mCherry)* is typically not visible by this stage. **(B, F)** Expression at 24 hpf is visible in the spinal cord, notochord and somites. Expression is the adjacent non-spinal cord tissues is more easily visible in the *Tg(β-actin:GDBD-RLBD);(UAS:EGFP)* embryos. **(C, D, G, H)** Expression is maintained in the spinal cord, notochord, and somites at 30 and 48 hpf. Expression is seen in the ventral eye by 48 hpf (arrow in D). Arrowhead in D indicates the somites. Expression in the eye of the *Tg(β-actin:GDBD-RLBD);(UAS:mCherry)* embryo is from the *α-cry:DsRed* used in the transgenic construct. Arrow in H indicates autofluorescent pigment cells. All views are lateral with anterior up.

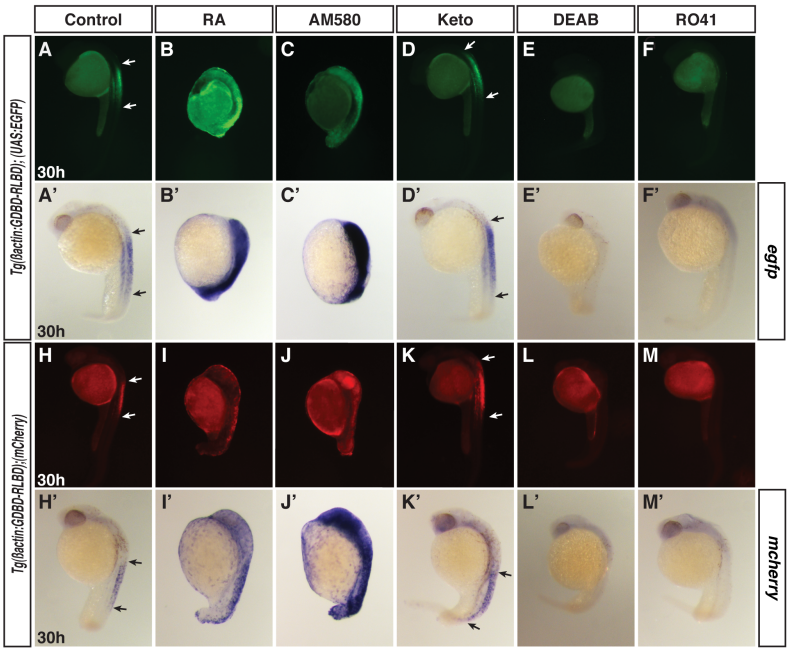

Figure 4. RA sensor lines are responsive to RAR agonists and antagonists. **(A, A', H, H')** Control untreated embryos. **(B, B', C, C', I, I', J, J')** RA or AM580 treated embryos show almost ubiquitous expression of the reporter. Embryos treated with RA or AM580 were posteriorized as a consequence of treatment with these agents. **(D, D', K, K')** Keto caused an expansion of reporter expression. **(E, E', F, F', L, L', M, M')** DEAB or RO41 treatment inhibited expression. None of the DEAB treated (0 of 17) or R041 treated (0 of 17) *Tg(β-actin:GDBD-RLBD);(UAS:EGFP)* embryos had expression compared to 28% (17 of 61) sibling embryos, which is close to the 25% of expected fluorescent embryos used from an intercross of *Tg(β-actin:GDBD-RLBD)* and *Tg(UAS:EGFP)* hemizygous individuals. None of DEAB treated (0 of 15) or R041 treated (0 of 14) *Tg(β-actin:GDBD-RLBD);(UAS:mCherry)* embryos had expression compared to 34% (18 of 53) sibling embryos, which is close to the 37.5% of expected fluorescent embryos used from an intercross of *Tg(β-actin:GDBD-RLBD);(UAS:mCherry)* hemizygous and *(UAS:mCherry)* hemizygous individuals. A-F and H-M are fluorescent images of live embryos. A'-F' and H'-M' are ISH. Arrows in A,A',D,D',H,H',K,K' indicate the length of the domain of reporter expression. All views are lateral with anterior up.

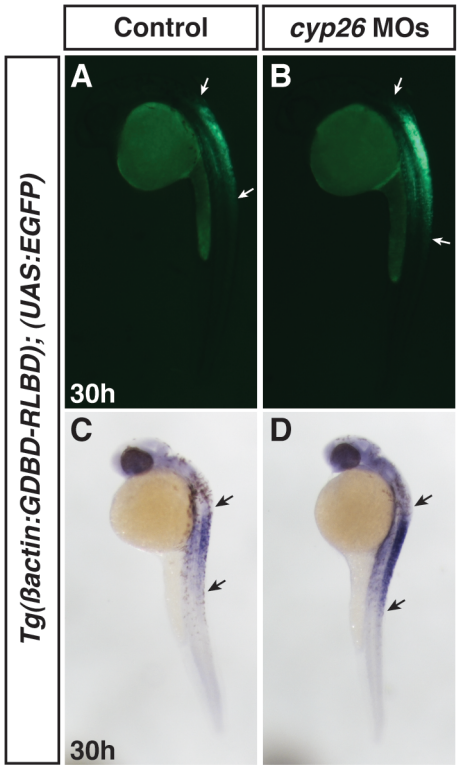

Figure 5. RA sensor expression is expanded in Cyp26 deficient embryos. **(A, C)** Control uninjected sibling embryos. **(B, D)** The domain of reporter expression is expanded in embryos injected with MOs targeting *cyp26a1* and *cyp26c1*. Arrows indicate the length of expression. Views are lateral with anterior up.

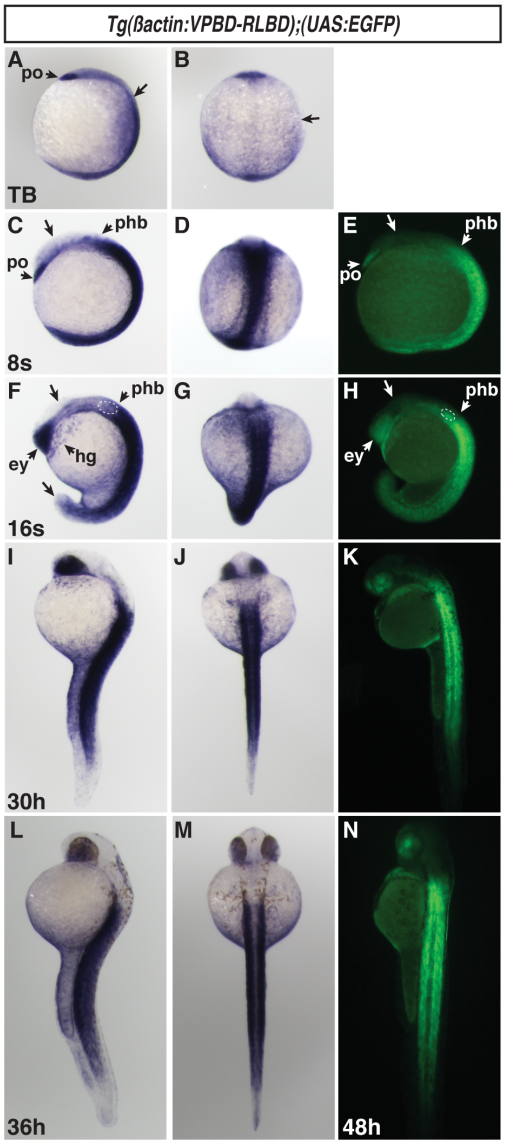

Figure 6. Expression in *Tg(β-actin:VPBD-RLBD);(UAS:EGFP)* embryos is consistent with the domains of RA producing and degrading enzymes. **(A, B)** VP16-RA sensor expression at the TB stage. Arrowhead indicates strong expression in the polster (po). Arrows in A and B indicate the boarder between the posterior reporter expression and the anterior of the embryo, which lacks reporter expression. **(C-E)** VP16-RA sensor expression via ISH and fluorescence at the 8s stage. Expression is maintained in the polster (po) and is largely absent in the anterior brain (arrows in C and E). There is strong expression throughout the posterior. Lower levels of expression extend into the posterior hindbrain (phb). **(F-H)** VP16-RA sensor expression via ISH and fluorescence at the 16s stage. There is expression in the eyes (ey) and anterior brain, hatching gland (hg), and posterior hindbrain. Expression extends into the posterior hindbrain up to the otic vesicle (dashed outlines in F and H), which forms at the rhombomeres 5 and 6. Expression is absent in the brain and tip of the tail (arrows in F and H). **(I-K)** RA reporter expression via ISH and fluorescence at 30 hpf. **(L, M)** VP16-RA sensor expression via ISH at 36 hpf. **(N)** VP16-RA sensor expression via fluorescence at 48 hpf. A, D, F, G, I, J, L, M, O are lateral views. B, E, H, K, N are dorsal views. In all images anterior is up.

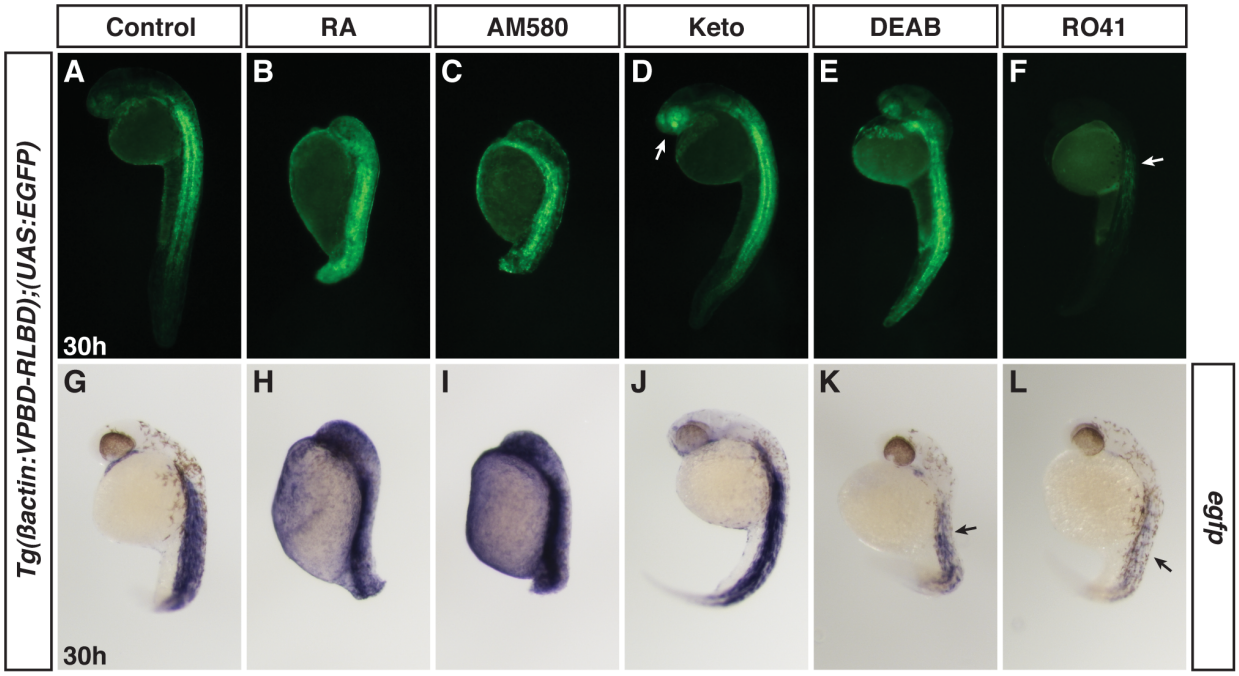

Figure 7. *Tg(β-actin:VPBD-RLBD);(UAS:EGFP)* embryos are sensitive to RAR agonists and antagonists. **(A, G)** Control sibling embryos at 30 hpf. **(B, C, H, I)** RA and AM580 treated VP16-RA sensor embryos have almost ubiquitous expression. Embryos are posteriorized due to RAR agonist treatment. **(D, J)** VP16-RA sensor embryos treated with Keto have expanded and enhanced expression, particularly in the anterior brain and eye. **(E, F, K, L)** VP16-RA sensor embryos treated with DEAB or RO41. By ISH, DEAB and RO41 reduced expression (arrows in K and L). However, RO41 was more effective. By fluorescence, it was often hard to distinguish a loss in reporter expression in DEAB treated embryos. While we observed reductions in reporter expression, particularly with RO41 treatment, we never completely lost expression in embryos treated with RAR or Aldh1a antagonists. All views are lateral with anterior up.

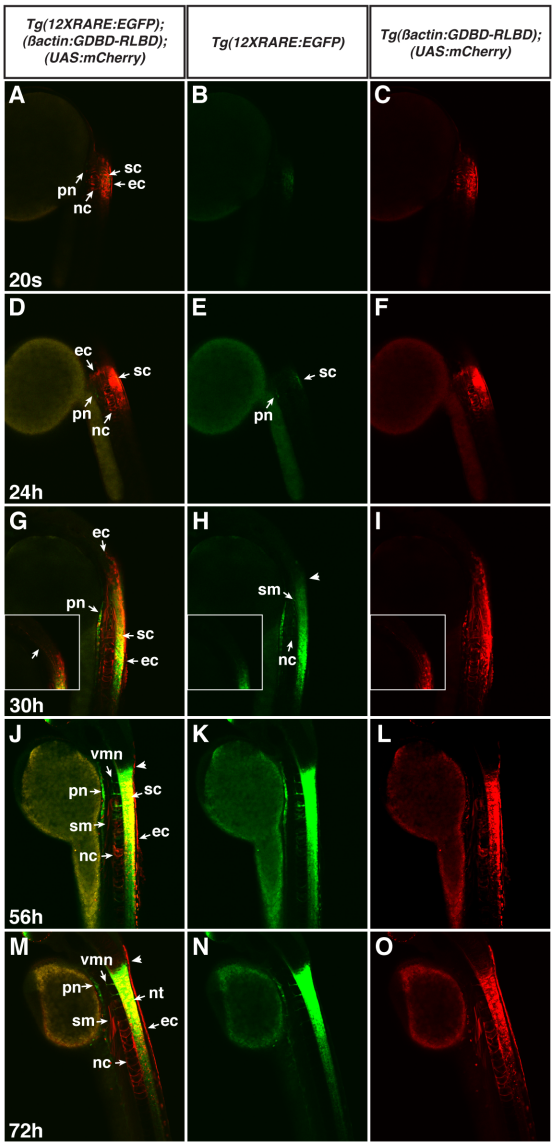

Figure 8. Direct comparison of the *12XRARE:EGFP* and *β-actin:GDBD-RLBD;UAS:mCherry* transgenes. **(A-F)** At the 20s stage and 24 hpf, the RA sensor is expressed in the skin epithelial cells (ec), the spinal cord (sc), the pronephros (pn) and the notochord (nc), while the *12XRARE:EGFP* transgene is less strongly visible in the spinal cord and pronephros. **(G-I)** By 30 hpf, mCherry expression from the *β-actin:GDBD-RLBD;UAS:mCherry* reporter has expanded in the anterior-posterior axis, but the tissue types expressing the reporter have not changed. MCherry can be seen in axons projecting anteriorly from the spinal cord (arrow in inset of G and I). *12XRARE:EGFP* reporter expression has also expanded in the A-P axis and the intensity of the reporter has increased. Low levels of expression are also in the somites (sm), though this is more obvious from mCherry. **(J-L)** By 56 hpf, expression of both reporters has expanded more posteriorly, while the anterior border of expression at the hindbrain-spinal cord boundary has become more distinct. Expression is also seen in the axonal projects from the ventral motor neurons (vmns). **(M-O)** Expression in these same tissues is maintained past 72 hpf. The ventral motor neurons can be seen elaborating further. All images are single confocal slices. Embryos are lateral views with anterior up.

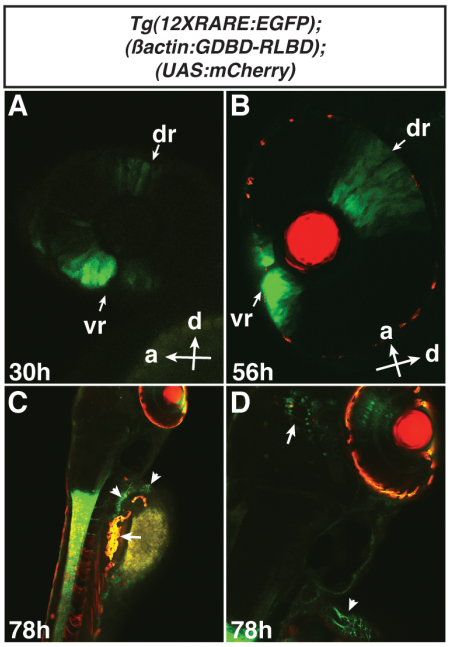

Figure 9. The *12XRARE:EGFP* transgene is expressed in the eye, pectoral fin motor neurons and brain. **(A)** The *12XRARE:EGFP* reporter is expressed in the dorsal retina (dr), by 30 hpf. The dorsal retina expression was visible due to PTU treatment. Expression in the ventral retina (vr) was reported previously [11]. **(B)** Expression of the *12XRARE:EGFP* reporter is maintained and expanded in the dorsal retina and ventral retina by 56 hpf. **(C, D)** At 78h, EGFP expression from the *12XRARE:EGFP* reporter is visible in the pectoral motor neuron axons and their termini at the base of the pectoral fin (arrowheads in C and D). Both transgenes are expressed in neurons in the brain (arrow in D). The red lenses in B-D are due *to α-cry:DsRed* expression, which was used in the Tol2 construct. The *β-actin:GDBD-RLBD;UAS:mCherry* reporter was not expressed in the eye. Red at the periphery of the eyes in B-D is due to auto-fluorescence from residual pigment cells. Auto-fluorescent cells are also found in the trunk at later stages, despite PTU treatment (arrow in C). Views in C and D are dorso-lateral. Magnification of images in A, B, and D is 200X. Magnification of images in C is 100X.

Chapter 3

Retinoic acid negatively regulates *dact3b* expression in the hindbrain of zebrafish embryos

Amrita Mandal[1,2] and Joshua Waxman[1]*

1 – Heart Institute, Molecular Cardiovascular Biology Division, Cincinnati Children's Hospital Medical Center, Cincinnati OH, USA

2 – Molecular and Developmental Biology Graduate Program, University of Cincinnati College of Medicine and Cincinnati Children's Hospital Medical Center, Cincinnati, OH 45208

*corresponding author: joshua.waxman@cchmc.org

Key Words: Dact, Dishevelled, Wnt signaling, retinoic acid signaling, vertebrate development

Highlights:

- We investigated *dact3a* and *dact3b* expression during early zebrafish development.
- Sequence alignments show strongest conservation in the PDZ-binding domains.
- *dact3a* is expressed in the lateral plate mesoderm, somites, and neural crest.
- *dact3b* is expressed in the dorsal forerunner cells (DFC) and hindbrain
- Retinoic acid signaling negatively regulates *dact3b* expression in the hindbrain

Abstract

Wnt signaling plays important roles in normal development as well as pathophysiological conditions. The Dapper antagonist of β-catenin (Dact) proteins are modulators of both canonical and non-canonical Wnt signaling via direct interactions with Dishevelled (Dvl) and Van Gogh like-2 (Vangl2). Here, we report the dynamic expression patterns of two zebrafish *dact3* paralogs during early embryonic development. Our whole mount i*n situ* hybridization (WISH) analysis indicates that specific *dact3a* expression starts by the tailbud stage in adaxial cells. Later, it is expressed in the anterior lateral plate mesoderm, somites, migrating cranial neural crest, and hindbrain neurons. By comparison, *dact3b* expression initiates on the dorsal side at the dome stage and soon after is expressed in the dorsal forerunner cells (DFCs) during gastrulation. At later stages, *dact3b* expression becomes restricted to the branchial neurons of the hindbrain and to the 2nd pharyngeal arch. To investigate how zebrafish *dact3* gene expression is regulated, we manipulated retinoic acid (RA) signaling during development and found it negatively regulates *dact3b* in the hindbrain. Our study is the first to document the expression of the paralogous zebrafish *dact3* genes during early development and demonstrate *dact3b* can be regulated by RA signaling. Therefore, our study opens up new avenues to study Dact3 function in the development of multiple tissues and suggests a previously unappreciated cross regulation of Wnt signaling by RA signaling in the developing vertebrate hindbrain.

1. Introduction

Wnt signaling regulates animal development and homeostasis through directing numerous fundamental cellular processes including cell specification, proliferation, differentiation, migration, and stem cell self-renewal [40, 41, 118]. The Dapper antagonist of β-catenin (Dact) protein family was initially isolated from yeast-two hybrid screens with the Dishevelled (Dvl) PDZ domain as bait [28, 65]. Since then, three Dact family members Dact1, Dact2, and Dact3 have been reported in vertebrates. All three have been reported in humans and mice, Dact1 and Dact2 have been reported in zebrafish and chicken [119], and Dact1 has been reported in *Xenopus* [28, 65]. Structurally, the Dact proteins share a number of conserved domains [29]. However, it is the conserved N-terminal leucine zipper domain (LZD) and C-terminal PDZ-binding (PDZB) domain that have been implicated in different Wnt-related functions [28, 29, 65, 120]. The N-terminal LZD of Dact1 has been shown to interact with LEF/TCF proteins and is involved in homo- and heterodimerization of Dact proteins [121, 122]. While the PDZ-binding domain is necessary and sufficient for interaction with Dvl [65], more recent studies have indicated that this domain is important for facilitating interactions with several other proteins, including Vangl2, PKA, PKC, CK1δ/ε, and p120ctn [122]. Thus, from the many interactions with regulators of Wnt signaling, in particular Dvl, Dact function in cellular signaling and proper embryonic development is likely very much dependent on the nature of the proteins it interacts with in a given context.

Dact1 orthologs have been the best studied of this protein family. In *Xenopus*, Dact1 can inhibit both β-catenin (canonical branch) and JNK (non-canonical branch) downstream of Dvl with a requirement in proper notochord and head development [28, 65]. Additionally, *dact1* was shown to mediate lysosome-inhibitor regulated Dvl degradation [123]. With respect to regulation

of canonical Wnt signaling, Dact1 can also act more downstream of Dvl. Dact1 associates with TCF3 independent of β-catenin in *Xenopus* [121], inhibits β-cat/LEF interactions in the nucleus, and promotes HDAC recruitment to LEF promoters [124]. Interestingly, Dact1 can also act as a positive regulator of canonical Wnt signaling [31, 65, 125-127]. Gain-of-function studies have found that co-injection of Dvl and Dact1 can promote canonical Wnt signaling. In zebrafish, depletion of Dact1 can enhance anteriorization due to the loss of canonical Wnt signaling in a *wnt8* hypomorphic background. While the molecular mechanism behind this context dependent switch in function of Dact proteins in canonical Wnt signaling remains elusive, phosphorylation status of Dact1 has been suggested to be a decisive factor [128]. Although studies in non-mammalian vertebrates primarily suggested that Dact1 proteins function to regulate canonical Wnt signaling, Dact1 knockout (KO) mice show severe urogenital defects and posterior body malformations, which has been associated with impaired Wnt-PCP signaling [31, 32]. In humans, *Dact1* mutations have been found in patients with neural tube defects (NTD) [129] and altered expression is found in many types of cancers [130-134]. Therefore, Dact1 has a multitude of functions regulating different types of Wnt signaling in developmental and disease contexts.

Similar to Dact1, Dact2 regulates different Wnt signals and has been proposed to also regulate TGF-β signaling [135]. During early zebrafish development, Dact2 regulates proper convergent extension movements. However, in mice, Dact2 functions as a negative regulator of canonical Wnt signaling in tooth development via interacting with and repressing *pitx2* expression [136]. Dact2 has also been shown to attenuate TGF-β/Nodal signaling by facilitating lysosomal degradation of type I receptors ALK4 and ALK5 during mesoderm induction [135, 137, 138]. Although *Dact2* null mice are viable, they exhibit accelerated wound healing due to enhanced TGF-β signaling [139].

To this point, *Dact3* has been the least studied Dact member. Its expression has only been described for mice and it had been suggested that it may only be specific to mammals [30]. Epigenetic repression of *Dact3* has been shown to be associated with increased canonical Wnt signaling in colorectal cancer, suggesting in this context Dact3 acts as a negative regulator of canonical Wnt signaling [34]. *Dact3* null mice did not display any obvious morphological abnormalities, but they have a slightly smaller body weight than wild type (WT) siblings indicating Dact3 has a role in postnatal development in mice [33]. Furthermore, unilateral ureteral obstruction in *Dact3* knockout mice produced noticeable kidney fibrosis along with increased Dvl2 and β-catenin, expression of several Wnt-responsive fibrotic, and epithelial-to-mesenchymal transition marker genes [33]. Together with a previous report, these observations support that Dact3 can act as a canonical Wnt signaling antagonist [34].

We wanted to better understand the evolution of the Dact family of proteins in vertebrates. Although the expression and function of *dact1* and *dact2* have been previously reported in zebrafish [125], the identity and putative expression pattern of any zebrafish ortholog(s) of Dact3 has not been determined. Here, we report the expression of two zebrafish Dact3 paralogs, *dact3a* and *dact3b*, during early development. Our finding also indicates that retinoic acid (RA) signaling negatively regulates *dact3b* expression in the zebrafish hindbrain, suggesting a previously unexplored regulation of Wnt signaling by RA signaling in the vertebrate hindbrain.

2. Results and discussions

2.1 Comparison of Dact protein sequences

Examining the current zebrafish genome (Zv9; ensemble.org), we found that there are two predicted zebrafish *dact3-like* paralogs. The first predicted zebrafish *dact3-like* gene (XM_005172584) is located on Chromosome (Chr) 10, has 4 exons, and encodes a 586 amino acid protein. The second *dact3-like* gene (XM_001340960) has 5 exons encoding a 533 amino acid protein. In order to determine the level of conservation of zebrafish *dact3-like* genes with the mammalian *dact3* orthologs, we performed sequence alignments using Clustal W for human (Hs), mice (Mm) and zebrafish (Dr) Dact3s. The zebrafish *dact3-like* gene on Chr 10 shares greater homology with both human and mice Dact3s compared to the *dact3-like* gene on Chr 18, so we now refer to them as *dact3a* and *dact3b*, respectively (Fig. 1A, B). While the overall amount of conservation is not high among the Dact3 proteins, there was greater conservation of an N-terminal coiled domain (CD1) and leucine zipper domains (LZD) [29]. Despite the overall higher conservation of *dact3a* with the mammalian Dact3 genes, its LZD was actually less conserved than *dact3b*. The C-terminal PDZ-binding (PDZB) domain for Dact3 homologs is completely conserved (Fig. 1A). Comparing the four zebrafish Dact homologs, we found greater conservation of sequence between zebrafish Dact1 and Dact2 than between either zebrafish Dact3 paralog (Fig 2A, B). The alignments between the four zebrafish Dact proteins indicate a strongly conserved PDZ-binding domain, except for a threonine (T) to leucine (L) change in Dact2 sequence. Interestingly, the N-terminal CD1 domain again is more highly conserved than the, LZD domain, which is not as easily identifiable (Fig. 2A) in the alignments of the zebrafish Dact proteins. The high conservation of the PDZ-binding domain is understandable, as deletion studies have reported that it is essential for interactions with multiple proteins [28]. Therefore,

this analysis of zebrafish Dact3a and Dact3b shows that Dact3 proteins are conserved in non-mammalian vertebrates.

2.3 *Dact3a* is expressed in the somites, neural crest cells and hindbrain neurons

To analyze the spatio-temporal expression patterns of *dact3a* and *dact3b*, we performed whole mount *in situ* hybridization (WISH) and reverse transcriptase-PCR (RT-PCR) at stages of zebrafish development starting from the dome stage until 48 hours post fertilization (hpf). Although we could detect *dact3a* expression with RT-PCR by the shield (SH) stage (Fig. 3), with WISH we were not able to detect specific *dact3a* expression until the tailbud (TB) stage, when it appeared in adaxial mesodermal cells (Fig. 4D). Initial expression of *dact3a* is seen much later than *dact1* and *dact2*, which appears to be present as early as the high stage with dorsal-specific expression [125]. At the 8 somite (s) stage, *dact3a* expression is observed in the anterior lateral plate mesoderm (ALPM) and prominently in the adaxial cells of the somites (Fig. 4B, E). By the 18s stage, *dact3a* is expressed in the posterior, newly forming somites, the 3 (mandibular, hyoid and branchial) streams of migrating cranial neural crest cells [140-142], the anterior brain, hindbrain neurons, and spinal cord neurons (Fig. 4C, F). Flat mounting of the probed embryos at 18s revealed that *dact3a* is expressed in the telencephalon and lines the inner periphery of eye. At this stage, *dact3a* is also expressed in the precursors to the cranial branchiomotor neurons (Fig 5A) and by 26 hpf in the trigeminal (V) the facial (VII) neurons (Fig 5B) [143-145]. The expression in the hindbrain persists through 48 hpf (Fig. 4H, I and Fig. 5C, D), while the *dact3a* expression in the cranial cartilage is consistent with it being derived from the cranial neural crest (Fig 4J) [140]. By 36hpf, *dact3a* expression also initiated in the pectoral fin bud (Fig. 4H). At 48

hpf, it is also interesting to notice that the pectoral fin bud expression of *dact3a* is present in two separate domains, consistent with expression in the pectoral muscle (Fig 5D) [146, 147]. By comparison, zebrafish *dact2* is also expressed in the pectoral fin bud [29]

2.4 *Dact3b* is expressed in the dorsal forerunner cells and brain

In contrast to *dact3a*, which did not have specific expression until the TB stage, localized *dact3b* expression begins at the dome stage in a cluster of cells at the dorsal blastoderm (Fig. 6A, E), very similar to what has been reported for zebrafish *dact1* [125]. The dorsal *dact3b* expression maintained through 40% epiboly (Fig. 6B, F). Compared to zebrafish *dact1* and *dact2* at the same developmental stages, the dorsal region expressing *dact3b* is narrower and the onset of expression is delayed [125]. By 60% epiboly, this scattered dorsal expressing cell population starts to reduce and become concentrated in only a few cells at the dorsal blastoderm margin (Fig. 6C, G). These dorsal expressing cells appear to be the dorsal forerunner cell population (DFC), because they are located below the blastoderm margin (Fig. 6C, G). Although the DFCs give rise to Kupffer's vesicle [148], we did not observe *dact3b* expression in the Kupffer's vesicle (data not shown), suggesting the DFC expression is not maintained in these cells after gastrulation. By the end of gastrulation at the TB stage, *dact3b* expression waned, as we did not detect specific expression via WISH or significant transcripts via RT-PCR (Fig. 3 and data not shown). Furthermore, even though dact3b expression increased by the 8s stage, we did not detect noticeable specific *dact3b* expression until late somitogenesis stages (Figs. 3 and 6D, H). The lack of expression from the end of gastrulation through early somitogenesis contrasts with

zebrafish *dact1*, *dact2*, and *dact3a*, which are all expressed throughout these stages in the somites, tailbud, brain, and spinal cord (Figs. 4 and 5) [149].

Beginning at the 18s stage, specific *dact3b* expression initiates in the hindbrain (Fig. 6H). As development proceeds, this expression persists and expands posteriorly by 24hpf (Fig. 6I). To examine the relative location of *dact3b* in the hindbrain, we performed double WISH at 24hpf with *krox-20.* This revealed *dact3b* expression resided in r2 through r6, with more medial expression in r3-r6 (Fig. 7A). At this stage, *dact3b* is also found in the 2nd pharyngeal arch (Fig. 7A). By 36hpf, we found expression begins in the anterior tectum/midbrain region (Fig. 6I and Fig. 7B) and extended up to the midbrain-hindbrain boundary. As development proceeds, the intensity of *dact3b* expression in these neural tissues becomes stronger through 48 hpf (Fig. 6K and 7C), with hindbrain expression in a striped pattern consistent with cranial branchiomotor neurons [150] (Fig. 7C). Interestingly, the hindbrain expression patterns for *dact3b* is more anterior compared to *dact3a* at the comparable stages (Fig. 5).

Comparing the previously reported expression patterns of zebrafish *dact1* and *dact2* to *dact3a and dact3b*, respectively, revealed that prior to gastrulation, *dact3b* is more similar to zebrafish *dact1* and *dact2* as they all share dorsally localized expression. After gastrulation, *dact3a* expression is more similar to *dact1* and *dact2* expression than its paralog *dact3b*, as *dact3a* shares broader expression in the somites, brain, and lateral plate mesoderm [29]. Although all four *dact* genes are expressed in the brain during development, *dact1* and *dact2* brain specific expression begins as early as the TB stage, while both *dact3a* and *dact3b* expression initiates after mid-somitogenesis stages.

In comparing zebrafish *dact3* paralog expression to the expression of the single mouse Dact3 gene, *dact3a* expression is more similar to the mouse Dact3 than *dact3b.* The_mouse *Dact3* is expressed in the somites, fore- and hind limb buds, otic vesicle, aortic arches, craniofacial mesenchyme, tail bud and central nervous system [30] . Likewise, *dact3a* is expressed in the somites, pectoral fin bud, cranial neural crest cells, and hindbrain neurons. Zebrafish *dact3b*, however, is not as broadly expressed as the mouse *Dact3*. While zebrafish *dact3b* is expressed only in the 2nd pharyngeal arch, mouse *Dact3* and zebrafish *dact3a* are both expressed throughout all the pharyngeal arches. Interestingly, although the mouse *Dact3* was not reported in the brain during development, it is prominently expressed in the adult brain and specifically in the cerebral cortex. We find specific regional expression of both *dact3a* and *dact3b* in the zebrafish brain during development that is reminiscent of the expression in the adult mouse.

2.5 RA signaling negatively regulates *dact3* expression in the hindbrain

We next wanted to understand if any of the major developmental signaling pathways, including canonical Wnt, FGF, BMP, and RA signaling regulate either *dact3a and dact3b* expression in the zebrafish hindbrain. To modulate RA signaling, we treated the embryos beginning at the 16s stage and 24 hpf with RA and diethylaminobenzaldehyde (DEAB), a retinaldehyde dehydrogenase inhibitor that inhibits RA synthesis [103]. Following treatment, embryos were fixed at 24hpf and 30hpf, respectively, and analyzed for *dact3b* expression. Examination of the embryos treated with exogenous RA revealed that at both stages RA induced a significant decrease in *dact3b* expression (Fig. 8A, B). Conversely, treatment with DEAB

resulted in expansion of *dact3b* expression within the hindbrain and extension posteriorly into the spinal cord (Fig. 8A, C). In the 30hpf embryos, treatment with RA also diminished the pharyngeal expression (Fig. 8D. E). Similar effects were not seen on the *dact3a* hindbrain expression when RA signaling was manipulated at these stages nor did we find that RA signaling affected *dact3a* expression at earlier stages (data not shown). Manipulation of Wnt, FGF, and BMP signaling pathways utilizing heat-shock inducible transgenic fish lines at similar stages did not affect *dact3b* expression in the hindbrain (data not shown). Together, our data suggest that RA signaling negatively regulates *dact3b* expression in the anterior hindbrain, but not *dact3a* in the posterior hindbrain, in zebrafish. Cross talk between Wnt and RA signaling has been studied in a variety of developmental contexts, including hematopoietic stem cell development, chondrocyte formation, and adipogenesis [69, 151, 152]. Our present findings suggest a previously unappreciated access point for the cross-regulation of Wnt signaling by RA signaling and provide a basis of future investigations targeting how Dact3 proteins function within the hindbrain to integrate the Wnt and RA signaling networks.

Experimental procedures:

Zebrafish husbandry and maintenance: Zebrafish (*Danio rerio*) were raised and maintained following standardized laboratory conditions [153]. Embryos were collected from crosses between WT strains and raised at 28.5°C in an incubator before fixing at desired stages for analysis. Staging was done as reported previously [154].

Generation of *dact3a* and *dact3b* probes: 629 bp of *dact3a* and 759 bp of *dact3b* sequence were amplified from mixed stage cDNA using the following primers: Forward *dact3a*: 5'-TGAAGGTGGACACAGAGAACAGC. Reverse *dact3a*: 5'-ATAGGTCGTGGGTCTTGCTTGG. Forward *dact3b*: 5'-ATTTTCTGCCCCATACCCCC Reverse *dact3b*: 5'-ACGCAACTGTCCTCTGAACGAG. The amplified products were cloned into pGemT-Easy (Promega), sequenced, and anti-sense probe was synthesized using standard methods. Probe used for *krox-20* was previously reported (ZDB-GENE-980526-283).

Phylogenetic analysis: Full-length sequence for all Dact members of human, mice and zebrafish was obtained from NCBI website. Sequence alignments were performed using Clustal W in MacVector.

RT-PCR analysis: 30 embryos at the designated stages were homogenization in TRIzol reagent (Ambion). RNA was prepared using Pure link RNA Micro Kit (In Vitrogen). cDNA was synthesized using the ThermoScript Reverse Transcriptase kit (Invitrogen). RT-PCR was performed using the primers that were used to make probe for the respective genes. Control for expression is *solo* a ubiquitously expressed gene at the stages mentioned.

Wholemount *in situ* hybridization (WISH): WISH was performed as described previously [155]. Images were taken using a Zeiss M2BioV12 stereomicroscope and Zeiss AxioImager 2. Pigmentation was prevented at later stages using 0.003% 1-phenyl-2-thiouera (PTU) treatment starting at 24 hpf.

Drug treatment: WT embryos were treated with 1 μm RA and 1μm DEAB and placed on a Nutator at 28.5°C. Treatment was performed beginning at 16hpf and 24hpf followed by fixation at 24hpf and 30hpf, respectively.

Figure Legends:

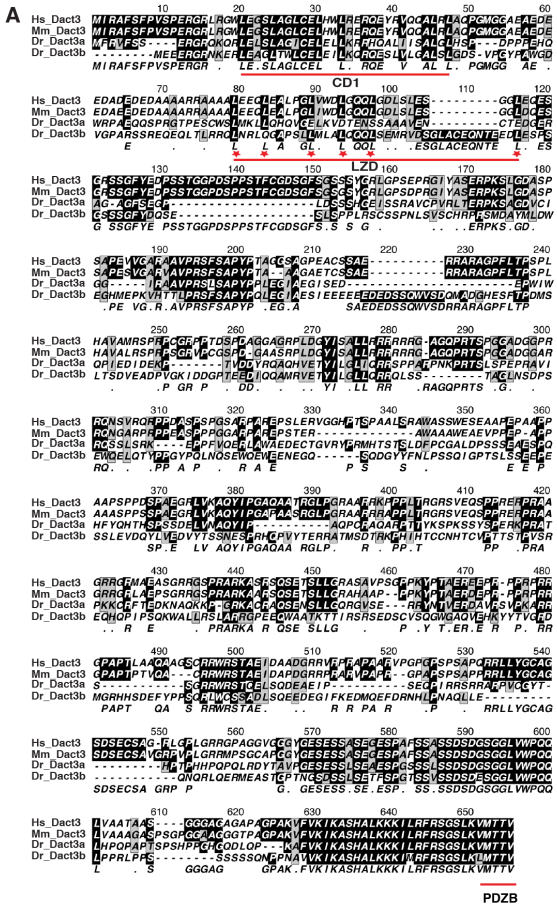

B

	Hs_Dact3	Mm_Dact3	Dr_Dact3a	Dr_Dact3b
Hs_Dact3	100.0	85.2	30.2	21.9
Mm_Dact3	88.6	100.0	30.0	20.5
Dr_Dact3a	41.6	33.4	100.0	24.8
Dr_Dact3b	31.7	30.4	37.8	100.0

Identity

Similarity

Figure 1. Sequence alignments of vertebrate Dact3 proteins. A: Comparison of human (Hs), mouse (Mm), and zebrafish (Dr) Dact3 protein sequences revealed conservation of the N-terminal CD1 and LZD domains and the C-terminal PDZ-binding domain. Conserved domains are underlined in red. 6 conserved leucines of the LZD are indicated with red stars. **B:** Table with the amino acid identity (Y-axis) and similarity scores (X-axis) of Hs, Mm and Dr Dact3 homologs.

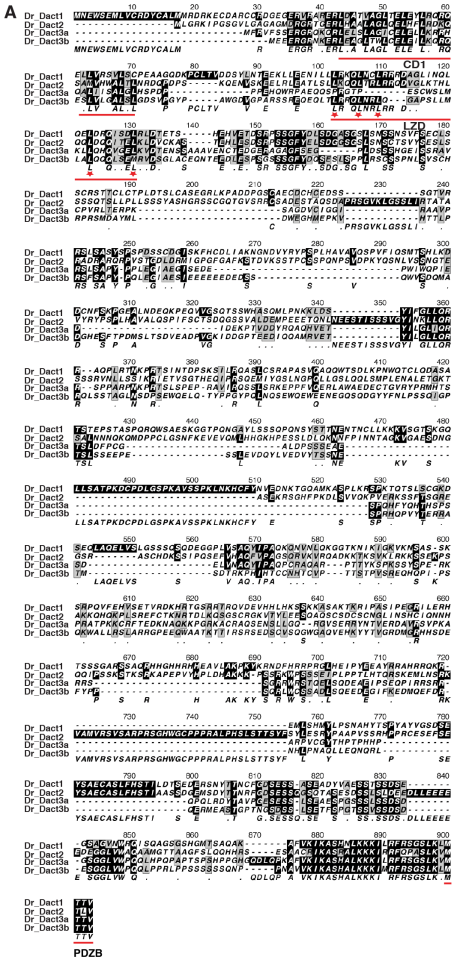

Figure 2. Sequence alignments of zebrafish Dact proteins. A: Comparison of zebrafish (Dr) Dact1, Dact2, and Dact3a and Dact3b protein sequences revealed greater conservation of the N-terminal CD1 and C-terminal PDZ-binding domains, with less conservation of the LZD domain. Conserved domains are underlined in red. 5 conserved leucines of the LZD are indicated with red stars. **B:** Table with the amino acid identity (Y-axis) and similarity scores (X-axis) of Dr Dact proteins.

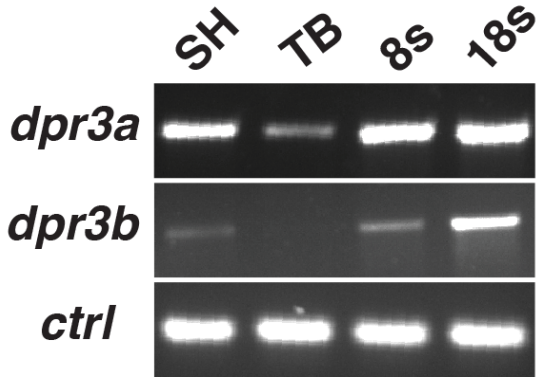

Figure 3. RT-PCR analysis of *dact3a* and *dact3b* gene expression: Expression of *dact3a* and *dact3b* analyzed by RT-PCR at the indicated stages. *Solo* served as a positive control.

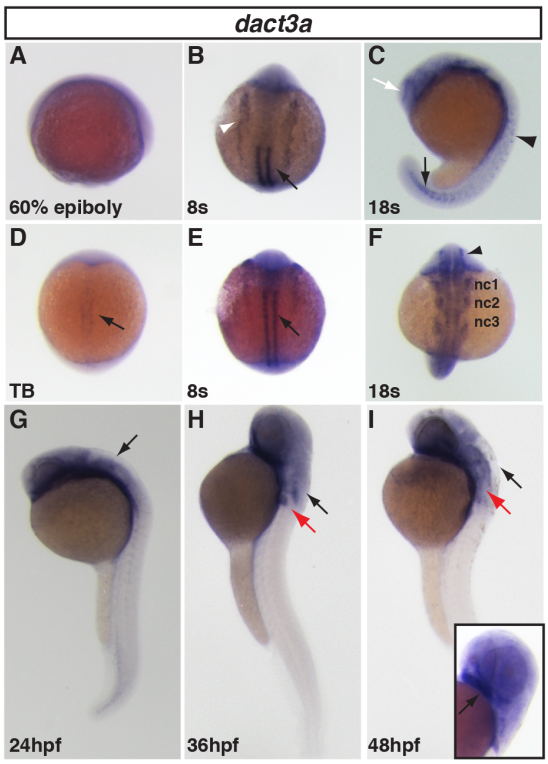

Figure 4. Zebrafish *dact3a* expression from 60% epiboly through 48hpf. A: Specific *dact3a* expression was not observed at 60% epiboly, even though it is detectable by RT-PCR (Fig. 3). **D:** *Dact3a* expression in the adaxial mesoderm at the TB stage (black arrow). **B,E:** *Dact3a* expression in the somites (black arrows) and anterior lateral plate mesoderm (white arrowhead) at the 8s stage. **C:** Expression at the telencephalon (white arrow), spinal cord neurons (black arrowhead), and the forming somites (black arrow) at the 18s stage. **F:** Mandibular (nc1), hyoid (nc2), and branchial (nc3) neural crest expression and medial eye expression (black arrowhead) at the 18s stage. **G-I:** Hindbrain expression at 24, 36 and 48hpf (black arrow). At 36 and 48 hpf, *dact3a* expression is visible in the pectoral fin bud (red arrow). **Inset:** Cartilage expression (black arrow) at 48hpf. A, C, G, H, I are lateral views. B, D, E, F are dorsal views. Anterior up in all the images.

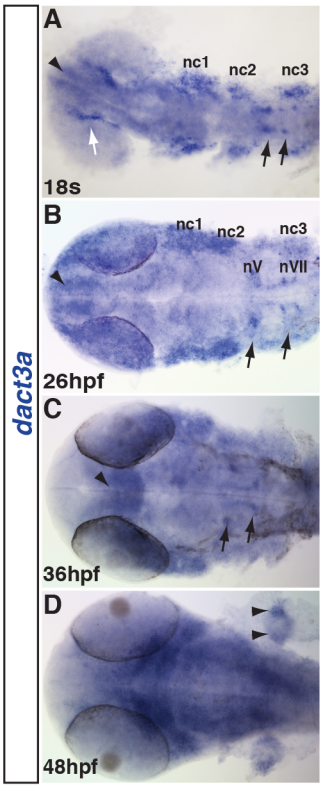

Figure 5: *Dact3a* expression in the brain. A: *Dact3a* expression in the telencephalon (black arrowhead), medial eye (white arrow), neural crest (nc1, 2, 3) and hindbrain neurons (black arrows). **B:** Expression in the nV (trigeminal) and nVII (facial) cranial branchiomotor neurons (black arrows). **C:** Expression in the diencephalon (black arrowhead) and branchiomotor neurons (black arrows). **D:** Pectoral fin bud expression in two distinct domains (black arrowheads). All the images are dorsal with anterior right.

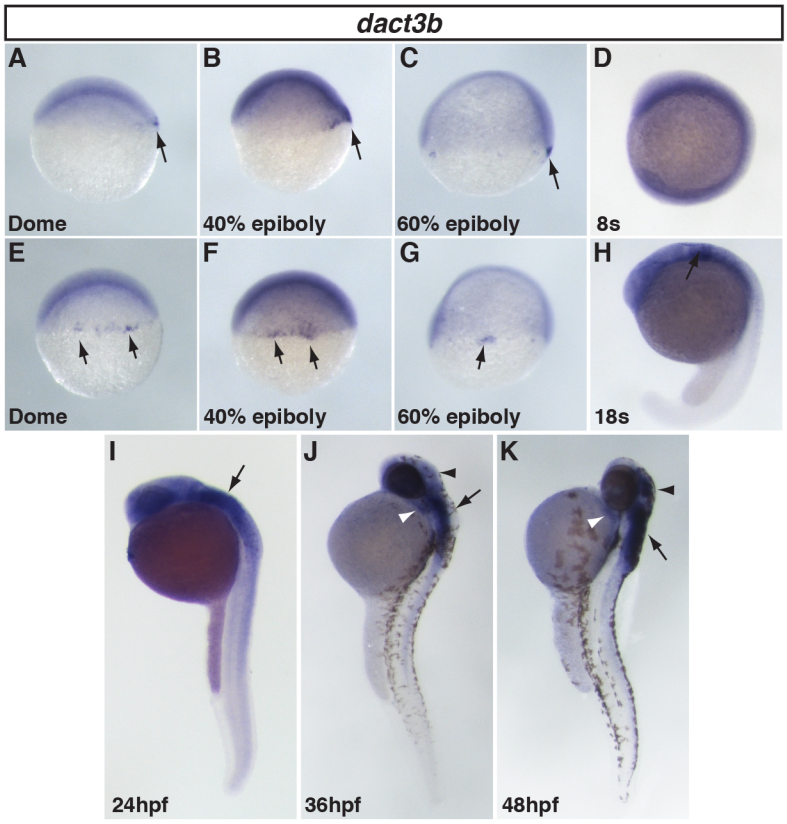

Figure 6. Zebrafish *dact3b* expression from dome through 48hpf. **A-C, E-G:** *Dact3b* expression in the dorsal blastoderm margin from dome through 60% epiboly stage (black arrow). **D:** Specific *dact3b* is not expressed at the 8s stage, even though we could detect it with RT-PCR (Fig. 3). **H,I:** *Dact3b* expression in the hindbrain starts at 18s and is maintained through 24 hpf embryos (arrow). **J,K:** *Dact3b* expression initiates in the 2nd pharyngeal arch (white arrowheads) and the dorsal region of the midbrain/tectum (black arrowheads) at 36hpf and is maintained through 48 hpf. *Dact3b* continues to be expressed in the hindbrain at 36 and 48hpf (black arrows). A-D and H-K are lateral views with dorsal rightward. E-G are dorsal views. In all images, anterior is up.

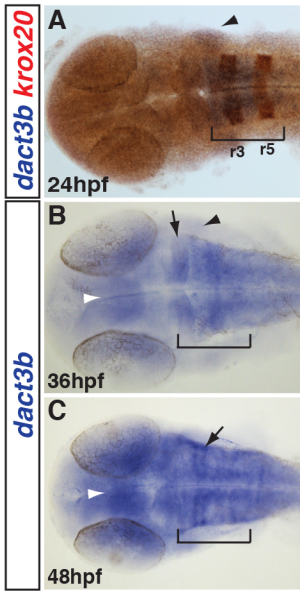

Figure 7: *Dact3b* expression in the hindbrain. A: Double WISH for *dact3b* and *krox-20* at 24 hpf. *Krox-20* (orange) is expressed in r3 and r5. *Dact3b* expression is from r2 through r6 (brackets). *dact3b* is expressed in the adjacent 2nd pharyngeal arch (black arrowhead). **B:** *Dact3b* expression extends more anteriorly past the midbrain-hindbrain boundary (black arrow) and is expressed in the tectum by 36 hpf (white arrowhead). 2nd pharyngeal arch expression is maintained (black arrowhead). **C:** By 48 hpf, *dact3b* expression is increased and is in stripes consistent with anterior branchiomotor neuron expression (black arrow) [150]. Embryos in images were flat mounted. Images are dorsal views with anterior to the left.

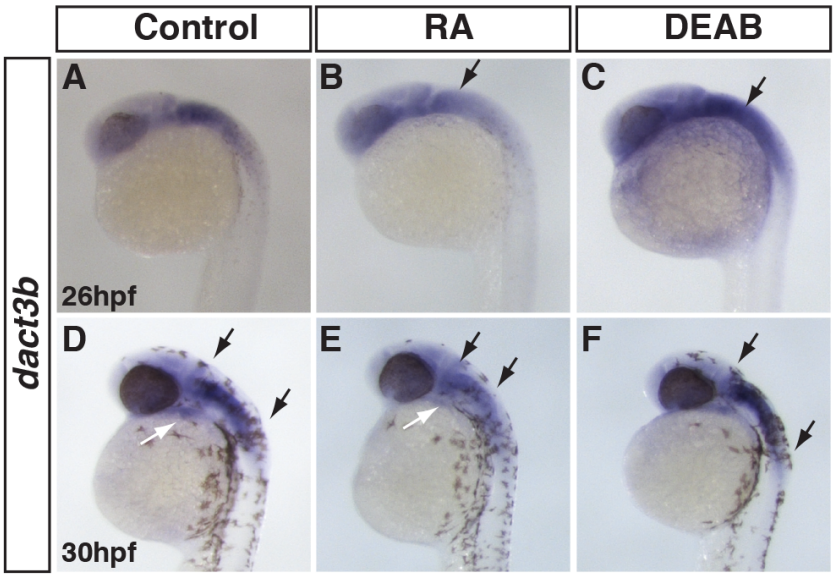

Figure 8: RA signaling negatively regulates *dact3b* expression. A, D: Control embryos **B, E:** Treatment with exogenous RA extinguishes *dact3b* expression in the hindbrain (black arrows) and 2nd pharyngeal arch (white arrow in E). **C, F:** Inhibition of RA signaling lead to an expansion of *dact3b* expression domain with the hindbrain (compare the length between arrows in D and F). Images are lateral views with anterior to upward.

Chapter 4

Wnt signaling balances specification of the cardiac and pharyngeal muscle fields

Amrita Mandal[1,2] and Joshua S. Waxman[1]*

1 – Heart Institute, Molecular Cardiovascular Biology Division, Cincinnati Children's Hospital Medical Center, Cincinnati OH, USA

2 – Molecular and Developmental Biology Graduate Program, University of Cincinnati College of Medicine and Cincinnati Children's Hospital Medical Center, Cincinnati, OH 45208

*corresponding author: joshua.waxman@cchmc.org

Running title: Balance of cardiac and pharyngeal fields

Keywords: Wnt signaling, zebrafish, cardiac, pharyngeal muscle, mesoderm patterning, organ fields

Abstract

Canonical Wnt/β-catenin (Wnt) signaling plays multiple conserved roles during fate specification of cardiac progenitors in developing vertebrate embryos. Although lineage analysis in ascidians and mice has indicated there is a close relationship between the cardiac second heart field (SHF) and pharyngeal muscle (PM) progenitors, the signals underlying directional fate decisions of the cells within the cardio-pharyngeal muscle field in vertebrates are not yet understood. Here, we examined the temporal requirements of Wnt signaling in cardiac and PM development. In contrast to a previous report in chicken embryos that suggested Wnt inhibits PM development during somitogenesis, we find that in zebrafish embryos Wnt signaling is sufficient to repress PM development during anterior-posterior patterning. Importantly, the temporal sensitivity of dorso-anterior PMs to increased Wnt signaling largely overlaps with when Wnt signaling promotes specification of the adjacent cardiac progenitors. Furthermore, we find that excess early Wnt signaling cell autonomously promotes expansion of the first heart field (FHF) progenitors at the expense of PM and SHF within the anterior lateral plate mesoderm (ALPM). Our study provides insight into an antagonistic developmental mechanism that balances the sizes of the adjacent cardiac and PM progenitor fields in early vertebrate embryos.

Introduction

Organogenesis begins with commitment of multi-potent overlapping organ progenitor fields into a specific fate. During the course of development, cardiac and PM progenitors, the latter of which give rise to cranio-facial muscles, lay in close physical proximity in the ALPM and anterior paraxial mesoderm, respectively [156, 157]. Multiple developmental syndromes feature cardiac and cranio-facial defects [156], with the most extensively studied being DiGeorge and velocardiofacial syndromes, suggesting defects in signaling pathways that affect distinct or common cardio-pharyngeal progenitors contribute to the molecular etiology of these syndromes.

Vertebrate heart development occurs in two waves. FHF progenitors differentiate earlier, primarily contributing to the left ventricle in mammals and birds and ~60% of the single ventricle and most of the atrium in the teleost zebrafish [158, 159]. Later differentiating SHF progenitors contribute to growth of the heart through progressively adding to both poles of the heart. In mammals, the SHF contributes to the right ventricle, outflow tract and parts of the atria [158, 160, 161]. In zebrafish, the SHF primarily contributes to the remaining 40% of ventricular cells [159, 162, 163]. A conserved aspect of vertebrate SHF progenitors is their ability to give rise to ventricular cardiomyocytes, endothelial, and smooth muscle of the outflow tract. In recent years, sophisticated retrospective clonal lineage tracing studies in mice have suggested there are also rare progenitors that give rise to both cardiac and PM, which fits with the close proximity of these progenitor fields within the anterior mesoderm [60, 164, 165].

Given the closeness of the cardiac and PM progenitor fields within the anterior mesoderm, which is exemplified by the existence of bi-potent cardio-pharyngeal progenitors, it is logical that there is significant overlap of genetic marker expression. In mice, the anterior

mesoderm that harbors both SHF progenitors and PMs, expresses markers including *Isl1, Tbx1,* and *Tcf21* [63, 166]. Knockout mice reveal that *Isl1* and *Tbx1*, the latter of which is the primary gene associated with DiGeorge syndrome in humans [58], are required to promote SHF and PM development [63, 166]. Additionally, *Tcf21* KO mice also have cardiac outflow tract and PM defects, although less severe than Tbx1 [63]. In zebrafish, while Isl1 does not have the broad role in SHF development that is found in mammals [162], Tbx1 has a conserved role in cardiac and facial muscle development [167, 168]. A recent study in zebrafish has suggested that *tcf21* is expressed in ventricular OFT and PM progenitors [157], although it was not determined if there are common cardio-pharyngeal progenitors in zebrafish. Therefore, shared conserved genetic regulators promote the development of SHF cardiomyocytes and PM in vertebrates.

Common cardio-pharyngeal progenitors that give rise to the heart and atrial siphon muscles (ASMs) have been described in the tunicate *Ciona,* indicating the relationship of these progenitors may have originated early in the chordate lineage [169]. Although analysis in vertebrates has identified signals that promote the generation of these progenitors, the comparably simple development of *Ciona* embryos has allowed for the detailed description of antagonistic relationships within cells of the SHF that generate the cardiac and ASMs. After secondary trunk ventral cells divide, differential gene expression within second heart precursors (SHPs) and ASM precursors determines their subsequent fates as cardiac and ASM [170]. Specifically, within the SHPs, NK4, the homolog of Nkx2.5 in vertebrates, inhibits Tbx1/10 expression, and promotes GATAa expression. Conversely, in the ASM precursors, Tbx1/10 promotes the muscle lineage through inhibition of GATAa expression. Thus, the simplicity of *Ciona* heart development has revealed a paradigm for antagonism between these conserved

transcriptional signals within SHF lineages, which specifies the appropriate number of cardiac and PM progenitors.

In vertebrates, despite the conservation of molecular players, comparable mechanisms as found in *Ciona* that affect the fate decision to become cardiac or PM have not been described. Canonical Wnt signaling is a viable candidate as studies have indicated it plays important roles in the development of cardiac and PMs. Wnt signaling plays multiple developmental stage specific roles during cardiogenesis [50, 171, 172]. Prior to gastrulation, Wnt signaling promotes cardiac specification [50, 171-174]. After gastrulation, Wnt inhibits cardiac differentiation [50, 171]. Additionally, early Wnt signaling can promote cardiac fates at the expense of adjacent hematovascular progenitors [172, 175, 176]. With respect to the role of Wnt signaling in PM development, however, there is currently a more limited understanding. Explant cultures and *in vivo* retrovirus injection in chicken embryos implicated canonical Wnt signaling from the dorsal neural tube and notochord as an inhibitor of PM. However, the conservation of this requirement for Wnt signaling has not been investigated [177].

In this study, we first sought to understand if there is a conserved requirement for Wnt in antagonizing PM development. Using transgenic heat-shock inducible lines to temporally manipulate Wnt signaling in zebrafish, we demonstrate that Wnt signaling primarily inhibits anterior PM development prior to gastrulation during anterior-posterior pattering, the developmental stage when it also promotes cardiac progenitor specification. Furthermore, excess Wnt signaling, through heat-shock induction of Wnt8a or co-depletion of the transcriptional repressors of Wnt signaling targets Tcf7la and Tcf7lb, promotes an expansion of the cardiac field into a region of the ALPM that typically harbors SHF and PM progenitors. Thus, Wnt signaling prior to gastrulation helps position the border between the FHF and the adjacent SHF and PM

progenitor fields. Furthermore, blastula transplantation data suggests Wnt signaling cell autonomously promotes cardiac specification and inhibits PM development. Altogether, our study provides evidence that canonical Wnt signaling establishes the proportions of the adjacent cardiac and PM fields during early anterior-posterior patterning of mesoderm in vertebrates.

Results

Wnt signaling inhibits dorso-anterior PM development before gastrulation

Previous studies in chicken embryos have suggested that Wnt signaling from the dorsal neural tube inhibits PM development [177]. However, the conservation of Wnt signaling in PM development has not been examined. To determine if, and when, Wnt signaling is sufficient to inhibit PM development in zebrafish, we crossed hemizygous *Tg(hsp70l:wnt8a-GFP)* fish to homozygous *Tg(α-actin:GFP)* fish. The resulting embryos were heat-shocked to induce Wnt8a-GFP at the sphere (SP) stage (prior to gastrulation), tailbud (TB) stage (end of gastrulation), the 16 somite (s) stage (mid-somitogenesis), and 24 hours post-fertilization (hpf; end of somitogenesis). The transgenic embryos were sorted from their siblings that did not carry the heat-shock transgene using GFP fluorescence and the PMs were examined at 72 hpf when the majority of these muscles have differentiated [178]. We found that increased Wnt signaling prior to gastrulation promoted maximal loss of dorso-anterior head muscles. Specifically, increased Wnt signaling prior to gastrulation inhibited development of the EOMs, which are derived from the prechordal mesoderm, and the 1st and 2nd arch muscles (Fig. 1A, E). While ventral muscles of the first two arches were reduced, the dorsal muscles of these arches were lost (Fig. 1E). More posterior pharyngeal wall muscles (PWMs) were also reduced, while the somite-derived sternohyoideus (SH) was not overtly affected. Wnt induction at the TB stage leads to comparatively less severe loss of dorso-anterior PMs (Fig. 1B, F), while induction at the 16s stage and 24 hpf appeared unaffected (Fig. 1C,D,G,H). Tcf7l transcription factors are transcriptional repressors that are required to limit posteriorization of early Wnt signaling [179]. To determine if endogenous Wnt signaling needs to be repressed to promote the PMs, we depleted Tcf7l1 proteins in the embryos using the previously validated *tcf71la* and *tcf71lb* MOs

(referred as Tcf7l1 depleted) [179]. Consistent with excess Wnt signaling prior to gastrulation, Tcf7l1 depleted embryos lost dorso-anterior PMs (Fig. 2A,B). Therefore, our data suggests that Wnt signaling is sufficient to inhibit PM development. However, in contrast to the analysis in chicken embryos that indicated a repressive role of Wnt signaling during somitogenesis, the PMs are most sensitive to excess Wnt signaling prior to gastrulation.

To determine if there is a requirement for Wnt signaling in PM development, hemizygous *Tg(hsp70l:dkk1-GFP)* fish were crossed to *Tg(α-actin:GFP)* fish. The resulting embryos were heat-shocked at SP, TB, 16s, and 24 hpf, sorted with GFP, and examined as described above. As would be expected, inhibition of Wnt signaling before gastrulation produced embryos with larger heads due to anteriorization (Fig. 3A,E) [180]. Embryos were less sensitive to Wnt inhibition after the SP stage, with no overt changes in head size observed with heat-shock beginning at the TB stage (Fig. 3B-D,F-H). In contrast to the ostensible loss of muscles from excess Wnt signaling, it was difficult to assess if there was an increase in PM number, despite their overtly larger heads. Therefore, we counted muscle nuclei number in the AM muscle of embryos with decreased Wnt signaling prior to gastrulation and found that the muscles were composed of more cells (Fig. 4A-C). Although we attempted to analyze the requirement of the bicistronic *wnt8a* genes that are required to posteriorize the mesoderm, the embryos were not viable at 72 hpf and precluded analysis at this later stage. Together, these results indicate Wnt signaling is necessary and sufficient to inhibit PM development prior to gastrulation when the organ progenitor fields are being established.

Wnt signaling limits anterior tcf21+ PM progenitors

Since we found that dorso-anterior PMs are most sensitive to perturbation of Wnt signaling during its requirement patterning the anterior-posterior axis, we wanted to understand the effects on distinct populations of the PM progenitors. A recent study demonstrated that *tcf21* marks PM progenitors that give rise to muscles in all the zebrafish pharyngeal arches (1-7) [157]. Initially there are two populations of *tcf21+* cells within the anterior mesoderm, with the anterior *tcf21+* population giving rise to the mandibular (1^{st}) and hyoid (2^{nd}) arches. Therefore, we predicted that the anterior *tcf21+* populations that give rise to the muscle within the 1^{st} and 2^{nd} pharyngeal arches would be lost or disrupted. To examine the PM progenitor populations after manipulation of Wnt signaling, we depleted Tcf7l1 and Wnt8a from *Tg(tcf21:nucEGFP)* embryos. We found that depletion of Tcf7l1 proteins inhibited the development of the anterior most population of *tcf21+* cells (we have designated field 1) at 24 hpf (Fig. 5A,B). Counting the *tcf21+* cells at 24hpf, which is facilitated by the nuclear GFP, indicated there was a significant decrease in the number of anterior *tcf21+* progenitors in field 1 (Fig. 5D). Conversely, inhibiting endogenous Wnt signaling via Wnt8a depletion led to an increased size of the anterior field 1 and number of *tcf21+* cells (Fig. 5A,C,D). Additionally, even though both field 1 and field 2 give rise to PMs in the both the 1^{st} and 2^{nd} arches [157], manipulation of Wnt signaling did not affect the number of adjacent field 2 *tcf21+* cells. Taken together, our data suggests manipulation of Wnt signaling affects the number of cells in the anterior most *tcf21+* progenitor fields, which give rise to the dorso-anterior PMs in the 1^{st} and 2^{nd} arches.

Wnt signaling affects the overlap of nkx2.5 and tcf21 fields

Previous studies demonstrated that increased Wnt signaling prior to gastrulation, when it patterns the anterior-posterior axis, produces increased cardiac specification in zebrafish [50, 171]. Therefore, we wanted to understand the relationship of the cardiac and PM progenitors after early Wnt signaling manipulation. We used the *Tg(nkx2.5:ZsYellow)* line to facilitate visualization of *nkx2.5*+ cells, which primarily mark cardiac progenitors at mid-somitogenesis [163], and the aforementioned heat-shock lines. Embryos were heat-shocked at the SP stage, as above, and we performed two-color in situ hybridization (ISH) with *tcf21* and *zsyellow* (*nkx2.5*+ cells), in order to examine the relative effects on these populations within the ALPM. While normally there is a small region of overlap with *nkx2.5* expression in the most anterior *tcf21*+ population ALPM (Fig. 6A,C), as has been reported previously [157], increasing Wnt signaling led to an expansion of *nkx2.5* expression into the *tcf21*+ pharyngeal field at 18s stage (Fig. 6A,B). Conversely, decreasing Wnt signaling caused less overlap of *tcf21* and *nkx2.5* expression (Fig. 6C,D). To further examine the relationship between these markers, we depleted Tcf7l1 and Wnt8a proteins in *Tg(nkx2.5:zsyellow);Tg(tcf21:nucEGFP)* embryos and performed immunohistochemistry (IHC). Surprisingly, measuring the expression domains revealed that the overall length of the anterior *tcf21*+ progenitor domain, which will give rise to PMs of the 1st and 2nd arches, was expanded at 18s in Tcf7l1 depleted embryos (Fig. 7A-C). Consistent with the ISH analysis of heat-shock Wnt induction, the overlap between *nkx2.5*+ and *tcf21*+ progenitor populations within this domain was also expanded (Fig. 7A-C). Conversely, in Wnt8a depleted embryos, the overall anterior *tcf21*+ population was minimally reduced, with the overlapping *tcf21*+ and *nkx2.5*+ domains also being reduced (Fig. 7D,E,F). Altogether, our data suggest that

enhancing or reducing Wnt signaling prior to gastrulation changes the overlap between *nkx2.5*+ and *tcf21*+ domains within the ALPM.

While it is understood that Wnt signaling promotes cardiac specification prior to gastrulation [50, 171], the source of the surplus cardiac cells is not clear. Specifically, *nkx2.5*+ cells give rise to both FHF and SHF-derived ventricular cardiomyocytes [163, 181]. Additionally, a fate map of the ALPM in zebrafish has suggested that SHF progenitors lie anterior and medial to the FHF progenitors [182]. Because anterior fates within the ALPM including the PM and hematovascular progenitors are lost [176], one possibility is that excess Wnt signaling promotes cardiomyocyte specification through differential effects on the first and SHFs. Specifically, we hypothesized that early Wnt signaling may promote FHF at the expense of SHF. In order to determine if the SHF derivatives are affected by excess early Wnt signaling, we first performed *in situ* hybridization for *elastin b* (*elnb*), which is expressed in the smooth muscle cells of the OFT [159, 182], after heat-shock induction of Wnt8a-GFP at the SP stage. Interestingly, embryos with increased Wnt signaling prior to gastrulation had reduced or complete absence of *elnb*+ cells (Fig. 8A-C). To further assay the effects on SHF progenitor markers after increased Wnt signaling, we used real-time quantitative PCR (RT-qPCR) for the SHF progenitor markers *mef2cb* and *ltbp3* at 24 hpf [159, 183]. At 24 hpf, when there was already increased FHF progenitor differentiation as indicated with *myl7* expression, there was a corresponding decrease in SHF progenitor expression (Fig. 8D). Altogether, our data suggest early Wnt signaling promotes an expansion of FHF progenitors at the expense of neighboring SHF and PM progenitors.

Wnt signaling acts cell-autonomously in PM progenitors

We next wanted to understand if Wnt signaling is acting directly within PM progenitors or indirectly through affecting the surrounding environment to inhibit PM development. To determine the cellular requirements of Wnt signaling, we performed blastula cell transplantation with Tcf7l1 depleted donor cells that were from embryos simultaneously carrying the *myl7:EGFP* and *α-actin:GFP* transgenes, which allowed unambiguous visualization of the differentiated CMs and PMs (Fig. 9A). After transplantation of cells at the SP stages, the frequency of donor cell contribution to heart and PMs, respectively, was assayed at 72 hpf (Fig. 9B,C). Consistent with what we have previously reported [176], when Tcf7l1 depleted donors cells were transplanted into the WT host embryos, we observed a significantly higher percentage of embryos with contribution to the cardiomyocyte lineage compared to WT donors transplanted into WT hosts. However, in the same set of experiments, the frequency of contribution to the PMs in embryos was significantly lower from Tcf7l1 depleted donor cells compared with WT donors transplanted to WT host embryos (Fig. 8D). One caveat of this experiment is that we rarely observed contribution to the dorsal 1st and 2nd arch muscles even from WT donor cells, suggesting these progenitors are a relatively rare population of cells. Overall, these results suggest Wnt signaling is cell autonomously required to repress PM development.

Discussion

In this study, we examined the role of Wnt signaling in allocating cardiac and PM cells during development. Using temporal activation and inhibition of Wnt signaling, as well as depletion of endogenous Wnt signaling ligand and transcriptional repressors, we found PM is most sensitive to manipulation of Wnt signaling prior to gastrulation in zebrafish. Increased Wnt signaling prior to gastrulation caused a severe reduction in anterior ventral 1st and 2nd arch muscles and loss of the dorsal 1st and 2nd arch muscles. Consistent with these phenotypes, increases and decreases in Wnt signaling reduce and expand, respectively, the most anterior *tcf21*+ cell population, which harbors PM progenitors. Despite an expansion of the overall domain containing anterior *tcf21*+ cells within the ALPM, the increased cardiomyocytes at the expense of PMs is due to early Wnt signaling promoting FHF specification at the expense of the more anterior fates, which include the adjacent PM and SHF progenitors. Finally, blastula cell transplantation demonstrates that early Wnt signaling cell autonomously controls the specification of PM progenitors.

Previous analysis of chick embryos had implicated Wnt and BMP signals from the neural tube as inhibitors of PM development [177]. It has been proposed that inhibition of Wnt signaling via Frzb, which is endogenously expressed in the pharyngeal ectoderm, is sufficient to promote PM development in chick explants. Based on these previous results, which implicated a role for Wnt signaling during somitogenesis, when the neural tube and pharyngeal arches had formed in chick embryos, we expected to observe later requirements for Wnt signaling in PM development. Thus, we did not anticipate that PM development would be most sensitive to modulation of Wnt signaling prior to gastrulation during anterior-posterior patterning in zebrafish. Although we cannot rule out very subtle defects in the PMs, we did not find any

evidence that PM development was perturbed when Wnt was manipulated after the end of gastrulation and during somitogenesis. Therefore, in contrast to the previous results examining chicken embryos, our results suggest that Wnt signaling inhibits PM development as part of its role establishing anterior-posterior patterning of the mesoderm in zebrafish.

Studies in mice have suggested there is a rare bi-potent pool of progenitors that can give rise to both SHF-derived cardiomyocytes and PMs [60, 165]. Based on the adjacent locations of cardiac and PM progenitors in the anterior lateral plate and paraxial mesoderm, it is has been proposed that bi-potential progenitors with cardiac and PM potential may lie at this border [61, 156]. Despite the close association of these progenitors and shared markers at later developmental stages, more recent lineage tracing studies using Confetti and MADM with Mesp1 inducible Cre-drivers indicate that cardiac FHF and SHF progenitors acquire their fates during gastrulation [164, 184]. Therefore, the proposed bi-potent cardio-pharyngeal progenitors may actually arise from progenitors at these early stages rather than existing at later stages. While our study does not directly address the existence of cardio-pharyngeal progenitors or when they emerge, our results highlight the closeness of these fields with the anterior mesoderm. Furthermore, in line with the idea that mesodermal lineage potential is established very early during vertebrate development, our results indicate that patterning events mediated by Wnt signaling prior to gastrulation partition the adjacent cardiac and PM progenitors through inverse effects on their specification.

Our data indicate that Wnt signaling affects the fates of cardiac and PM progenitors as part of its role during anterior-posterior mesoderm patterning. However, it was counterintuitive that during later somitogenesis, after an early increase in Wnt signaling, the overlap of the anterior-most *tcf21*+ and *nkx2.5*+ progenitors was expanded, while decreasing early Wnt

signaling had the opposite effect. The overlapping anterior-most *tcf21*+ and *nkx2.5*+ expressing cells within the ALPM give rise to the ventral 1st and 2nd arch muscles [157]. Therefore, given the expansion of the *tcf21+/nkx2.5*+ field after increased Wnt signaling prior to gastrulation, it is unexpected that these ventral PMs were actually overtly reduced, and not expanded,. By comparison, the dorsal 1st and 2nd arch muscles are derived from the adjacent, more anterior progenitors that only express *tcf21* [157]. Thus, the loss of these dorsal PMs is consistent with posteriorization from excess early Wnt signaling and the reduction in the anterior most *tcf21*+ progenitor field. Clearly, our data indicate Wnt signaling helps to define the border between the *tcf21*+ and *tcf21+/nkx2.5*+ progenitors within the anterior mesoderm. However, because we observe increased overlap of the *tcf21*+ and *nkx2.5*+ populations and not strictly an expansion of *nkx2.5* at the expense of *tcf21*, our data support that the expansion of genes promoting FHF cardiac potential from excess Wnt signaling overrides some of the developmental potential of the ventral 1st and 2nd arch muscle progenitors. It is unlikely to be Nkx2.5 alone that confers this potential as a recent study indicated overexpression of Nkx2.5 does not promote cardiac specification [181]. Another possible interpretation of our results could be that Wnt signaling promotes SHF-derived cardiac specification at the expense of PM and SHF-derived smooth muscles and endothelial cells. However, we think this interpretation is unlikely given expression of the established SHF progenitor markers is reduced. Taking into account our and others' studies of the effects on anterior vascular progenitors [50, 185], our results suggest that during anterior-posterior patterning Wnt signaling promotes FHF specification at the expense of the adjacent more anterior hematovascular, PMs, and SHF cardiac progenitors.

In conclusion, our study provides insight into a previously unappreciated role of Wnt signaling in balancing cardiac and PM development of vertebrates. Our results indicate that at

least in zebrafish the major inhibitory effects of Wnt signaling on PM development occur during anterior-posterior patterning of the mesoderm, which coincides with recent data supporting very early lineage restriction of mesodermal progenitors in mammals [60, 184]. Regulation of the molecular interface between FHF, SHF and PM specification is an exciting field open for further investigation. Knowledge of mechanisms that direct the fate choices of progenitors within the cardio-pharyngeal field is necessary to enhance our potential of preventing congenital syndromes with both cardiac and cranio-facial malformations.

Experimental Procedures

Zebrafish husbandry and transgenic lines

Zebrafish were raised and maintained following standard laboratory conditions [186]. Transgenic lines used were: *Tg(hsp70l:wnt8a-GFP)*^{w34} [187] *Tg(hsp70l:dkk1-GFP)*^{w32} [188], *Tg(α-actin:GFP)* [189], *Tg(tcf21:nucEGFP)*^{pd41}*[190], TgBAC(−36nkx2.5:ZsYellow) [159], Tg(−5.1myl7:EGFP)*^{twu2} [191].

Heat-shock experiments and imaging of live embryos

For heat-shock experiments hemizygous *Tg(hsp70l:wnt8a-GFP)* and *Tg(hsp70l:dkk1-GFP)* were crossed with *Tg(α-actin-GFP), Tg(tcf21:nucEGFP) TgBAC(−36nkx2.5:ZsYellow),* and *Tg(−5.1myl7:EGFP)* fish. Embryos were heat-shocked at 37ºC for 30 min in a BioRad PCR machine. 1 hour post heat-shock GFP+ transgenic siblings were sorted from the GFP- siblings, which served as controls, using a Zeiss M2BioV12 Stereomicroscope. Embryos heat-shocked at early stages exhibited dorsalized and ventralized phenotypes upon Wnt modulation as described previously [187, 188], which served as a confirmation that we are manipulating Wnt signaling properly. At 72 hpf, embryos were anesthetized with Tricaine (Sigma) and imaged with a Zeiss AxioImager with Apotome. To prevent pigmentation, 0.003% 1-phenyl-2-thiourea (PTU) treatment starting from 24hpf was used.

Zebrafish morpholino (MO) oligonucleotide injection

Zebrafish embryos were injected at the one cell stage with a mixture of 3.5 ng *tcf71la* and 2.5 ng *tcf71lb* MOs, as previously reported [176]. *Wnt8a.1* and *wnt8a.2* MOs were injected at a dose of 2 ng of each [180]. For all MO injections, 1 ng of *p53* MO was co-injected to prevent non-specific induced cell death [116].

Whole mount Immunohistochemistry and cell counting

Immunohistochemistry (IHC) was performed as described previously [171]. The following antibodies were used: chicken anti-GFP primary antibody (1:250; Abcam), anti-chicken FITC secondary antibody (1:100; Southern Biotech), anti-RCFP rabbit polyclonal primary antibody (1:50; Clontech), anti-rabbit TRITC secondary antibody (1:200; Southern Biotech), anti-MHC monoclonal antibody (MF20) (1:10; Gift of D. Yelon). Embryos were imaged using a Zeiss AxioImager with Apotome. To determine the number of *tcf21*+ progenitors at 24 hpf, after IHC was performed, embryos were mounted laterally and the GFP expressing cells were imaged. Fluorescent nuclei were then counted. To determine the overlap of *tcf21*+ and *nkx2.5*+ progenitors at the 18s stage, the embryos were mounted dorsally and the different populations were imaged. Measurement of the length of domains was performed using ImageJ. Statistical significance for cell counting and length measurements was assessed using Student's t-test with $p<0.05$ being considered statistically significant.

In situ hybridization (ISH)

Single and two-color ISH were done as described previously [180, 192]. All probes were reported previously: *tbx1* (ZDB-GENE-030805-5), *tcf21* (ZDB-GENE-051113-88), *dlx2* (ZDB-GENE-980526), *six1b* (ZDB-GENE-040426-2308), and, *zsyellow* (accession number: Q9U6Y4). INT-BCIP (Roche) and Fast red (Sigma) were used for two-color ISH. For images, embryo yolks were manually removed, the embryos were flat mounted and imaged using a Zeiss AxioImager2 compound microscope.

Quantitative real time PCR (RT-qPCR)

RT-qPCR was performed as described previously [193]. Briefly, total RNA was extracted from a pool of 30 whole embryos. Embryos were homogenized using Trizol (Ambion) and RNA was extracted using Purelink RNA Microkit (Invitrogen). 1ug of RNA was used to prepare cDNA using the ThermoScript Reverse Transcriptase kit (Invitrogen). PCR was performed in a BioRad CFX-96 PCR machine with Power SYBR Green PCR Master Mix (Applied Biosystems). Gene expression levels were standardized to β-actin and analyzed using the 2-ΔΔCT Livak Method and Student's *t*-test. *Myl7* and *ltbp3* primer sequences were described previously [193] and [159]. Sequences for *mef2cb* primers are: F-ctatggaaaccaccgcaact and R-tgcgcagactgagagttgtt.

Blastula cell transplantation

For blastula cell transplantation, homozygous *Tg (myl7:EGFP)* and *Tg(α-actin:GFP)* adults were crossed. The resulting embryos were used as donors and injected at one-cell stage with rhodamine-dextran lineage tracer along with the *tcf7l1* MOs. Approximately 30 cells from the control or *tcf7l1* depleted embryos were transplanted to the margin of control host blastula margin at SP stage. Embryos were raised and scored for CM and PM contribution at 48 and 72 hpf, respectively. The statistical significance of differences in the different populations was compared using a Chi-squared test with $p<0.05$ being considered statistically significant.

Acknowledgments

The authors are grateful to A. Rydeen and J. Schumacher for comments on the manuscript. This research was supported by grants March of Dimes Grant 6-FY14-389 and NIH Grant R01 HL112893 to JSW.

Figure Legends

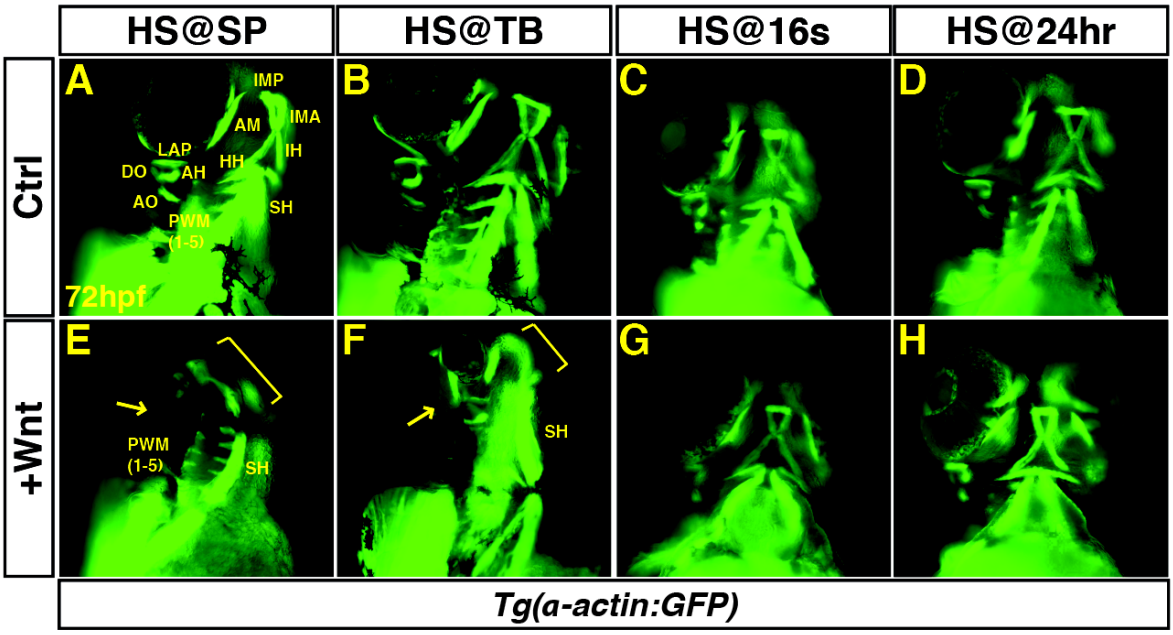

Figure 1. Excess Wnt signaling inhibits PM development during gastrulation. (A-P) *Tg(α-actin:GFP)* control sibling embryos and embryos with increased Wnt signaling (*hsp70l:wnt8a-GFP+*). (A,E) After increasing Wnt signaling from heat-shock (HS) at the SP stage, the EOMs, dorsal 1st and 2nd arch PMs are lost (arrow), while the ventral 1st and 2nd arch PMs are reduced (bracket). PW muscles are also lost and reduced, while the SH was overtly unaffected. (B,F) After increasing Wnt signaling at the TB stage, there is a similar but less severe loss of EOMs, 1st and 2nd arch PMs (dorsal PMs – arrow; ventral PMs bracket). (C, G, D, H) Wnt signaling does not overtly affect PM development at later stages. Muscle nomenclature used is from [178]. 1st arch muscles - intermandibularis anterior (IMA), intermandibularis posterior (IMP), adductor mandibulae (AM), levator arcus palatine (LAP), dilatator opercula (DO). 2nd (hyoid) arch muscles - hyohyal (HH), interhyal (IH), adductor hyomandibulae (AH), adductor opercula (AO), and levator opercula (LO). Embryos are at 72 hpf. Images are anterior ventro-lateral views. Anterior is up in all images. Heat-shock (HS).

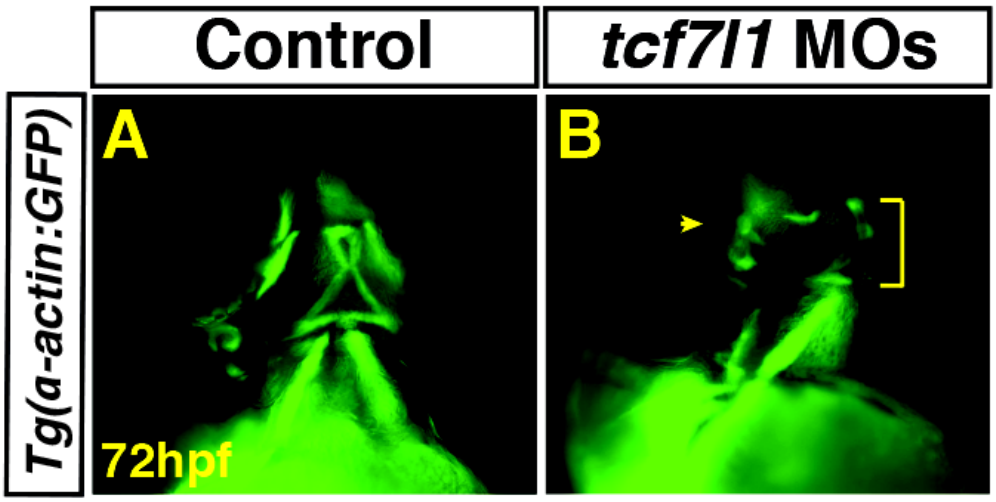

Figure 2. Tcf7l1 depletion causes loss of dorso-anterior PMs. (A-B) Control and Tcf7l1 depleted *Tg(α-actin:GFP)* embryos at 72 hpf. Tcf7l1 depletion resulted in similar loss of dorso-anterior PMs loss as increasing Wnt signaling prior to gastrulation. EOMs (arrows), 1st, 2nd, and dorsal PWMs are severely reduced and misorganized or lost (arrowhead). Ventral 1st and 2nd arch muscles are reduced (bracket). Views are anterior ventro-lateral.

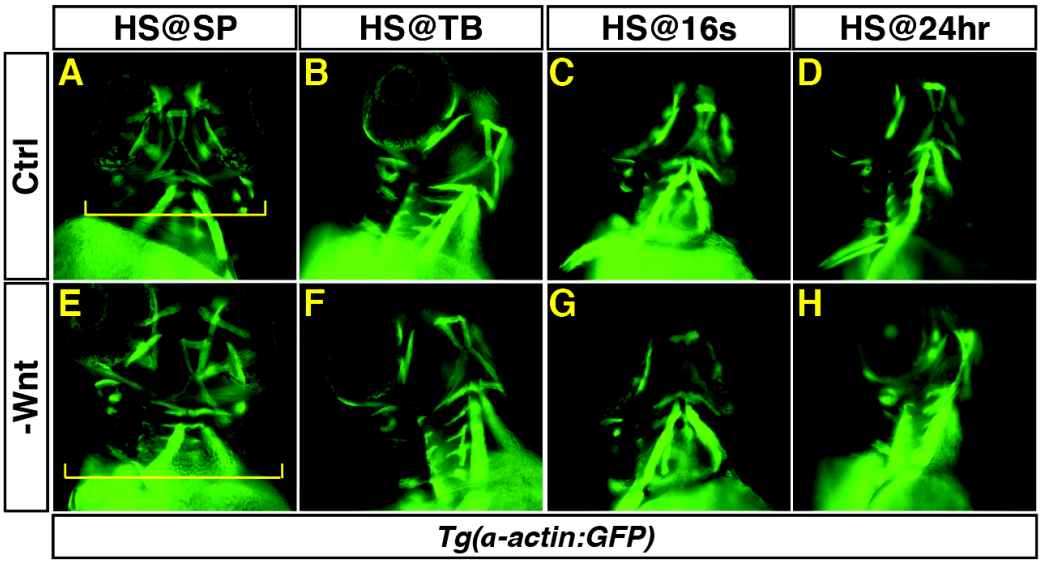

Figure 3. Decreased Wnt signaling inhibits PM development during gastrulation. (A-H) *Tg(α-actin:GFP)* control sibling embryos and embryos with decreased Wnt signaling (*hsp70l:dkk1-GFP*+). (A,E) After decreasing Wnt signaling at the SP stage, the embryos have enlarged heads (brackets). (B-D, F-H) After decreasing Wnt signaling at later stages, there was no discernible effect on pharyngeal muscles. Embryos are at 72 hpf. Images in A,E are anterior ventral views. Images in B-D, F-H are anterior ventro-lateral views. Anterior is up in all images. Heat-shock (HS).

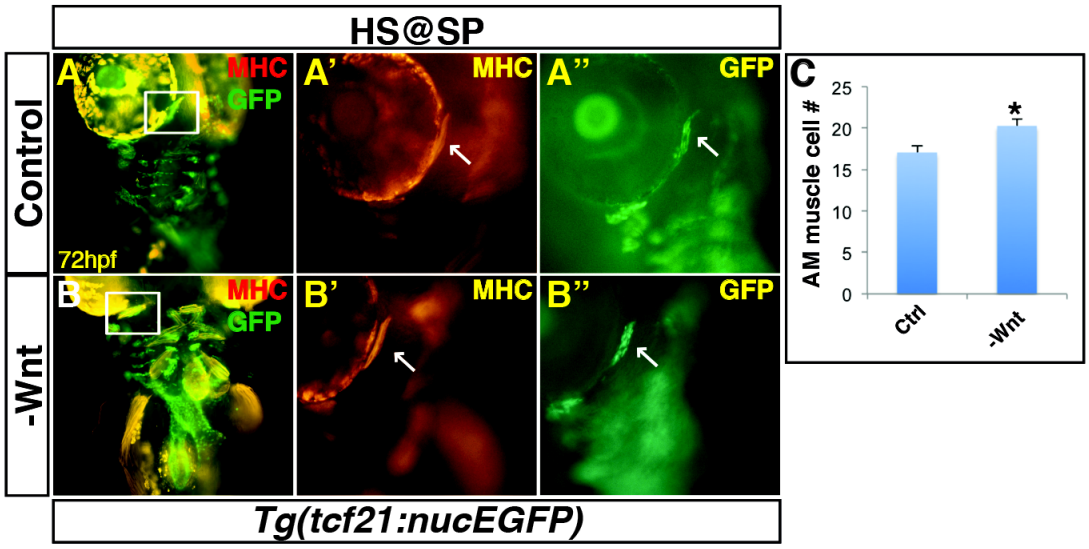

Figure 4. Decreased Wnt signaling causes an increase in 1st arch PM cells. (A, B) *Tg(tcf21:nucEGFP)* control sibling embryos and embryos with decreased Wnt signaling at the SP stage. Decreased Wnt signaling causes enlargement of the 1st arch AM muscle (boxes). Sarcomeric myosin (MHC; red). NucGFP (green). (A', B') MHC alone of AM muscles (arrow) (A", B") NucEGFP alone of AM (arrow). (G) Graph depicting quantification of nuclei in the AM muscles. Decreasing Wnt signaling at the SP stage produces a significant increase in AM muscle nuclei. Control embryos n=15, *Tg(hsp70l:dkk1-GFP)* embryos n=7. Asterisks in all graphs indicate $p<0.05$. Error bars in all graphs indicate S.E.M.

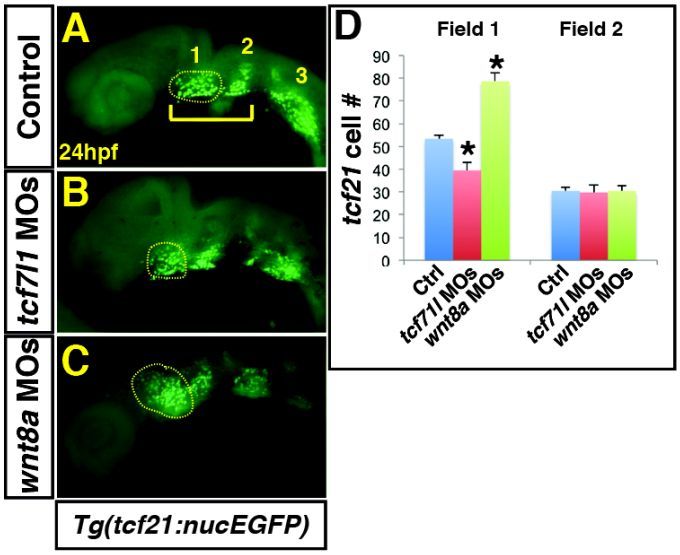

Figure 5. Endogenous Wnt signaling components restrict *tcf21*+ PM progenitor development. (A, B, C) *Tg(tcf21:nucEGFP)* control, Tcf7l1 depleted, and Wnt8a depleted embryos at 24 hpf. Bracket in A indicates the anterior *tcf21*+ field of cells that give rise to the 1st and 2nd arch muscles. Numbers 1 and 2 indicate the two anterior tcf21+ fields of cells. Number 3 indicates the more posterior *tcf21*+ population that gives rise to PM in arches 3-7 [157]. (B) Tcf7l1 depletion produces a loss of the anterior most *tcf21*+ progenitors (yellow outline). (C) Wnt8a depletion results in expansion of the anterior most pharyngeal *tcf21*+ progenitors. (D) Graph depicting quantification of *tcf21*+ progenitors. There is a significant decrease in *tcf21*+ progenitors with Tcf7l1 depletion and conversely a significant increased in tcf21+ progenitors following Wnt8a depletion. Images are lateral views with anterior left. Field 1 control embryos n=11; Tcf7l1 depleted embryos n=7; Wnt8a depleted embryos n=9. Field 2 control embryos n=11; Tcf7l1 depleted embryos n=6; Wnt8a depleted embryos n=8.

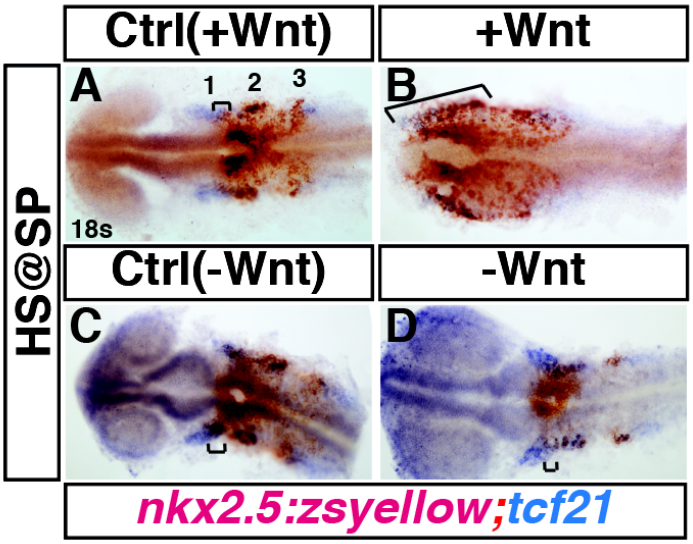

Figure 6. Manipulation of Wnt signaling affects the overlap of *nkx2.5*+ and *tcf21*+ domains within the ALPM. (A-D) *Tg(nkx2.5:ZsYellow)* control sibling embryos and embryos with increased and decreased Wnt signaling at the SP stage. (A,B) Two-color ISH of *nkx2.5:zsyellow* (red) and *tcf21* (blue) at the 18s stage shows expansion of the lateral *nkx2.5*+ domains into the anterior *tcf21*+ domain after increased Wnt signaling. Numbers in A indicate the three *tcf21*+ fields depicted in Figure 5. (C, D) Decreasing Wnt signaling prior to gastrulation causes a decrease in the overlap of *nkx2.5* and *tcf21*. Images are dorsal views with anterior to left. Brackets indicate overlap of *nkx2.5*+ and *tcf21*+ domains. For each group >15 embryos were examined.

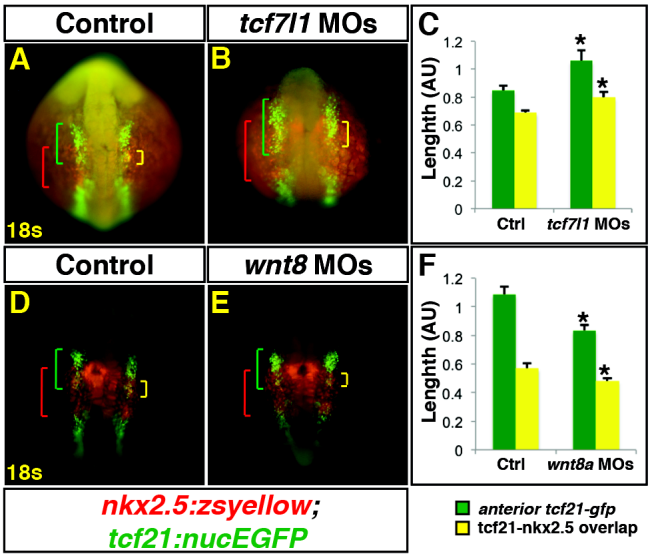

Figure 7. Manipulation of endogenous Wnt signaling affects the size of the *nkx2.5*+ and *tcf21*+ domains. (A,B,D,E) *Tg(nkx2.5:ZsYellow);Tg(tcf21:nucEGFP)* control, Tcf7l1 depleted, and Wnt8a depleted embryos at the 18s stage. Tcf7l1 depletion expands the total anterior *tcf21*+ progenitor domain length (green brackets) as well as the overlapping expression (yellow brackets) within the ALPM. (C) Graph depicting measurements of the total *tcf21*+ progenitors and overlap with *nkx2.5*+ progenitors from Tcf7l1 depleted embryos. Control embryos n=10, Tcf7l1 depleted embryos n=9. (D, E) Wnt8a depletion reduces the overall length of the *tcf21*+ domain and the overlap with the *nkx2.5*+ progenitor domain. (F) Graph depicting measurements of the total *tcf21*+ progenitors and overlap with *nkx2.5*+ progenitors from Wnt8a depleted embryos. Control embryos n=8, Wnt8a depleted embryos n=10. Green brackets - anterior *tcf21*+ progenitors. Red brackets - *nkx2.5*+ progenitors. Yellow brackets – regions of overlap between *tcf21*+ and *nkx2.5*+ domains.

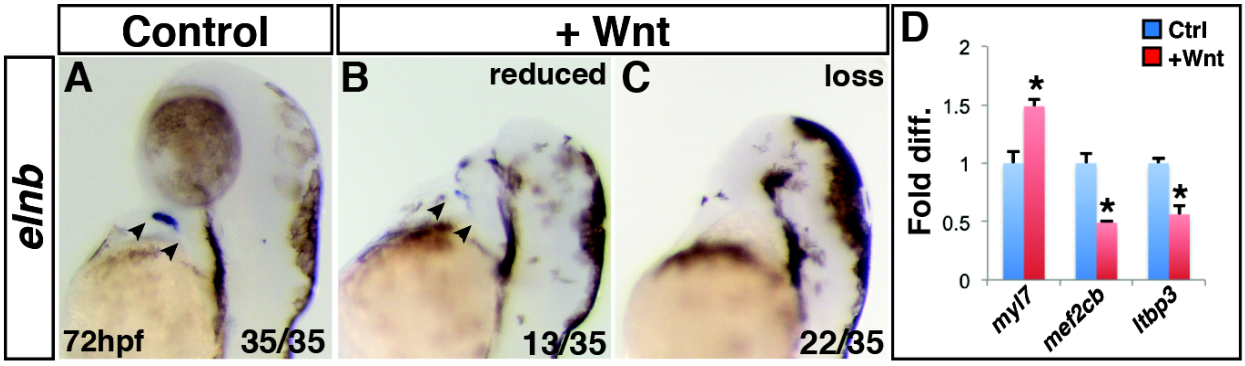

Figure 8. Increased Wnt signaling promotes loss of the SHF. (A-C) Control sibling embryos and embryos after increased Wnt signaling at the SP stage. Increasing Wnt signaling prior to gastrulation leads to loss of the SHF-derived OFT smooth muscle (*elnb)*. (D) RT-qPCR for cardiac differentiation and SHF progenitor marker expression at 24 hpf. Increasing Wnt signaling prior to gastrulation promotes increased expression of the pan-cardiac differentiation marker *myl7* and decreased expression of the SHF markers *mef2cb* and *ltbp3* compared to WT sibling controls. Images are lateral views with anterior upward.

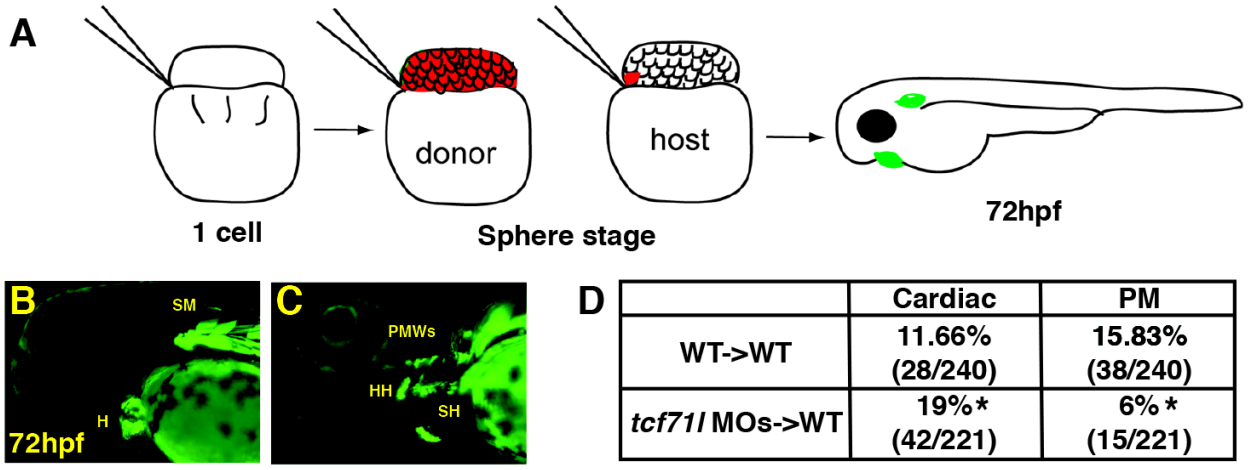

D

	Cardiac	PM
WT->WT	11.66% (28/240)	15.83% (38/240)
tcf7l1 MOs->WT	19%* (42/221)	6%* (15/221)

Figure 9. Wnt signaling cell-autonomously inhibits PM specification: (A) Schematic of blastula cell transplantation method. (B, C) Representative donor cells that incorporated into the heart and PMs at 72 hpf. (D) Frequency of donor cell contribution to the heart and the PMs. Numbers in brackets indicate the number of embryos that had donor cell contribution out of the total number of host embryos. Tcf7l1 depleted donor cells contributed significantly more to the cardiomyocytes and less frequently to the PMs compared to WT donors. Images are lateral views with anterior leftwards.

Chapter 5:

Discussion

Discussion Part I: Generation and characterization of a novel RA reporter

Previous RA reporters in mice and zebrafish were created using the consensus-binding site for RAR/RXR i.e. RARE. Although there was improvement in reporter activity by increasing the copy number of DR5 RARE sequences in these transgenics, it did not reflect all possible areas of active RA signaling [11, 23, 25]. This limitation can be attributed to the fact that synthetic promoters often lack necessary enhancers and local chromatin and epigenetic conformation essential for transcription in vivo. Other than local availability of RA, these RARE driven lines depend on proper RAR/RXR heterodimer formation for reporter activity. Our novel RA sensor was created based on a ligand trap method where GFP expression is dependent only on ligand (RA) availability. Thus, it avoids additional factors (co-activators, co-repressors, receptor dimerization etc.), which might hinder reporter activity. Expression in this novel sensor initiated earlier than the previously characterized transcriptional reporters since ligand availability precedes transcription. This novel RA sensor has been used in studies from our lab as an accurate readout of embryonic RA. For example, this novel stable line was used to asses the effect of functional interactions between RAR and RA degrading enzyme Cyp26 on embryonic RA level [194]. Another study has used the RA sensor line to gain insight about the effect of hyperactive RAR expression on embryonic RA [195]. These studies further enhance the applicability of the novel reporter to study RA biology.

Although there are some advantages, there are some caveats to the sensor line. The expression was broader in the novel GDBD sensors still it was comparatively restricted and could not reflect all available endogenous RA. Previous studies have shown that co-operation between the N and C terminal transcriptional activation domain of both the RXR and RAR is required for maximal transcriptional output and tissue specific co-activator recruitment.

Additionally, *in vitro* assays have shown the extent of this co-operation is cell type and promoter context dependent and specific for each type of RAR/RXR isoform [94]. These observations suggest combinatorial factors acting at various levels need to act synergistically to achieve maximal transcription of RA target genes. For our transgenic RA sensor, we have used the C-terminal ligand-binding domain of RARαb. This construct lacks the N-terminal domain, which might not be optimal for RA induced transcriptional activation in certain cells or tissues. Maximal and efficient reporter activity depends on various factors such as the choice of targeting vectors, promoters, reporter proteins etc. Although expression from the RA sensor is consistently high in the mid region of the embryo where there is known high endogenous RA, but it was still not present in all tissues known to have RA [11, 26, 100]. This absence in reporter expression might be attributed to the fact that synthetic reporters lack *in vivo* epigenetic, genetic and non-genomic signature, which have profound effect on tissue specific gene expression. Transcriptional activity of RA can also mediate via another family of nuclear receptor PPARβ/δ. Thus, tissues in which RA acts through these receptors would not be detected by this sensor [196]. One caveat of the VP16-GDBD line was treatment with RA pathway antagonists were not able to completely eliminate reporter expression. This might give a false negative result in the context of testing novel drugs against RA signaling.

Nuclear receptors are being widely studied due to their potential application in the pharmaceutical industry [64]. We have knowledge of transcriptional co-activators and repressors binding to RAR/RXR heterodimer, but identification of tissue and stage specific ligands will add immense value to discover novel drug targets for RA pathway. Addition of desired protein tags in the ligand trap vector and subsequent extraction and analysis of bound cofactors at different

developmental stage and tissues will unravel a huge amount of valuable information about factors that interact with RA signaling pathway at a precise spatial and temporal resolution.

Discussion Part II: *Dact3* expression and regulation

Dact proteins are known to directly interact with *disheveled* and *vangl2* thus regulating both canonical and non-canonical branches of Wnt signaling [28]. In zebrafish, knockdown of *dact1* using MO results in subtle defect in the midbrain-hindbrain boundary and diencephalon. Injection of both *dact1* and *wnt8* MOs phenocopy loss of canonical Wnt signaling, suggesting Dact1 is a positive regulator of canonical Wnt signaling in zebrafish within this context. In contrast to Dact1, *dact2* morphants have a stronger early phenotype, which includes defects in convergent extensions movement during gastrulation. To understand if *dact2* functionally interacts with canonical or non-canonical Wnt pathways similar to Dact1, double morphant phenotypes were assessed. It was found *dact2* interacts with the non-canonical Wnt member *wnt11*, suggesting it regulates non-canonical Wnt signaling. Thus, *dact1* and *dact2* can play distinct role during zebrafish development [29]. Although Dact1 and Dact2 have been functionally characterized in zebrafish and mice, less is known about Dact3. Here, we have analyzed the expression and regulation of the *dact3* paralogous genes *dact3a* and *dact3b* in zebrafish. Some areas of expression for *dact3a* were cranial neural crest cells, somites, pectoral fin bud and various populations of hindbrain neurons. Dact3b was specifically expressed in populations of hindbrain neurons of rhombomere (r) 4 to 6. We have also found that treatment with the RA antagonist DEAB results in posterior expansion of *dact3b* in the hindbrain and spinal cord. This might suggest endogenous RA is required to keep those more posterior tissues

free from *dact3b*. *Dact3b* is expressed in the 2nd pharyngeal arch where RA is generally absent but late treatment with RA can diminish the pharyngeal expression. Although we did not observe any specific early phenotype for the *dact3b* morphants, generating *dact3b* zebrafish mutant using the CRISPR/Cas9 system may give us insight into the requirement of *dact3* in these tissues. Additional experiments such as co-immunoprecipitation and promoter analysis is necessary to decide if RA directly binds with *dact3b.* Additionally, because Dact proteins are known regulators for canonical and non-canonical Wnt signaling, it would be interesting to study if *dact3b* is acting as a linker between these two pathways during hindbrain development. RA is well known for its role in hindbrain patterning [26, 106]. The RA signaling gradient is high in the posterior hindbrain while Wnt is present consistently along the A-P axis. Different levels of RA might regulate how Wnt influence the hindbrain development. Further study is required to establish if *dact3b* plays a role in cross-regulation of Wnt and RA signaling during hindbrain development.

Discussion Part III: Wnt signaling in cardiac & PM specification

A previous study has shown Wnt inhibits head muscle formation at somitogenesis [55]. However, it is not known if there is any temporal requirement for Wnt during head muscle development. Our study has shown an increase in Wnt signaling leads to loss of the dorso-anterior mandibular and hyoid arch derived muscles. Recent work in zebrafish has shown these specific anterior muscles originate from the anterior *tcf21*+ progenitors in the ALPM [157] (Figure 1). This anterior ALPM harbors progenitors for other lineages such as vessels and blood [197]. In the absence of a hemato-angiogenic signal, the anterior most ALPM can form cardiac

lineage. This data suggests the anterior most part of the ALPM also has latent cardiogenic potential. Lineage tracing studies from our lab and others have found *tcf21*+ cells in zebrafish can give rise to both cardiac and PM cells [157]. Based on this, we can hypothesize Wnt signaling forces the anterior *tcf21*+ population to become FHF derived CMs instead of PM and SHF. The proposed mechanism by which Wnt might favor one fate over another is discussed here.

A recent paper by Nagelberg et al. performed detailed lineage analysis of the mesodermal progenitors in the zebrafish ALPM [157]. According to their data, the ALPM can be subdivided into four distinct regions depending on the lineage contribution (Figure 1). Anterior to posterior the divisions are as follows: 1) the most anterior *pitx2* expressing prechordal mesoderm gives rise to the muscles surrounding the eye (EOM muscles); 2) anterior *tcf21*+ and *tcf21+/nkx2.5*+ populations gives rise to the pharyngeal arch (PA) 1 and 2 derived muscles; 3) the posterior *tcf21*+ and *tcf21+/nkx2.5*+ are specified into the posterior pharyngeal muscles 3-7. Additionally, the anterior *tcf21+/nk2.5*+ population specifically gives rise to the ventral muscles of the PA 1 - 2 and hypobranchial arch artery (HA). Our analysis (Chapter 4, Figure 7) suggested upon Wnt increase length of the anterior *tcf21+/nkx2.5*+ population of overlapping cell is expanded. According to the lineage analysis, this population gives rise to the ventral muscles derived from PA 1 and 2 as well as the HA. In contrast to an increase in ventral muscles, we found they are reduced in size and severely mispatterned. This discrepancy suggests two hypotheses: 1) In the context of excess Wnt, cardio-pharyngeal progenitors cannot form ventral head muscles appropriately and are forced towards FHF derived cardiac lineage. Previous data where it has been shown excess Wnt promotes mesoderm progenitors to form CMs at the expense of other mesoderm-derived lineages further supports this hypothesis [52, 198]. 2) Alternatively, this

anterior *tcf21+/nkx2.5+* population can form the HA at the expense of ventral head muscles. Although this outcome is mostly unlikely since Wnt is known to inhibit vascular specification. Altogether similar genetic requirements, transcription factor expression and signaling molecules suggest there is significant plasticity among hematovascular, cardiac and head muscle progenitors across species. A complete and clear understating of the network regulating the specification of these progenitors will aid in regenerative therapies of many craniofacial and cardiac birth defects.

Our results have shown Wnt promotes loss of muscles originating from pharyngeal mesoderm as well as prechordal plate mesoderm. *Pitx2+* prechordal plate mesoderm is distinct and anterior to *tcf21+* population (Figure 2). Although our data suggests a loss of *tcf21+* progenitors, total length of *tcf21+* ALPM is not changed. One possibility might be that anterior tissue loss includes only *pitx2+* prechordal mesoderm and not the *tcf21+* population. Loss of the *tcf21+* population can be due to changing fate to some other adjacent lineages possible cardiac. Also, it is also very much likely that both posteriorization and the fate change are acting together for the loss of *tcf21* derived PM and SHF. There are a few outstanding questions that follow our findings. Is there any role of the surrounding matrix in fate specification? Do other signaling pathways act in concert with Wnt? Does Wnt act at the chromatin level to balance fate in the CPF? These possibilities are discussed below in the light of evidence from existing literature based on work in the ascidian model organism *Ciona sp*.

Differential fate induction in the CPF of *Ciona* has been attributed to polarized matrix adhesion. B7.5 blastomere founder cell accumulates cell adhesion factors, such as actin and talin, only on ventral side where it is attached to the epidermal matrix [199]. Next, asymmetric cell division redistributes actin only to the daughter cell on the ventral side, which goes on to become

pre-cardiac lineage (TVC) and the dorsal daughter cell becomes atrial tail muscle (ATM) (Figure 3). After cell division of the two daughter cells, they are exposed to different niche/microenvironment, which directs differential downstream signals and subsequent fate induction. Progressive fate induction in *Ciona* has been attributed to external cues from epidermal protrusion and matrix adhesion as well as intrinsic mitotic processes. Protrusion and invasion enhances FGF/MAPK signaling and this acts as an induction to mediate cell fate in *Ciona* [68]. Wnt signaling is known to regulate cell adhesion from multiple studies. Role of Wnt upstream of regulating differential actin accumulation of progenitor cells in the CPF is an exciting question for future studies.

In mice BMP signaling plays important roles in cardiac and PM development [55]. There are reports for interaction between BMP and Wnt during cardiac development [200]. While Wnt signaling plays biphasic role in cardiac development, high level of BMP is required during cardiogenesis at specification, maintenance and differentiation. BMP is known to play inhibitory role in both head and somite derived trunk myogenesis. Since at the time of progenitor specification in the CPF (pre-gastrulation) BMP is present in the ventral mesoderm along with Wnt, there might be interaction among signaling pathways that fine-tune the CPF patterning [201]. Further experiments are required to tease out if BMP signaling plays any role during CPF development along with Wnt.

Another interesting aspect will be to study if Wnt signaling differentially regulates cardiac and pharyngeal gene expression at the level of chromatin. One in vitro report has shown Wnt inhibits histon deacetylase 1 *(HDAC1)* expression, which results in upregulation of cardiac specification gene *nkx2.5* and subsequent increase in early cardiomyogenesis [202]. Addressing the question if Wnt plays any role at the chromatin level to differentially regulate cardiac and

pharyngeal muscle progenitor specification would provide valuable insight into the mechanistic aspect of CPF development. Together, these analyses will help to decipher the mechanism by which Wnt regulates CPF development.

Alternative approaches and future directions:

Generation and characterization of a novel RA reporter

For the RA sensor reporter construct we used GFP as readout for reporter expression. GFP has a long half-life (8hrs), the stability of GFP hinders the ability to monitor rapidly changing early cell signaling dynamics [203]. One approach would be to use a destabilize GFP with a shorter half-life, which would allow to asses rapid changes in the endogenous RA level. *12XRARE:EGFP* line was created using concatenation of 12 synthetic RARE sites. While this line was more sensitive to RA compared to the previous zebrafish transgenic lines with three copies of *RARE*, expression was restricted to few tissues such as ventral eye, pronephros and anterior spinal cord [11]. As mentioned above, one possible reason for this limitation is synthetic promoters often lack necessary enhancers and local chromatin and epigenetic conformation essential for transcription in vivo. One-way to overcome this would be to use RARE sequences from promoters of other RA responsive genes and make reporter constructs. RARE sequence is present in the promoters of *Cyp26, Hox* and *Hnf* genes [204]. It would be interesting to analyze the expression from reporters using these natural promoters and what additional information those lines can give.

Wnt signaling in cardiac & PM specification

Our blastula cell transplantion experiments established cell autonomous roles of Wnt signaling in restricting PM fate. The blastula transplantation in this study was performed using ~20-30 donor cells which increases the probability for multi lineage contribution. One way to address this limitation is to perform single cell transplantation, which will give us an accurate view on lineage relationships since progeny of a single cell typically gives rise to lineage restricted contribution. Our studies did not rule out the possibility of a cell non-autonomous role for Wnt signaling too. A previous study in chicken demonstrated that Wnt signaling from the notochord and dorsal neural tube acts antagonistically during head muscle development [55]. PM progenitors are in close physical proximity to surrounding pharyngeal endoderm, ectoderm and cranial neural crest cells. It is possible Wnt signal from the adjacent tissues also affects PM development significantly. We could use the *Tg (hsp70:ΔTCF-GFP)* line to test the hypothesis if Wnt also plays cell-non-autonomous role during PM development [205].

According to previous zebrafish fate map cardiac progenitors lies more ventral to the head muscle progenitors in the lateral marginal zone [206, 207]. Creating a high-resolution fate map of the cardio-pharyngeal progenitors before gastrulation would also provide further information about the source of excess CMs upon Wnt signaling increase [206]. To generate a fate map of the pre-gastrula embryos, we could use caged-fluorescein mediated fate mapping. For this technique, one-cell stage embryos are injected with caged fluorescein (lineage tracer) and control MO or t*cf7l1ab* MOs. A few cells in the lateral marginal zone of blastula staged embryos would be uncaged using a pulse UV laser and then the contribution of the labeled progenitors are to be traced by performing anti-fluorescein immunostaining. If Wnt signaling is acting to promote cardiac at the expense of PM fate, we expect to see labeled progenitors from

the more ventral lateral margin contributing to cardiac structures instead of pharyngeal in the *tcf7l1ab* morphants. Scoring and comparing contribution to cardiac and pharyngeal lineage between control and Wnt increased embryos will give us further insight on the fate decision in the CPF. Because it appears Wnt promotes loss of *tcf21*+ anterior population, it brings up the question if the excess CMs comes from this *tcf21*+ lineage. A previous lineage study from our lab (data not shown) has shown *tcf21*+ cells in zebrafish can contribute to both PM and cardiac derivatives. The inducible *Tg(tcf21:Cre^{ERT2})* and color-switch *Tg(ubi::CsY)* lines can be used to permanently labels *tcf21*+ expressing cells. We can then treat the embryos with tamoxifen to activate *cre* at 30% epiboly before *tcf21* is turned on to mark all the uncommitted *tcf21* progeny in yellow. If Wnt signaling is acting upstream of *tcf21* to balance the fate decision in CPF then we would expect to see more *tcf21*+ cell in FHF derived structure and less in PM and SHF in the *tcf71lab* morphants (Wnt+) compared to control. This experiment would reveal a direct correlation between cardiac and PM progenitors.

A previous study has shown that the anterior *nkx2.5+/tcf21*+ cells contributes to PM and HA artery. Since our data suggest Wnt can affect the size of this overlapping population. It would be interesting to determine the fate of this *nkx2.5+/tcf21*+ population upon Wnt modulation. One way to determine that would be to use time lapse video analysis using the *tcf21:GFP;nkx2.5:zsyellow* double transgenic embryos. One-cell stage embryos would be injected with the previously mentioned *tcf7l1ab* MO combination to increase and decrease Wnt signaling. Then, we would follow what the overlapping cell population contributes to at 72 hpf when the heart, PM and HA artery are all fully formed by segmenting the movies based on fluorescence intensity from GFP and zsyellow. With these proposed experiments, it will be possible to further elucidate the role of RA and Wnt signaling during vertebrate development.

Discussion Part IV: RA and Wnt in patterning the organ field

RA Wnt and *dact3* in head mesoderm:

The role of RA as a morphogen has been studied extensively with respect to anterior-posterior patterning of the hindbrain [208] . RA is required for the formation of posterior rhombomeres (r5-r7) and anterior spinal cord [21, 85]. More posterior hindbrain rhombomeres require higher levels of RA compared to the more anterior rhombomeres. The RA degrading enzyme *cyp26* is known to maintain a RA free zone in the anterior forebrain and hindbrain. RA increases *cyp26* levels in the anterior hindbrain, thus maintaining self-degradation. In contrast, the synthesizing enzyme *raldh2*, which is present in the posterior presomitic mesoderm and later in the somites, maintains high levels of RA in the posterior part of the hindbrain [112, 208, 209]. Other anterior-posterior patterning morphogens such as FGF and Wnt inhibit RA induced *cyp26* expression, thereby maintaining posterior hindbrain fates [210]. Detailed analysis of head mesoderm patterning in chicken has shown anterior head mesoderm markers, such as *pitx2* and *myoR,* that eventually forms the EOM and mandibular arch muscles require very low level of RA [211]. *Tbx1*, which is expressed towards the caudal end of the anterior hindbrain mesoderm, requires reduction of RA and concomitant increase in FGF level [211]. Dose dependent RA agonist and antagonist treatments have shown anterior head markers are more sensitive to RA compared to posterior genes. In the posterior part of the head mesoderm, RA levels are high enough to inhibit anterior genes, such as *pitx2,* but low enough to allow *tbx1* expression (Figure 4).

Wnt signaling plays critical role in midbrain-hindbrain (MHB) boundary formation via its interaction with FGF and Pax family members [212]. Combinatorial knockdown of canonical Wnt members *wnt3a*, *wnt1* and *wnt10b* in zebrafish leads to loss of a significant part of the midbrain and cerebellum [213]. Critical Wnt members are expressed in the boundary of rhombomores and known to maintain proper rhombomeric boundary formation and neurogenesis in the hindbrain [214]. Thus, we can speculate Wnt and RA act antagonistic to each other during patterning of the anterior fates in the head mesoderm.

In Chapter 3, we discussed a novel observation that RA signaling negatively regulates the Wnt signaling modulator gene *dact3b* in the hindbrain of zebarfish embryos. *Dact3b* expression spans from r4 to r6 and absent in r7. Mutation in *raldh2* leads to loss of r7 signifying the requirement of RA in proper formation of the most posterior hindbrain segment. It is interesting to note that treatment with the RA inhibitor DEAB results in posterior expansion of *dact3b* into r7. From this observation we can speculate RA helps in maintaining low *dact3b* levels in the posterior head mesoderm and Dact3b is required for proper formation of the more anterior head mesoderm. Since Wnt family members are expressed all along the hindbrain segments we can hypothesize anterior *dact3b* and posterior RA expression modifies the activity of Wnt during hindbrain patterning. Previous studies have shown Dact3 acts upstream of Wnt to negatively regulate Wnt signaling in the context of colon cancer as well as kidney fibrosis model in mice [33, 34]. From these information we can hypothesize in the absence of RA excess *dact3b* will repress Wnt signaling leading to mis-patterned rhombomere formation (Figure 6). Similarly *dact3b* inhibition will lead to the release of Wnt suppression and excess Wnt can then inhibit *cyp26* in the anterior forebrain leading to anterior shift of the posterior rhombomeres.

RA and Wnt in cardiac specification:

With respect to early heart development, RA signaling restricts cardiac progenitor specification [22]. Zebrafish mutants for the RA synthesizing enzyme *raldh2,* as well as treatment with RA antagonists, result in expansion of cardiac markers *nkx2.5* and *myl7* [22, 215]. Fate map studies have found inhibition of RA results in excess cardiomyocytes with a concomitant decrease in other adjacent organ fields such as pancreas, pharyngeal pouch and pectoral fin [22]. Treatment with RA antagonists before gastrulation results in expansion of cardiac markers, at the same time point when increase in Wnt signaling lead to similar increase in those cardiac markers [216]. These observations suggest RA and Wnt acts antagonistically in the ALPM to maintain cardiac fate (Figure 5).

Conclusion

In summary, the work presented in this thesis provides valuable insight into the roles of RA and Wnt signaling during zebrafish development. First, we have generated and characterized novel stable transgenic lines to study RA signaling. These RA sensor reporters have already been used in our lab to measure embryonic RA levels in two distinct studies. The RA sensors will add further value to study RA signaling *in vivo* as well as the anatomy of nephrons and motor neurons independent of RA. Next, we have analyzed the expression pattern and regulation of Wnt modulator proteins Dact3a and Dact3b in zebrafish and found that RA negatively regulates *dact3b* expression in the hindbrain. This finding opens up new avenues to study the molecular intersection of RA and Wnt signaling during hindbrain development in zebrafish. Finally, we

have looked into the role of Wnt signaling in balancing cardiac and PM fate in the cardio-pharyngeal field. In this study, we have found Wnt plays a developmental stage specific role in PM development in zebrafish and negatively regulate SHF and PM formation. This is an important field of study providing multiple congenital abnormalities include both cardiac and craniofacial abnormalities. Further work studying the mechanism of how progenitors are fate restricted during cardio-pharyngeal development will help create these types of cells in a dish for regenerative therapy purposes.

Figures

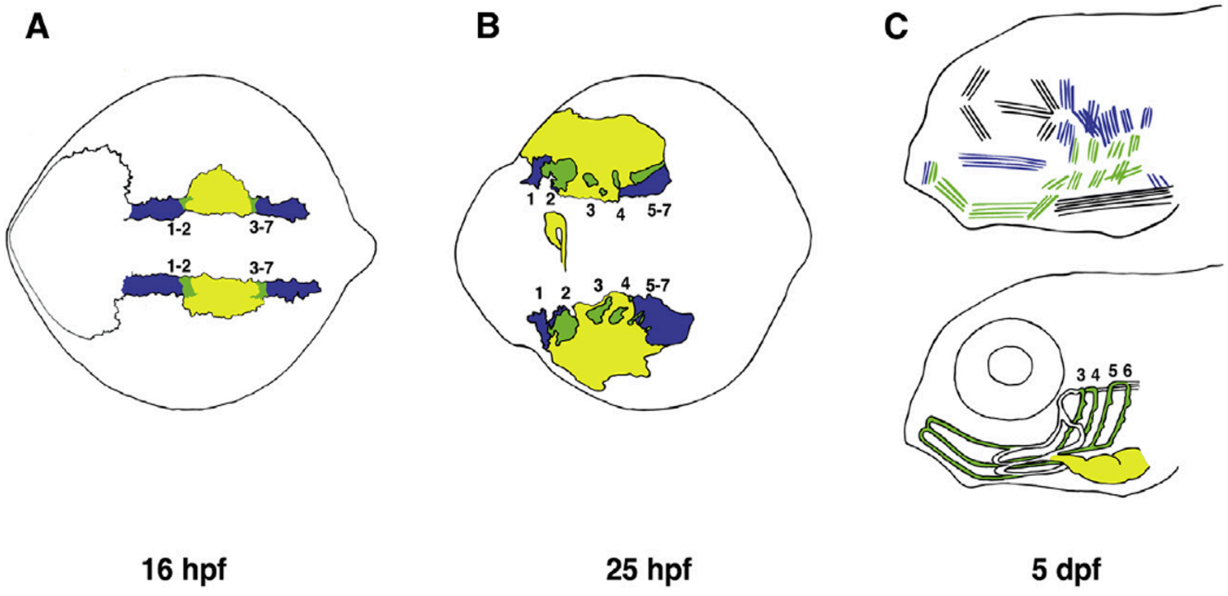

Figure 1: Contribution of *tcf21*+ and *nkx2.5*+ population to head muscle, vasculature and heart

Color code for the schematic*:* *tcf21*+=blue, *nkx2.5*=yellow, *tcf21*+*/nkx2.5*+=green (double positive)

A) Anterior *tcf21*+ and double positive population give rise to PM 1-2 and posterior *tcf21*+ and double positive population will form PM 3-7. B) *tcf21*+ and *nkx2.5*+ population is clustered in to mesodermal cores of respective PM. C) *tcf21*+ cells form the dorsal muscles of the PM 1-7, *tcf21*+*/nkx2/5*+ cells form mostly the ventral muscles. Eye and neck muscles (in black) are not derived from *tcf21*+ or *nkx2.5*+ population. Adapted from Nagelberg et al., [217]

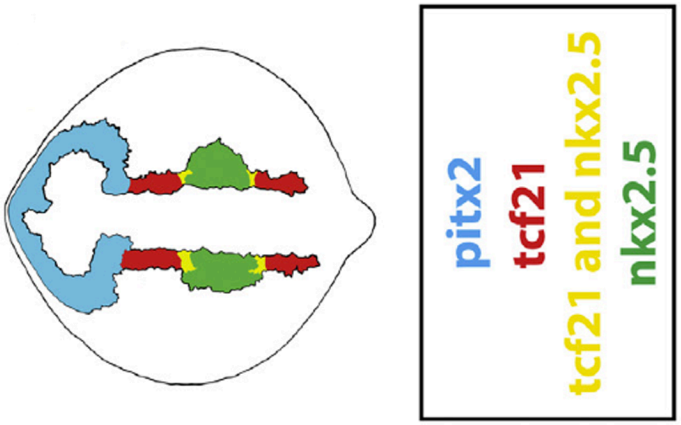

Figure 2: Schematic of *pitx2*, *tcf21* and *nkx2.5* expression in the lateral plate mesoderm

At 16 hpf zebrafish lateral mesoderm can be divided in to *pitx2* expressing prechordal mesoderm which give rise to the extra ocular muscles. *tcf21* and *nkx2.5* expressing pharyngeal mesoderm which eventually forms parts of the heart and PM. Adapted from Nagelberg et al., [217]

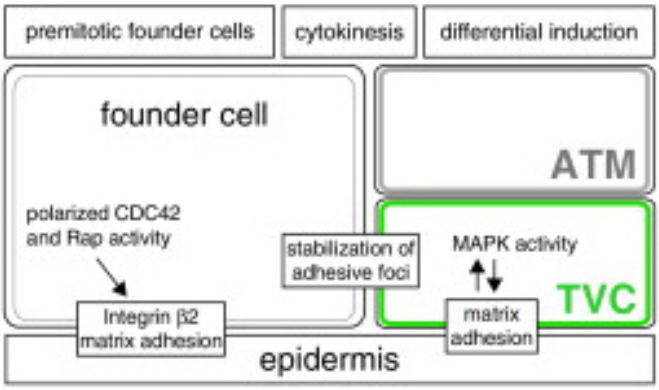

Figure 3: Role of cell-adhesion in differential after induction

After founder cell division polarized matrix adhesion occurs only at the daughter cell on the dorsal side (TVC). Matrix adhesion leads to MAPK activation and TVC induction. TVC is the pre-cardiac progenitor in *Ciona*. While the ventral daughter cell give rise to anterior tail muscle (ATM). Adapted from Kaplan et al., [68]

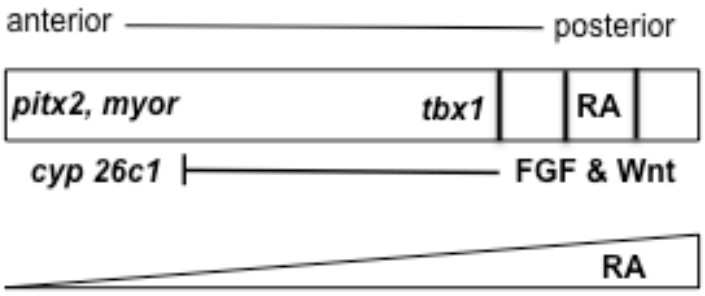

Figure 4: Role of RA in head mesoderm

RA level is high in the posterior part of the head mesoderm. The anterior head markers need low endogenous RA for proper specification. FGF and Wnt inhibit RA degrading enzyme cyp26 in the anterior head mesoderm thus promoting posterior hindbrain patterning. Adapted from Nagelberg et al., [217]

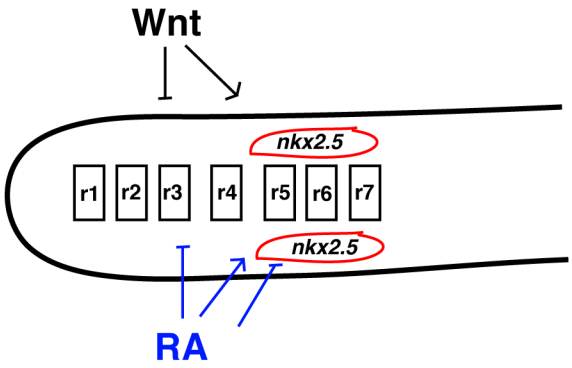

Figure 5: RA and Wnt in ALPM progenitor fate

RA promotes posterior rhombomere formation and inhibits anterior rhombomeres. RA restricts cardiac progenitor specification. Wnt inhibits head formation and promotes cardiac specification. *Nkx2.5* is a cardiac progenitor marker. RA regulation in blue. Wnt regulation in black.

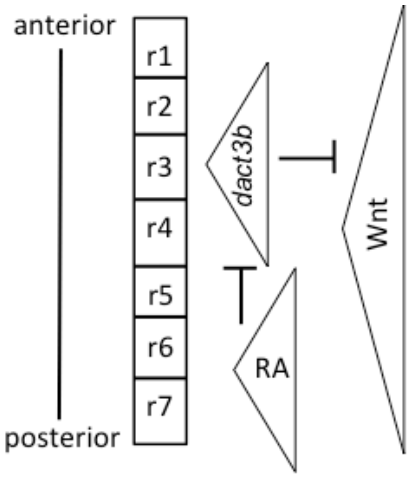

Figure 6: Hypothetical model of RA, *dact3b* and Wnt in hindbrain

Dact3b is robustly expressed in the r4-r6. RA is required for r4-r7 formation. Wnt is uniformly expressed throughout the hindbrain. We speculate here RA is required to keep dact3b low in the posterior rhombomeres. Anterior rhombomere formation requires high dact3b and low RA. Cross-antagonism between dact3b and RA specifies the function of Wnt in distinct rhombomeres across all of the hindbrain segments.

References:

1. Quadro, L., et al., *Impaired retinal function and vitamin A availability in mice lacking retinol-binding protein.* Embo Journal, 1999. **18**(17): p. 4633-4644.
2. Kawaguchi, R., et al., *A membrane receptor for retinol binding protein mediates cellular uptake of vitamin A.* Science, 2007. **315**(5813): p. 820-825.
3. Ang, H.L., et al., *Retinoic acid synthesis in mouse embryos during gastrulation and craniofacial development linked to class IV alcohol dehydrogenase gene expression.* Journal of Biological Chemistry, 1996. **271**(16): p. 9526-9534.
4. Sandell, L.L., et al., *RDH10 is essential for synthesis of embryonic retinoic acid and is required for limb, craniofacial, and organ development.* Genes & Development, 2007. **21**(9): p. 1113-1124.
5. Mic, F.A., et al., *Novel retinoic acid generating activities in the neural tube and heart identified by conditional rescue of Raldh2 null mutant mice.* Development, 2002. **129**(9): p. 2271-2282.
6. Pittlik, S., et al., *Expression of zebrafish aldh1a3 (raldh3) and absence of aldh1a1 in teleosts.* Gene Expression Patterns, 2008. **8**(3): p. 141-147.
7. Noy, N., *Retinoid-binding proteins: mediators of retinoid action.* Biochemical Journal, 2000. **348**: p. 481-495.
8. Duester, G., *Retinoic acid synthesis and signaling during early organogenesis.* Cell, 2008. **134**(6): p. 921-31.
9. Bastien, J. and C. Rochette-Egly, *Nuclear retinoid receptors and the transcription of retinoid-target genes.* Gene, 2004. **328**: p. 1-16.
10. Aranda, A. and A. Pascual, *Nuclear hormone receptors and gene expression.* Physiol Rev, 2001. **81**(3): p. 1269-304.
11. Waxman, J.S. and D. Yelon, *Zebrafish retinoic acid receptors function as context-dependent transcriptional activators.* Developmental Biology, 2011. **352**(1): p. 128-40.
12. Lammer, E.J., et al., *Retinoic acid embryopathy.* N Engl J Med, 1985. **313**(14): p. 837-41.
13. Waxman, J.S. and D. Yelon, *Comparison of the expression patterns of newly identified zebrafish retinoic acid and retinoid X receptors.* Dev Dyn, 2007. **236**(2): p. 587-95.
14. Mic, F.A., et al., *Retinoid activation of retinoic acid receptor but not retinoid X receptor is sufficient to rescue lethal defect in retinoic acid synthesis.* Proc Natl Acad Sci U S A, 2003. **100**(12): p. 7135-40.
15. Chawla, A., et al., *Nuclear receptors and lipid physiology: opening the X-files.* Science, 2001. **294**(5548): p. 1866-70.

16. Moutier, E., et al., *Retinoic acid receptors recognize the mouse genome through binding elements with diverse spacing and topology.* J Biol Chem, 2012. **287**(31): p. 26328-41.
17. Maden, M., et al., *Vitamin A-deficient quail embryos have half a hindbrain and other neural defects.* Curr Biol, 1996. **6**(4): p. 417-26.
18. Niederreither, K., et al., *Embryonic retinoic acid synthesis is essential for early mouse post-implantation development.* Nat Genet, 1999. **21**(4): p. 444-8.
19. Niederreither, K., et al., *Retinoic acid synthesis and hindbrain patterning in the mouse embryo.* Development, 2000. **127**(1): p. 75-85.
20. Niederreither, K., et al., *Embryonic retinoic acid synthesis is essential for heart morphogenesis in the mouse.* Development, 2001. **128**(7): p. 1019-31.
21. Begemann, G., et al., *The zebrafish neckless mutation reveals a requirement for raldh2 in mesodermal signals that pattern the hindbrain.* Development, 2001. **128**(16): p. 3081-94.
22. Keegan, B.R., et al., *Retinoic acid signaling restricts the cardiac progenitor pool.* Science, 2005. **307**(5707): p. 247-9.
23. Rossant, J., et al., *Expression of a retinoic acid response element-hsplacZ transgene defines specific domains of transcriptional activity during mouse embryogenesis.* Genes Dev, 1991. **5**(8): p. 1333-44.
24. Balkan, W., et al., *Transgenic indicator mice for studying activated retinoic acid receptors during development.* Proc Natl Acad Sci U S A, 1992. **89**(8): p. 3347-51.
25. Perz-Edwards, A., N.L. Hardison, and E. Linney, *Retinoic acid-mediated gene expression in transgenic reporter zebrafish.* Dev Biol, 2001. **229**(1): p. 89-101.
26. White, R.J., et al., *Complex regulation of cyp26a1 creates a robust retinoic acid gradient in the zebrafish embryo.* PLoS biology, 2007. **5**(11): p. e304.
27. Shimozono, S., et al., *Visualization of an endogenous retinoic acid gradient across embryonic development.* Nature, 2013. **496**(7445): p. 363-6.
28. Cheyette, B.N., et al., *Dapper, a Dishevelled-associated antagonist of beta-catenin and JNK signaling, is required for notochord formation.* Developmental cell, 2002. **2**(4): p. 449-461.
29. Waxman, J.S., et al., *Zebrafish Dapper1 and Dapper2 play distinct roles in Wnt-mediated developmental processes.* Development (Cambridge, England), 2004. **131**(23): p. 5909-5921.
30. Fisher, D.A., et al., *Three Dact gene family members are expressed during embryonic development and in the adult brains of mice.* Developmental dynamics : an official publication of the American Association of Anatomists, 2006. **235**(9): p. 2620-2630.
31. Suriben, R., et al., *Posterior malformations in Dact1 mutant mice arise through misregulated Vangl2 at the primitive streak.* Nature genetics, 2009. **41**(9): p. 977-985.
32. Wen, J., et al., *Loss of Dact1 disrupts planar cell polarity signaling by altering dishevelled activity and leads to posterior malformation in mice.* The Journal of biological chemistry, 2010. **285**(14): p. 11023-11030.
33. Xue, H., et al., *Disruption of the Dapper3 gene aggravates ureteral obstruction-mediated renal fibrosis by amplifying Wnt/β-catenin signaling.* The Journal of biological chemistry, 2013. **288**(21): p. 15006-15014.
34. Jiang, X., et al., *DACT3 is an epigenetic regulator of Wnt/beta-catenin signaling in colorectal cancer and is a therapeutic target of histone modifications.* Cancer cell, 2008. **13**(6): p. 529-541.

35. Easwaran, V., et al., *Cross-regulation of beta-catenin-LEF/TCF and retinoid signaling pathways.* Curr Biol, 1999. **9**(23): p. 1415-8.
36. Liu, T., et al., *Activation of the beta-catenin/Lef-Tcf pathway is obligate for formation of primitive endoderm by mouse F9 totipotent teratocarcinoma cells in response to retinoic acid.* J Biol Chem, 2002. **277**(34): p. 30887-91.
37. Otero, J.J., et al., *Beta-catenin signaling is required for neural differentiation of embryonic stem cells.* Development, 2004. **131**(15): p. 3545-57.
38. Yasuhara, R., et al., *Wnt/beta-catenin and retinoic acid receptor signaling pathways interact to regulate chondrocyte function and matrix turnover.* J Biol Chem, 2010. **285**(1): p. 317-27.
39. Miller, J.R., et al., *Mechanism and function of signal transduction by the Wnt/beta-catenin and Wnt/Ca2+ pathways.* Oncogene, 1999. **18**(55): p. 7860-72.
40. Clevers, H. and R. Nusse, *Wnt/β-catenin signaling and disease.* Cell, 2012. **149**(6): p. 1192-1205.
41. Logan, C. and R. Nusse, *The Wnt signaling pathway in development and disease.* Annual review of cell and developmental biology, 2004. **20**: p. 781-810.
42. Abu-Issa, R. and M.L. Kirby, *Heart field: from mesoderm to heart tube.* Annu. Rev. Cell Dev. Biol., 2007.
43. Srivastava, D., *Making or breaking the heart: from lineage determination to morphogenesis.* Cell, 2006.
44. Fishman, M.C. and K.R. Chien, *Fashioning the vertebrate heart: earliest embryonic decisions.* Development, 1997. **124**(11): p. 2099-117.
45. Vincent, S.D. and M.E. Buckingham, *How to make a heart: the origin and regulation of cardiac progenitor cells.* Curr Top Dev Biol, 2010. **90**: p. 1-41.
46. Kelly, R.G., *The second heart field.* Current topics in developmental biology, 2012. **100**: p. 33-65.
47. Kwon, C., K.R. Cordes, and D. Srivastava, *Wnt/beta-catenin signaling acts at multiple developmental stages to promote mammalian cardiogenesis.* Cell Cycle, 2008. **7**(24): p. 3815-8.
48. Atsuhiko, T.N., et al., *Developmental stage-specific biphasic roles of Wnt/Œ≤-catenin signaling in cardiomyogenesis and hematopoiesis.* Proceedings of the National Academy of Sciences, 2006. **103**(52): p. 19812-19817.
49. Tzahor, E., *Wnt/beta-catenin signaling and cardiogenesis: timing does matter.* Dev Cell, 2007. **13**(1): p. 10-3.
50. Ueno, S., et al., *Biphasic role for Wnt/beta-catenin signaling in cardiac specification in zebrafish and embryonic stem cells.* Proc Natl Acad Sci U S A, 2007. **104**(23): p. 9685-90.
51. Dohn, T.E. and J.S. Waxman, *Distinct phases of Wnt/beta-catenin signaling direct cardiomyocyte formation in zebrafish.* Dev Biol, 2012. **361**(2): p. 364-76.
52. Liu, F., et al., *ER71 specifies Flk-1+ hemangiogenic mesoderm by inhibiting cardiac mesoderm and Wnt signaling.* Blood, 2012. **119**(14): p. 3295-305.
53. Buckingham, M. and P.W. Rigby, *Gene regulatory networks and transcriptional mechanisms that control myogenesis.* Dev Cell, 2014. **28**(3): p. 225-38.
54. Buckingham, M. and F. Relaix, *The role of Pax genes in the development of tissues and organs: Pax3 and Pax7 regulate muscle progenitor cell functions.* Annu Rev Cell Dev Biol, 2007. **23**: p. 645-73.

55. Tzahor, E., *Antagonists of Wnt and BMP signaling promote the formation of vertebrate head muscle.* Genes & Development, 2003. **17**(24).
56. Kaplan, N., F. Razy-Krajka, and L. Christiaen, *Regulation and evolution of cardiopharyngeal cell identity and behavior: insights from simple chordates.* Curr Opin Genet Dev, 2015. **32**: p. 119-28.
57. Jacobson, A.G. and A.K. Sater, *Features of embryonic induction.* Development, 1988. **104**(3): p. 341-59.
58. Baldini, A., *DiGeorge syndrome: the use of model organisms to dissect complex genetics.* Hum Mol Genet, 2002. **11**(20): p. 2363-9.
59. Wang, W., et al., *NK4 antagonizes Tbx1/10 to promote cardiac versus pharyngeal muscle fate in the ascidian second heart field.* PLoS biology, 2013. **11**(12).
60. Lescroart, F., et al., *Early lineage restriction in temporally distinct populations of Mesp1 progenitors during mammalian heart development.* Nat Cell Biol, 2014. **16**(9): p. 829-40.
61. Tzahor, E. and S.M. Evans, *Pharyngeal mesoderm development during embryogenesis: implications for both heart and head myogenesis.* Cardiovascular research, 2011. **91**(2): p. 196-202.
62. Lescroart, F., et al., *Clonal analysis reveals common lineage relationships between head muscles and second heart field derivatives in the mouse embryo.* Development (Cambridge, England), 2010. **137**(19): p. 3269-3279.
63. Harel, I., et al., *Pharyngeal mesoderm regulatory network controls cardiac and head muscle morphogenesis.* Proceedings of the National Academy of Sciences of the United States of America, 2012. **109**(46): p. 18839-44.
64. Tiefenbach, J., et al., *A live zebrafish-based screening system for human nuclear receptor ligand and cofactor discovery.* PLoS One, 2010. **5**(3): p. e9797.
65. Gloy, J., H. Hikasa, and S.Y. Sokol, *Frodo interacts with Dishevelled to transduce Wnt signals.* Nature cell biology, 2002. **4**(5): p. 351-357.
66. Baker, K.D., M.C. Ramel, and A.C. Lekven, *A direct role for Wnt8 in ventrolateral mesoderm patterning.* Dev Dyn, 2010. **239**(11): p. 2828-36.
67. Rui, D., et al., *A new heart for a new head in vertebrate cardiopharyngeal evolution.* Nature, 2015. **520**(7548): p. 466-473.
68. Kaplan, N., F. Razy-Krajka, and L. Christiaen, *Regulation and evolution of cardiopharyngeal cell identity and behavior: insights from simple chordates.* Regulation and evolution of cardiopharyngeal cell identity and behavior: insights from simple chordates, 2015.
69. Chanda, B., et al., *Retinoic acid signaling is essential for embryonic hematopoietic stem cell development.* Cell, 2013. **155**(1): p. 215-227.
70. Etchamendy, N., et al., *Alleviation of a selective age-related relational memory deficit in mice by pharmacologically induced normalization of brain retinoid signaling.* J Neurosci, 2001. **21**(16): p. 6423-9.
71. Ono, K., et al., *Vitamin A exhibits potent antiamyloidogenic and fibril-destabilizing effects in vitro.* Exp Neurol, 2004. **189**(2): p. 380-92.
72. Lieschke, G.J. and P.D. Currie, *Animal models of human disease: zebrafish swim into view.* Nat Rev Genet, 2007. **8**(5): p. 353-67.
73. Warkany, J. and E. Schraffenberger, *Congenital malformations induced in rats by maternal vitamin A deficiency; defects of the eye.* Archives of Ophthalmology, 1946. **35**: p. 150-69.

74. Wilson, J.G., C.B. Roth, and J. Warkany, *An analysis of the syndrome of malformations induced by maternal vitamin A deficiency. Effects of restoration of vitamin A at various times during gestation.* The American journal of anatomy, 1953. **92**(2): p. 189-217.
75. Wilson, J.G. and J. Warkany, *Aortic-arch and cardiac anomalies in the offspring of vitamin A deficient rats.* The American journal of anatomy, 1949. **85**(1): p. 113-55.
76. Rizzo, R., et al., *Limb reduction defects in humans associated with prenatal isotretinoin exposure.* Teratology, 1991. **44**(6): p. 599-604.
77. Niederreither, K., et al., *Embryonic retinoic acid synthesis is essential for early mouse post-implantation development.* Nature Genetics, 1999. **21**(4): p. 444-8.
78. Li, E., et al., *Normal development and growth of mice carrying a targeted disruption of the alpha 1 retinoic acid receptor gene.* Proceedings of the National Academy of Sciences of the United States of America, 1993. **90**(4): p. 1590-4.
79. Lohnes, D., et al., *Function of retinoic acid receptor gamma in the mouse.* Cell, 1993. **73**(4): p. 643-58.
80. Lohnes, D., et al., *Function of the retinoic acid receptors (RARs) during development (I). Craniofacial and skeletal abnormalities in RAR double mutants.* Development, 1994. **120**(10): p. 2723-48.
81. Mendelsohn, C., et al., *Function of the retinoic acid receptors (RARs) during development (II). Multiple abnormalities at various stages of organogenesis in RAR double mutants.* Development, 1994. **120**(10): p. 2749-71.
82. Abu-Abed, S., et al., *The retinoic acid-metabolizing enzyme, CYP26A1, is essential for normal hindbrain patterning, vertebral identity, and development of posterior structures.* Genes & development, 2001. **15**(2): p. 226-40.
83. Emoto, Y., et al., *Retinoic acid-metabolizing enzyme Cyp26a1 is essential for determining territories of hindbrain and spinal cord in zebrafish.* Developmental Biology, 2005. **278**(2): p. 415-27.
84. Sakai, Y., et al., *The retinoic acid-inactivating enzyme CYP26 is essential for establishing an uneven distribution of retinoic acid along the anterio-posterior axis within the mouse embryo.* Genes & development, 2001. **15**(2): p. 213-25.
85. Grandel, H., et al., *Retinoic acid signalling in the zebrafish embryo is necessary during pre-segmentation stages to pattern the anterior-posterior axis of the CNS and to induce a pectoral fin bud.* Development, 2002. **129**(12): p. 2851-65.
86. Heine, U.I., et al., *Effects of retinoid deficiency on the development of the heart and vascular system of the quail embryo.* Virchows Arch B Cell Pathol Incl Mol Pathol, 1985. **50**(2): p. 135-52.
87. Niederreither, K. and P. Dolle, *Retinoic acid in development: towards an integrated view.* Nature reviews. Genetics, 2008. **9**(7): p. 541-53.
88. Mark, M., N.B. Ghyselinck, and P. Chambon, *Function of retinoic acid receptors during embryonic development.* Nuclear receptor signaling, 2009. **7**: p. e002.
89. Campo-Paysaa, F., et al., *Retinoic acid signaling in development: tissue-specific functions and evolutionary origins.* Genesis, 2008. **46**(11): p. 640-56.
90. Braitsch, C.M., et al., *Pod1/Tcf21 is regulated by retinoic acid signaling and inhibits differentiation of epicardium-derived cells into smooth muscle in the developing heart.* Developmental Biology, 2012. **368**(2): p. 345-57.
91. Chen, T.H., et al., *Epicardial induction of fetal cardiomyocyte proliferation via a retinoic acid-inducible trophic factor.* Dev Biol, 2002. **250**(1): p. 198-207.

92. Cooper, K.L., et al., *Initiation of proximal-distal patterning in the vertebrate limb by signals and growth.* Science, 2011. **332**(6033): p. 1083-6.
93. Li, P., M. Pashmforoush, and H.M. Sucov, *Retinoic acid regulates differentiation of the secondary heart field and TGFbeta-mediated outflow tract septation.* Developmental Cell, 2010. **18**(3): p. 480-5.
94. Nagpal, S., et al., *Promoter context- and response element-dependent specificity of the transcriptional activation and modulating functions of retinoic acid receptors.* Cell, 1992. **70**(6): p. 1007-19.
95. Allenby, G., et al., *Retinoic acid receptors and retinoid X receptors: interactions with endogenous retinoic acids.* Proceedings of the National Academy of Sciences of the United States of America, 1993. **90**(1): p. 30-4.
96. Waxman, J.S. and D. Yelon, *Comparison of the expression patterns of newly identified zebrafish retinoic acid and retinoid X receptors.* Developmental dynamics : an official publication of the American Association of Anatomists, 2007. **236**(2): p. 587-95.
97. Hale, L.A., et al., *Characterization of the retinoic acid receptor genes raraa, rarab and rarg during zebrafish development.* Gene expression patterns : GEP, 2006. **6**(5): p. 546-55.
98. Asakawa, K., et al., *Genetic dissection of neural circuits by Tol2 transposon-mediated Gal4 gene and enhancer trapping in zebrafish.* Proceedings of the National Academy of Sciences of the United States of America, 2008. **105**(4): p. 1255-60.
99. Davison, J.M., et al., *Transactivation from Gal4-VP16 transgenic insertions for tissue-specific cell labeling and ablation in zebrafish.* Developmental Biology, 2007. **304**(2): p. 811-24.
100. Feng, L., et al., *Dhrs3a regulates retinoic acid biosynthesis through a feedback inhibition mechanism.* Developmental Biology, 2010. **338**(1): p. 1-14.
101. Waxman, J.S. and D. Yelon, *Increased Hox activity mimics the teratogenic effects of excess retinoic acid signaling.* Developmental dynamics : an official publication of the American Association of Anatomists, 2009. **238**(5): p. 1207-13.
102. Goll, M.G., et al., *Transcriptional silencing and reactivation in transgenic zebrafish.* Genetics, 2009. **182**(3): p. 747-55.
103. Russo, J.E., D. Hauguitz, and J. Hilton, *Inhibition of mouse cytosolic aldehyde dehydrogenase by 4-(diethylamino)benzaldehyde.* Biochem Pharmacol, 1988. **37**(8): p. 1639-42.
104. Zhang, L.X., et al., *Evidence for the involvement of retinoic acid receptor RAR alpha-dependent signaling pathway in the induction of tissue transglutaminase and apoptosis by retinoids.* J Biol Chem, 1995. **270**(11): p. 6022-9.
105. Waxman, J.S., et al., *Hoxb5b acts downstream of retinoic acid signaling in the forelimb field to restrict heart field potential in zebrafish.* Developmental Cell, 2008. **15**(6): p. 923-34.
106. Maves, L. and C.B. Kimmel, *Dynamic and sequential patterning of the zebrafish posterior hindbrain by retinoic acid.* Dev Biol, 2005. **285**(2): p. 593-605.
107. Hernandez, R.E., et al., *vhnf1 integrates global RA patterning and local FGF signals to direct posterior hindbrain development in zebrafish.* Development, 2004. **131**(18): p. 4511-20.
108. Liang, D., et al., *Expressions of Raldh3 and Raldh4 during zebrafish early development.* Gene expression patterns : GEP, 2008. **8**(4): p. 248-53.

109. Pittlik, S., et al., *Expression of zebrafish aldh1a3 (raldh3) and absence of aldh1a1 in teleosts.* Gene expression patterns : GEP, 2008. **8**(3): p. 141-7.
110. French, C.R., et al., *Gdf6a is required for the initiation of dorsal-ventral retinal patterning and lens development.* Developmental Biology, 2009. **333**(1): p. 37-47.
111. Ma, L.H., et al., *Ancestry of motor innervation to pectoral fin and forelimb.* Nature communications, 2010. **1**: p. 49.
112. Hernandez, R.E., et al., *Cyp26 enzymes generate the retinoic acid response pattern necessary for hindbrain development.* Development, 2007. **134**(1): p. 177-87.
113. Lee, Y., et al., *Maintenance of blastemal proliferation by functionally diverse epidermis in regenerating zebrafish fins.* Developmental Biology, 2009. **331**(2): p. 270-80.
114. Kwan, K.M., et al., *The Tol2kit: a multisite gateway-based construction kit for Tol2 transposon transgenesis constructs.* Developmental dynamics : an official publication of the American Association of Anatomists, 2007. **236**(11): p. 3088-99.
115. Kawakami, K., *Transposon tools and methods in zebrafish.* Developmental dynamics : an official publication of the American Association of Anatomists, 2005. **234**(2): p. 244-54.
116. Robu, M.E., et al., *p53 activation by knockdown technologies.* PLoS genetics, 2007. **3**(5): p. e78.
117. Oxtoby, E. and T. Jowett, *Cloning of the zebrafish krox-20 gene (krx-20) and its expression during hindbrain development.* Nucleic Acids Research, 1993. **21**(5): p. 1087-95.
118. MacDonald, B., K. Tamai, and X. He, *Wnt/beta-catenin signaling: components, mechanisms, and diseases.* Developmental cell, 2009. **17**(1): p. 9-26.
119. Alvares, L., et al., *Chicken dapper genes are versatile markers for mesodermal tissues, embryonic muscle stem cells, neural crest cells, and neurogenic placodes.* Developmental dynamics : an official publication of the American Association of Anatomists, 2009. **238**(5): p. 1166-1178.
120. Brott, B. and S. Sokol, *Frodo proteins: modulators of Wnt signaling in vertebrate development.* Differentiation; research in biological diversity, 2005. **73**(7): p. 323-329.
121. Hikasa, H. and S. Sokol, *The involvement of Frodo in TCF-dependent signaling and neural tissue development.* Development (Cambridge, England), 2004. **131**(19): p. 4725-4734.
122. Kivimäe, S., X. Yang, and B. Cheyette, *All Dact (Dapper/Frodo) scaffold proteins dimerize and exhibit conserved interactions with Vangl, Dvl, and serine/threonine kinases.* BMC biochemistry, 2011. **12**: p. 33.
123. Zhang, L., et al., *Dapper 1 antagonizes Wnt signaling by promoting dishevelled degradation.* The Journal of biological chemistry, 2006. **281**(13): p. 8607-8612.
124. Gao, X., et al., *Dapper1 is a nucleocytoplasmic shuttling protein that negatively modulates Wnt signaling in the nucleus.* The Journal of biological chemistry, 2008. **283**(51): p. 35679-35688.
125. Waxman, J.S., *Regulation of the early expression patterns of the zebrafish Dishevelled-interacting proteins Dapper1 and Dapper2.* Developmental dynamics : an official publication of the American Association of Anatomists, 2005. **233**(1): p. 194-200.
126. Park, J.-i., et al., *Frodo links Dishevelled to the p120-catenin/Kaiso pathway: distinct catenin subfamilies promote Wnt signals.* Developmental cell, 2006. **11**(5): p. 683-695.
127. Yang, X., D. Fisher, and B. Cheyette, *SEC14 and Spectrin Domains 1 (Sestd1), Dishevelled 2 (Dvl2) and Dapper Antagonist of Catenin-1 (Dact1) co-regulate the*

Wnt/Planar Cell Polarity (PCP) pathway during mammalian development. Communicative & integrative biology, 2013. **6**(6).
128. Teran, E., A. Branscomb, and J. Seeling, *Dpr Acts as a molecular switch, inhibiting Wnt signaling when unphosphorylated, but promoting Wnt signaling when phosphorylated by casein kinase Idelta/epsilon.* PloS one, 2009. **4**(5).
129. Shi, Y., et al., *Identification of novel rare mutations of DACT1 in human neural tube defects.* Human mutation, 2012. **33**(10): p. 1450-1455.
130. Yin, X., et al., *DACT1, an antagonist to Wnt/β-catenin signaling, suppresses tumor cell growth and is frequently silenced in breast cancer.* Breast cancer research : BCR, 2013. **15**(2).
131. Yau, T.-O., et al., *HDPR1, a novel inhibitor of the WNT/beta-catenin signaling, is frequently downregulated in hepatocellular carcinoma: involvement of methylation-mediated gene silencing.* Oncogene, 2005. **24**(9): p. 1607-1614.
132. Astolfi, A., et al., *A molecular portrait of gastrointestinal stromal tumors: an integrative analysis of gene expression profiling and high-resolution genomic copy number.* Laboratory investigation; a journal of technical methods and pathology, 2010. **90**(9): p. 1285-1294.
133. Yang, Z.-Q., et al., *Downregulation of HDPR1 is associated with poor prognosis and affects expression levels of p120-catenin and beta-catenin in nonsmall cell lung cancer.* Molecular carcinogenesis, 2010. **49**(5): p. 508-519.
134. Yuan, G., et al., *Oncogenic function of DACT1 in colon cancer through the regulation of β-catenin.* PloS one, 2012. **7**(3).
135. Su, Y., et al., *The evolutionally conserved activity of Dapper2 in antagonizing TGF-beta signaling.* FASEB journal : official publication of the Federation of American Societies for Experimental Biology, 2007. **21**(3): p. 682-690.
136. Li, X., et al., *Dact2 represses PITX2 transcriptional activation and cell proliferation through Wnt/beta-catenin signaling during odontogenesis.* PloS one, 2013. **8**(1).
137. Zhang, L., et al., *Zebrafish Dpr2 inhibits mesoderm induction by promoting degradation of nodal receptors.* Science (New York, N.Y.), 2004. **306**(5693): p. 114-117.
138. Lee, W.-C., et al., *Dact2 is expressed in the developing ureteric bud/collecting duct system of the kidney and controls morphogenetic behavior of collecting duct cells.* American journal of physiology. Renal physiology, 2010. **299**(4): p. 51.
139. Meng, F., et al., *Accelerated re-epithelialization in Dpr2-deficient mice is associated with enhanced response to TGFbeta signaling.* Journal of cell science, 2008. **121**(Pt 17): p. 2904-2912.
140. Schilling, T.F. and C.B. Kimmel, *Musculoskeletal patterning in the pharyngeal segments of the zebrafish embryo.* Development (Cambridge, England), 1997. **124**(15): p. 2945-2960.
141. Diogo, R., Y. Hinits, and S.M. Hughes, *Development of mandibular, hyoid and hypobranchial muscles in the zebrafish: homologies and evolution of these muscles within bony fishes and tetrapods.* BMC developmental biology, 2007. **8**: p. 24.
142. Sperber, S.M., et al., *Zebrafish dlx2a contributes to hindbrain neural crest survival, is necessary for differentiation of sensory ganglia and functions with dlx1a in maturation of the arch cartilage elements.* Developmental biology, 2008. **314**(1): p. 59-70.

143. Chandrasekhar, A., *Turning heads: development of vertebrate branchiomotor neurons.* Developmental dynamics : an official publication of the American Association of Anatomists, 2003. **229**(1): p. 143-161.
144. Auclair, F., N. Vald√©s, and R. Marchand, *Rhombomere-specific origin of branchial and visceral motoneurons of the facial nerve in the rat embryo.* The Journal of comparative neurology, 1996. **369**(3): p. 451-461.
145. Studer, M., et al., *Altered segmental identity and abnormal migration of motor neurons in mice lacking Hoxb-1.* Nature, 1995. **384**(6610): p. 630-634.
146. Ahn, D. and R.K. Ho, *Tri-phasic expression of posterior Hox genes during development of pectoral fins in zebrafish: implications for the evolution of vertebrate paired appendages.* Developmental biology, 2008. **322**(1): p. 220-33.
147. Thorsen, D.H. and M.E. Hale, *Development of zebrafish (Danio rerio) pectoral fin musculature.* Journal of morphology, 2005. **266**(2): p. 241-55.
148. Cooper, M.S. and L.A. D'Amico, *A cluster of noninvoluting endocytic cells at the margin of the zebrafish blastoderm marks the site of embryonic shield formation.* Developmental biology, 1996. **180**(1): p. 184-198.
149. Gillhouse, M., et al., *Two Frodo/Dapper homologs are expressed in the developing brain and mesoderm of zebrafish.* Developmental dynamics : an official publication of the American Association of Anatomists, 2004. **230**(3): p. 403-409.
150. Chandrasekhar, A., et al., *Development of branchiomotor neurons in zebrafish.* Development, 1997. **124**(13): p. 2633-44.
151. Yasuhara, R., et al., *Wnt/beta-catenin and retinoic acid receptor signaling pathways interact to regulate chondrocyte function and matrix turnover.* The Journal of biological chemistry, 2010. **285**(1): p. 317-327.
152. Kim, D., et al., *Retinoic acid inhibits adipogenesis via activation of Wnt signaling pathway in 3T3-L1 preadipocytes.* Biochemical and biophysical research communications, 2013. **434**(3): p. 455-459.
153. Westerfield, M., *The Zebrafish book. A guide for the laboratory use of zebrafish (Danio rerio).* . University of Oregon Press, Eugene. 2000.
154. Kimmel, C., et al., *Stages of embryonic development of the zebrafish.* Developmental dynamics : an official publication of the American Association of Anatomists, 1995. **203**(3): p. 253-310.
155. Waxman, J., et al., *Hoxb5b acts downstream of retinoic acid signaling in the forelimb field to restrict heart field potential in zebrafish.* Developmental cell, 2008. **15**(6): p. 923-934.
156. Diogo, R., et al., *A new heart for a new head in vertebrate cardiopharyngeal evolution.* Nature, 2015. **520**(7548): p. 466-73.
157. Nagelberg, D., et al., *Origin, Specification, and Plasticity of the Great Vessels of the Heart.* Curr Biol, 2015. **25**(16): p. 2099-110.
158. Dyer, L.A. and M.L. Kirby, *The role of secondary heart field in cardiac development.* Dev Biol, 2009. **336**(2): p. 137-44.
159. Zhou, Y., et al., *Latent TGF-beta binding protein 3 identifies a second heart field in zebrafish.* Nature, 2011. **474**(7353): p. 645-8.
160. Kelly, R.G., *The second heart field.* Curr Top Dev Biol, 2012. **100**: p. 33-65.
161. Zaffran, S. and R.G. Kelly, *New developments in the second heart field.* Differentiation, 2012. **84**(1): p. 17-24.

162. de Pater, E., et al., *Distinct phases of cardiomyocyte differentiation regulate growth of the zebrafish heart.* Development, 2009. **136**(10): p. 1633-41.
163. Guner-Ataman, B., et al., *Zebrafish second heart field development relies on progenitor specification in anterior lateral plate mesoderm and nkx2.5 function.* Development, 2013. **140**(6): p. 1353-63.
164. Lescroart, F., et al., *Clonal analysis reveals a common origin between nonsomite-derived neck muscles and heart myocardium.* Proc Natl Acad Sci U S A, 2015. **112**(5): p. 1446-51.
165. Lescroart, F., et al., *Clonal analysis reveals common lineage relationships between head muscles and second heart field derivatives in the mouse embryo.* Development, 2010. **137**(19): p. 3269-79.
166. Nathan, E., et al., *The contribution of Islet1-expressing splanchnic mesoderm cells to distinct branchiomeric muscles reveals significant heterogeneity in head muscle development.* Development, 2008. **135**(4): p. 647-57.
167. Nevis, K., et al., *Tbx1 is required for second heart field proliferation in zebrafish.* Dev Dyn, 2013. **242**(5): p. 550-9.
168. Piotrowski, T., et al., *The zebrafish van gogh mutation disrupts tbx1, which is involved in the DiGeorge deletion syndrome in humans.* Development, 2003. **130**(20): p. 5043-52.
169. Stolfi, A., et al., *Early chordate origins of the vertebrate second heart field.* Science, 2010. **329**(5991): p. 565-8.
170. Wang, W., et al., *NK4 antagonizes Tbx1/10 to promote cardiac versus pharyngeal muscle fate in the ascidian second heart field.* PLoS Biol, 2013. **11**(12): p. e1001725.
171. Dohn, T.E. and J.S. Waxman, *Distinct phases of Wnt/beta-catenin signaling direct cardiomyocyte formation in zebrafish.* Developmental Biology, 2012. **361**(2): p. 364-76.
172. Naito, A.T., et al., *Developmental stage-specific biphasic roles of Wnt/beta-catenin signaling in cardiomyogenesis and hematopoiesis.* Proc Natl Acad Sci U S A, 2006. **103**(52): p. 19812-7.
173. Kwon, C., et al., *Canonical Wnt signaling is a positive regulator of mammalian cardiac progenitors.* Proc Natl Acad Sci U S A, 2007. **104**(26): p. 10894-9.
174. Paige, S.L., et al., *Endogenous Wnt/beta-catenin signaling is required for cardiac differentiation in human embryonic stem cells.* PLoS One, 2010. **5**(6): p. e11134.
175. Liu, F., et al., *ER71 specifies Flk-1+ hemangiogenic mesoderm by inhibiting cardiac mesoderm and Wnt signaling.* Blood, 2012.
176. Sorrell, M.R., et al., *Tcf7l1 proteins cell autonomously restrict cardiomyocyte and promote endothelial specification in zebrafish.* Developmental Biology, 2013.
177. Tzahor, E., et al., *Antagonists of Wnt and BMP signaling promote the formation of vertebrate head muscle.* Genes Dev, 2003. **17**(24): p. 3087-99.
178. Schilling, T.F. and C.B. Kimmel, *Musculoskeletal patterning in the pharyngeal segments of the zebrafish embryo.* Development, 1997. **124**(15): p. 2945-60.
179. Dorsky, R.I., et al., *Two tcf3 genes cooperate to pattern the zebrafish brain.* Development, 2003. **130**(9): p. 1937-47.
180. Lekven, A.C., et al., *Zebrafish wnt8 encodes two wnt8 proteins on a bicistronic transcript and is required for mesoderm and neurectoderm patterning.* Dev Cell, 2001. **1**(1): p. 103-14.

181. George, V., S. Colombo, and K.L. Targoff, *An early requirement for nkx2.5 ensures the first and second heart field ventricular identity and cardiac function into adulthood.* Dev Biol, 2015. **400**(1): p. 10-22.
182. Hami, D., et al., *Zebrafish cardiac development requires a conserved secondary heart field.* Development, 2011. **138**(11): p. 2389-98.
183. Lazic, S. and I.C. Scott, *Mef2cb regulates late myocardial cell addition from a second heart field-like population of progenitors in zebrafish.* Dev Biol, 2011. **354**(1): p. 123-33.
184. Devine, W.P., et al., *Early patterning and specification of cardiac progenitors in gastrulating mesoderm.* Elife, 2014. **3**.
185. Sorrell, M.R. and J.S. Waxman, *Restraint of Fgf8 signaling by retinoic acid signaling is required for proper heart and forelimb formation.* Developmental Biology, 2011. **358**(1): p. 44-55.
186. Westerfield, M., *The Zebrafish Book: A guide for the labratory use of zebrafish (Danio rerio)*. 3 ed. 1995: University of Oregon Press.
187. Weidinger, G., et al., *The Sp1-related transcription factors sp5 and sp5-like act downstream of Wnt/beta-catenin signaling in mesoderm and neuroectoderm patterning.* Curr Biol, 2005. **15**(6): p. 489-500.
188. Stoick-Cooper, C.L., et al., *Distinct Wnt signaling pathways have opposing roles in appendage regeneration.* Development, 2007. **134**(3): p. 479-89.
189. Higashijima, S., et al., *High-frequency generation of transgenic zebrafish which reliably express GFP in whole muscles or the whole body by using promoters of zebrafish origin.* Dev Biol, 1997. **192**(2): p. 289-99.
190. Wang, J., et al., *The regenerative capacity of zebrafish reverses cardiac failure caused by genetic cardiomyocyte depletion.* Development, 2011. **138**(16): p. 3421-30.
191. Huang, C.J., et al., *Germ-line transmission of a myocardium-specific GFP transgene reveals critical regulatory elements in the cardiac myosin light chain 2 promoter of zebrafish.* Developmental dynamics : an official publication of the American Association of Anatomists, 2003. **228**(1): p. 30-40.
192. Oxtoby, E. and T. Jowett, *Cloning of the zebrafish krox-20 gene (krx-20) and its expression during hindbrain development.* Nucleic Acids Res, 1993. **21**(5): p. 1087-95.
193. D'Aniello, E., et al., *Depletion of Retinoic Acid Receptors Initiates a Novel Positive Feedback Mechanism that Promotes Teratogenic Increases in Retinoic Acid.* PLoS genetics, 2013. **9**(8): p. e1003689.
194. D'Aniello, E., et al., *Depletion of retinoic acid receptors initiates a novel positive feedback mechanism that promotes teratogenic increases in retinoic acid.* PLoS Genet, 2013. **9**(8): p. e1003689.
195. Rydeen, A., et al., *Excessive feedback of Cyp26a1 promotes. cell non-autonomous loss of retinoic acid signaling.* Developmental Biology, 2015. **405**(1): p. 47-55.
196. Schug, T.T., et al., *Opposing effects of retinoic acid on cell growth result from alternate activation of two different nuclear receptors.* Cell, 2007. **129**(4): p. 723-733.
197. Schoenebeck, J.J., B.R. Keegan, and D. Yelon, *Vessel and blood specification override cardiac potential in anterior mesoderm.* Dev Cell, 2007. **13**(2): p. 254-67.
198. Wang, H., et al., *Wnt2 coordinates the commitment of mesoderm to hematopoietic, endothelial, and cardiac lineages in embryoid bodies.* J Biol Chem, 2007. **282**(1): p. 782-91.

199. Norton, J., et al., *Matrix adhesion polarizes heart progenitor induction in the invertebrate chordate Ciona intestinalis.* Development, 2013. **140**(6).
200. Klaus, A. and W. Birchmeier, *Developmental signaling in myocardial progenitor cells: a comprehensive view of Bmp- and Wnt/beta-catenin signaling.* Pediatr Cardiol, 2009. **30**(5): p. 609-16.
201. Hoppler, S. and R.T. Moon, *BMP-2/-4 and Wnt-8 cooperatively pattern the Xenopus mesoderm.* Mech Dev, 1998. **71**(1-2): p. 119-29.
202. Liu, Z., et al., *WNT signaling promotes Nkx2.5 expression and early cardiomyogenesis via downregulation of Hdac1.* Biochim Biophys Acta, 2009. **1793**(2): p. 300-11.
203. Chalfie, M., et al., *Green Fluorescent Protein as a Marker for Gene-Expression.* Science, 1994. **263**(5148): p. 802-805.
204. Balmer, J.E. and R. Blomhoff, *Gene expression regulation by retinoic acid.* J Lipid Res, 2002. **43**(11): p. 1773-808.
205. Lewis, J.L., et al., *Reiterated Wnt signaling during zebrafish neural crest development.* Development, 2004. **131**(6): p. 1299-308.
206. Keegan, B.R., D. Meyer, and D. Yelon, *Organization of cardiac chamber progenitors in the zebrafish blastula.* Development, 2004. **131**(13): p. 3081-3091.
207. Kimmel, C.B., R.M. Warga, and T.F. Schilling, *Origin and organization of the zebrafish fate map.* Development, 1990. **108**(4): p. 581-94.
208. Schilling, T.F., Q. Nie, and A.D. Lander, *Dynamics and precision in retinoic acid morphogen gradients.* Curr Opin Genet Dev, 2012. **22**(6): p. 562-9.
209. White, R.J., et al., *Complex regulation of cyp26a1 creates a robust retinoic acid gradient in the zebrafish embryo.* PLoS Biol, 2007. **5**(11): p. e304.
210. Kudoh, T., S.W. Wilson, and I.B. Dawid, *Distinct roles for Fgf, Wnt and retinoic acid in posteriorizing the neural ectoderm.* Development, 2002. **129**(18): p. 4335-46.
211. Bothe, I., et al., *Dynamic control of head mesoderm patterning.* Development, 2011. **138**(13): p. 2807-21.
212. Rhinn, M. and M. Brand, *The midbrain--hindbrain boundary organizer.* Curr Opin Neurobiol, 2001. **11**(1): p. 34-42.
213. Buckles, G.R., et al., *Combinatorial Wnt control of zebrafish midbrain-hindbrain boundary formation.* Mech Dev, 2004. **121**(5): p. 437-47.
214. Amoyel, M., et al., *Wnt1 regulates neurogenesis and mediates lateral inhibition of boundary cell specification in the zebrafish hindbrain.* Development, 2005. **132**(4): p. 775-85.
215. Waxman, J.S., et al., *Hoxb5b acts downstream of retinoic acid signaling in the forelimb field to restrict heart field potential in zebrafish.* Developmental cell, 2008. **15**(6): p. 923-934.
216. Dohn, T.E. and J.S. Waxman, *Distinct phases of Wnt/Œ≤-catenin signaling direct cardiomyocyte formation in zebrafish.* Developmental biology, 2012. **361**(2): p. 364-376.
217. Danielle, N., et al., *Origin, Specification, and Plasticity of the Great Vessels of the Heart.* Current biology : CB, 2015. **25**(16): p. 2099-2110.